

POLITECNICO DI TORINO

UNIVERSITY OF ALBERTA

Master's Degree in Biomedical Engineering (Bionanotechnology)



Master's Degree Thesis

**Design and evaluation of albumin
nanoparticles for the delivery of a β -
tubulin polymerization inhibitor**

Supervisors

Dr Jack Tuszynski

Dr Afsaneh Lavasanifar

Co-supervisor

Dr Jaber Emami

Candidate

Alessandra Spada

October 21, 2020

Abstract

One of the major limitations of chemotherapy in cancer treatment is the wide range of side effects caused by anti-cancer drugs, due to their toxicity, their non-selective distribution and their action on both cancer and normal dividing cells. The ultimate goal of this study is to develop a novel delivery system for the potent and cytotoxic compound CCI-001, which is a novel β -tubulin polymerization inhibitor, to protect it from degradation, help its transport through the body, improve its therapeutic efficacy and reduce its harmful side effects.

Albumin, one of the most abundant proteins in blood plasma, has shown to be non-toxic, non-immunogenic, biocompatible and biodegradable. Furthermore, it strongly interacts with both hydrophilic and hydrophobic compounds. Therefore, it is an ideal and versatile substance to fabricate nanoparticles for drug delivery. The albumin carrier could specifically target the desired site of action due to the active recognition by the albumin receptors, gp60 and SPARC, which are overexpressed in tumours. Therefore, the uniqueness of using albumin lies in the facts that firstly, it is a natural component of our body and secondly, it can potentially provide both passive and active targeting, without the use of any external ligands.

CCI-001, a tubulin polymerization inhibitor, which has been synthesized and patented in the Department of Oncology, University of Alberta, Edmonton, Canada, has shown potent anti-cancer activity in various cancer cell lines, *in vitro* (IC_{50} s of 3.28 and 4.29 nM in pancreatic and bladder cancer, respectively). Moreover, CCI-001 has been particularly effective in cancer cells which have demonstrated to be resistant to paclitaxel. However, its applications are limited by its extremely low water solubility, poor uptake into the tumour site and non-selective distribution and uptake by healthy cells. These limitations can reduce the efficacy of the compound and also could cause undesirable side effects, upon *in vivo* administration. In the current study, CCI-001 was loaded into serum albumin, both bovine and human, generating CCI-001-BSA and CCI-001-HSA nanoparticles, using a modified version of the desolvation method, based on an incubation process. Already formed and crosslinked albumin nanoparticles were incubated overnight at 37°C with different drug solutions. The obtained CCI-001-loaded albumin

nanoparticles were assessed for particle size, zeta potential, drug loading, release, morphology and cell toxicity against SW620 and HCT116 colorectal cancer cell lines.

The spherical nanoparticles were negatively charged (zeta potential of ~ -30 mV) and had an average diameter of ~ 130 nm, with a narrow size distribution. The *in vitro* release of CCI-001 from the albumin nanoparticles showed a sustained release pattern over 24-25 hours without any initial burst release, compared to the fast release of the free drug. Due to the extremely high lipophilicity of the drug (solubility in water at pH 7.4 of 0.007 mg/mL), the drug loading resulted to be around 6 $\mu\text{g}/\text{mg}$ albumin, which is still high enough to be tested on the cell lines investigated, because of the extremely high cytotoxicity of the compound. In fact, cellular toxicity studies of the CCI-001-loaded albumin nanoparticles showed a similar activity to the free drug, with IC_{50} s even slightly lower in the cancer cell lines investigated.

These data support the advantages of the potential use of these versatile nanoparticles as drug carriers in biological systems. However, the formulation of such CCI-001-loaded albumin nanoparticles could be further improved (the drug loading could be increased and toxicity of the carrier could be reduced, by replacing the crosslinking agent with a less toxic one) for efficient delivery to tumours and future animal and human studies.

Acknowledgments

I would like to express my deepest gratitude and appreciation to all of the following people:

- My supervisors Dr Jack Tuszynski and Dr Afsaneh Lavasanifar for giving me the opportunity to pursue my Master's Thesis in Canada. Their encouragement, guidance, support and inspiration helped me throughout the program and allowed me to develop an understanding of the field. Even during a global pandemic, Dr Tuszynski was always there to give his advice and cheer me up.
- This thesis would not have been possible unless with the guiding advices and support of my co-supervisor Dr Jaber Emami, who assisted me every day in my research. I cannot thank him enough for his endless help and motivation. Without his patient guidance, I would have been lost in miscellaneous problems and obstacles encountered during the research.
- My lab mates Waleed Mohamad Saied, Igor Paiva, Julian Ethier-Hopwood, Parnian Mehinrad and Sams Sadat, for their help, support and fruitful discussions.
- Dr Foroughalsadat Sanaee, for her patience and help with the HPLC analysis.
- Dr Mohamed Reza Vakili, for his help and advice in chemistry and polymer synthesis.
- My beloved parents and sister, for their love, support and encouragement throughout my whole life. This experience has been really tough and hard, being so far away from home during a pandemic. Our weekly Skype videocalls allowed me to stay strong and positive and to keep going with my project.
- My best friend Simona, whose calls and texts always stimulated me to stay positive and happy throughout the experience. Although physical far away, she was always there when I needed her the most.
- Last but not least, I would like to extend my sincere thanks to my boyfriend Antonio, who went through this journey with me in Canada. His love, patience, thoughtfulness and never-ending support helped me during this experience and allowed me to become a better person. We experienced laughter and tears, joy and frustration, but we have overcome all the obstacles together. I love you (and I am also grateful for all of your delicious and exquisite dishes that brought a bit of Italy here in Canada).

Table of contents

1	Introduction.....	1
1.1	The clinical problem: cancer.....	1
1.2	Microtubules and tubulin.....	5
1.2.1	Main components of the cytoskeleton.....	5
1.2.2	Microtubule dynamic instability.....	7
1.2.3	The tubulin code.....	8
1.2.3.1	Tubulin isotypes.....	8
1.2.3.2	Tubulin PTMs.....	9
1.2.3.3	The tubulin code in cell division.....	10
1.3	Microtubule-targeting agents.....	11
1.3.1	Mechanisms of action.....	11
1.3.2	Mechanisms of resistance.....	14
1.3.2.1	ABC transporters.....	15
1.3.2.2	Glutathione detoxification system.....	16
1.3.2.3	p53 and Bcl-2 proteins.....	18
1.3.2.4	Mutations and overexpressions of tubulin isotypes.....	21
1.3.3	Main classes of microtubule-targeting agents.....	23
1.3.3.1	Vinca domain-binding agents.....	23
1.3.3.2	Taxol domain-binding agents.....	25
1.3.3.3	Colchicine domain-binding agents.....	25
1.4	Novel derivatives and CCI-001.....	32
1.5	Albumin.....	38
1.5.1	Characteristics and features of albumin.....	38
1.5.1.1	Human serum albumin.....	39
1.5.1.2	Serum albumin from other species.....	40
1.5.1.3	Roles of albumin in drug delivery.....	41
1.5.2	The unique properties of albumin in tumour targeting.....	42

1.5.2.1	Passive targeting	42
1.5.2.2	Active targeting and albumin receptors.....	43
1.5.2.3	Stealth nanoparticles.....	45
1.5.3	ABI-007 (Abraxane [®])	46
1.5.3.1	Advantages of ABI-007 over Taxol.....	46
1.5.4	Albumin: more than a carrier for anticancer drugs	49
1.5.5	Future perspectives	50
2	Aim of the work	52
3	Materials and methods	55
3.1	Materials	55
3.1.1	Chemicals and cell lines.....	55
3.1.2	Instruments.....	56
3.2	Methods	57
3.2.1	Preparation of CCI-001-loaded albumin nanoparticles.....	57
3.2.1.1	First strategy: Nab-technology [®]	58
3.2.1.2	Second strategy: Desolvation.....	62
3.2.1.3	Modified version of desolvation	65
3.2.2	Freeze-drying.....	67
3.2.3	Characterization of CCI-001-loaded albumin nanoparticles	68
3.2.3.1	Size and zeta potential	68
3.2.3.2	Nanoparticles morphology.....	69
3.2.3.3	Yield.....	69
3.2.3.4	Drug entrapment efficiency and drug loading	69
3.2.4	<i>In vitro</i> drug release studies.....	70
3.2.5	HPLC analysis of CCI-001.....	72
3.2.6	Cell culture	72
3.2.6.1	Cell freezing.....	73
3.2.6.2	Cells thawing	73

3.2.6.3	Sub-culture.....	74
3.2.7	MTT assay (<i>in vitro</i> cytotoxicity).....	75
3.2.7.1	Free CCI-001	77
3.2.7.2	CCI-001-loaded HSA nanoparticles.....	77
3.2.7.3	Blank HSA nanoparticles	78
4	Results and discussion	79
4.1	Preparation of CCI-001-loaded albumin nanoparticles	79
4.1.1	Nab-technology®.....	79
4.1.1.1	Sonication	79
4.1.1.2	High-pressure homogenization	80
4.1.2	Desolvation.....	81
4.1.3	Modified version of desolvation.....	81
4.2	Characterization of CCI-001-loaded albumin nanoparticles.....	83
4.2.1	Size and zeta potential.....	86
4.2.2	Freeze-drying.....	89
4.2.3	Encapsulation efficiency and drug loading	90
4.2.4	Yield.....	91
4.2.5	Morphology	91
4.2.6	Effect of the stirring speed	92
4.2.7	Effect of pH.....	93
4.2.8	Effect of the glutaraldehyde	94
4.3	<i>In vitro</i> drug release.....	96
4.4	Cell toxicity.....	97
5	Conclusions.....	101
6	Limitations and future directions.....	104
7	References.....	108

List of figures

Figure 1: Microtubule. From THE CELL, Fourth Edition, Figure 12.42.....	6
Figure 2: Dynamic instability. From ref[24] with permission.	7
Figure 3: Chemical structure of colchicine.....	25
Figure 4: Chemical structure of CCI-001.....	32
Figure 5: Comparison between the activity of control, CCI-001 (6 mg/kg) and CCI-001 (3 mg/kg) on T24 cell line xenografts in vivo. From ref [126] with permission.	35
Figure 6: Comparison between the activity of CCI-001 and gemcitabine/cisplatin on T24 xenografts in vivo. From ref [126] with permission.	35
Figure 7: Structure of albumin. From ref [131] with permission.....	38
Figure 8: Nab-technology process. From ref [149] with permission.	58
Figure 9: Desolvation process. From ref [149] with permission.	63
Figure 10: Modified version of desolvation process. Adapted from ref [149] with permission.	66
Figure 11: Reduction of MTT to Formazan crystals.....	75
Figure 12: 96-wells plate.....	76
Figure 13: A) λ_{\max} CCI-001 B) Calibration curve of CCI-001.....	84
Figure 14: Size distribution of A) CCI-loaded BSA nanoparticles (batch 6) and C) CCI-00-loaded HSA nanoparticles (batch 8). Zeta potential of B) CCI-001-loaded BSA nanoparticles and D) CCI-001-loaded HSA nanoparticles.	87
Figure 15: A) Size comparison of CCI-001-loaded BSA/HSA nanoparticles and blank BSA/HSA nanoparticles. B) Zeta potential comparison of CCI-001-loaded BSA/HSA nanoparticles and blank BSA/HSA nanoparticles. Data represent average \pm SD (n=3). * means statistically different from the blank NPs ($\alpha < 0.05$, Student t-test).....	88
Figure 16: Stability of CCI-001-loaded albumin nanoparticles. Data represent average \pm SD (n=3).....	89
Figure 17: Influence of the use of trehalose on the size and zeta potential of freeze-dried nanoparticles. Data represent average \pm SD (n=3). ** means statistically different from the formulation with trehalose ($\alpha < 0.01$, Student t-test). * means statistically different from the formulation with trehalose ($\alpha < 0.05$, Student t-test).....	90
Figure 18: Encapsulation efficiency (%) and amount of drug/albumin ($\mu\text{g}/\text{mg}$). Data represent average \pm SD (n=3).....	91
Figure 19: Sem images of A) CCI-001-loaded HSA NPs 45k-fold magnification, B) CCI-001-loaded HSA NPs 16k-fold magnification, C) CCI-001-loaded BSA NPs 45k-fold magnification, D) CCI-001-loaded BSA NPs 16k-fold magnification.	92

Figure 20: Influence of the stirring speed on the size of the nanoparticles. Data represent average \pm SD (n=3).....	93
Figure 21: Influence of the pH on the size of the nanoparticles. Data represent average \pm SD (n=3).....	94
Figure 22: Glutaraldehyde.....	94
Figure 23: In vitro CCI-001 release profiles. Data represent average \pm SD (n=3).	97
Figure 24: Comparison between the cytotoxicity of CCI-001-loaded HSA NPs, blank NPs and free CCI-001 in: A) SW-620 48h, B) SW-620 72h, C) HCT-116 48h, D) HCT-116 72h. Data represent average \pm SD (n=3). * means statistically different from free drug (α <0.05, Student t-test). ** means statistically different from free drug (α <0.01, Student t-test).....	99
Figure 25: Comparison of the drug-loaded NPs effects at 48 and 72h in: A) SW-620, B) HCT-116. Data represent average \pm SD (n=3). * means statistically different from 72h (α <0.05, Student t-test). ** means statistically different from 72h (α <0.01, Student t-test).....	100

List of tables

Table 1: Summary of the nano-delivery systems of colchicine.	29
Table 2: Other drugs combined with HSA in albumin-based formulations.....	48
Table 3: Albumin-based formulations in other diseases.....	49
Table 4: Formulations prepared with nab-technology.....	62
Table 5: Formulations prepared with desolvation.....	65
Table 6: Formulations prepared with a modified version of desolvation.	67
Table 7: Characterization of the CCI-001-loaded BSA/HSA nanoparticles. Data represent average \pm SD (n=3).....	85
Table 8: Influence of glutaraldehyde concentration on the particle size. Data represent average \pm SD (n=3). ** means statistically different from the other glutaraldehyde concentration ($\alpha<0.01$, Student t-test).....	95
Table 9: IC _{50S} of CCI-001-loaded HSA nanoparticles and free CCI-001, in SW-620 and HCT-116 cancer cell lines, at 48 and 72 hours. Data represent average \pm SD (n=3). * means statistically different from free drug ($\alpha<0.05$, Student t-test). ** means statistically different from free drug ($\alpha<0.01$, Student t-test).....	98

List of abbreviations

EPR	Enhanced permeability and retention effect
NO	Nitric oxide
PEO	Polyethylene oxide
PEG	Polyethylene glycol
FDA	Food and Drug Administration
SPARC	Secreted protein acidic and rich in cysteine
GTP	Guanosine triphosphate
GDP	Guanosine diphosphate
MAPs	Microtubule-associated proteins
MT	Microtubule
PTMs	Post-translational modifications of tubulin
AiAs	Angiogenesis-inhibiting agents
VDAs	Vascular-disrupting agents
VEGF	Vascular endothelial growth factor
VEGFR	Vascular endothelial growth factor receptor
ABCs	ATP binding cassette transporters
P-gp	P-glycoprotein
GSH	Glutathione
GST	Glutathione S-transferases
ROS	Reactive oxygen species
MRP	Multiple resistance-associated protein
MTAs	Microtubule-targeting agents
TGFBI	Transforming growth factor- β induced
PLA	Polylactic acid
HSA	Human serum albumin
Trp	Tryptophan

ADMET	Administration, Distribution, Metabolism, Elimination, Toxicity
PDI	Polydispersity index
BSA	Bovine serum albumin
RSA	Rat serum albumin
OVA	Ovalbumin
pI	Isoelectric point
SNO-HSA	S-nitrosated human serum albumin
PVP	Polyvinyl pyrrolidone
PVA	Polyvinyl alcohol
PAA	Polyacrilic acid
HUVEC	Human umbilical vascular endothelial cells
HPLC	High-performance liquid chromatography
DMEM	Dulbecco's Modified Eagle Medium
NaOH	Sodium Hydroxide
EtOH	Ethanol
DMSO	Dimethyl sulfoxide
FBS	Fetal bovine serum
P/S	Penicillin-streptomycin
SEM	Scanning electron microscope
NP	Nanoparticle
RES	Reticuloendothelial system

1 Introduction

1.1 The clinical problem: cancer

This chapter is a general introduction, aimed at highlighting the biological background and the reasons that led to the experimental work of this research project. Then, the structure and function of microtubules, important part of the cytoskeleton of eukaryotic cells, are outlined. The most studied and investigated microtubule-targeting drugs, which are compounds that take advantage of the overexpression in cancer of some isotypes of tubulin in order to fight the disease, their mechanisms of action, their mechanisms of resistance, the toxicities and the possibility of improvement of the formulations are described. In particular, the attention is focused on CCI-001, which is a novel colchicine derivative, designed and synthesized by the Department of Oncology, University of Alberta, Edmonton, Canada. It is described and compared with other colchicine-binding agents, highlighting the advantages and the differences. Finally, albumin, the most abundant protein in blood plasma, its characteristics, the sources of extraction and its roles and advantages as a smart carrier in drug delivery are depicted.

Cancer is the second leading cause of death globally (right after cardiovascular diseases) and, in 2018, it was responsible for 9.6 million deaths worldwide: 1 in 6 deaths was due to cancer. It is a genetic disease, caused by changes in the genes that modulate the way our cells function: in particular, how they proliferate and migrate. These genetic changes can be inherited (germline mutations) or acquired during the lifetime (somatic mutations) because of damage to DNA, arisen for certain environmental exposures. Cancer cells are¹: able to ignore signals that usually tell cells to stop dividing and to begin the process of programmed death (apoptosis), less specialized than healthy cells, able to escape the immune system and take advantage of it for their proliferation, able to influence the tumour microenvironment, able to promote a general state of inflammation, able to induce angiogenesis, able to activate invasion and metastasis. Cancer is characterized by the sudden growth and proliferation of some cells which begin to divide without control and, eventually, spread into surrounding tissues. A cancer that has spread from its primary site is called “*metastatic cancer*” and the tumour cells begin to travel to other parts of the body through the bloodstream and the lymphatic system. The final purpose of any cancer

treatment would be to destroy as many cancer cells as possible, without causing harm to the healthy cells. The most popular cancer treatments are²:

- Surgery³ (e.g.: cryosurgery, laser treatment, hyperthermia, photodynamic therapy), that physically removes the tumour tissue, but has the inability to eliminate completely all the tumour cells from the patient's body. Therefore, it may affect the patient's quality of life after the removal of a certain organ;
- Radiotherapy⁴, which uses high energy radiation (external beam radiation therapy or internal radiation therapy) to kill cancer cells, producing DNA damage. However, it may cause harm to surrounding tissues depending on the dose of the radiation, the accuracy and the specific site of the cancer;
- Chemotherapy⁵, that uses anti-cancer drugs interfering with cell division. However, it may be unable to kill a tumour on its own (it needs to be combined with another treatment) and it may be toxic to healthy cells as well, such as the ones that proliferate fast: digestive tract, hair follicles, cells of the bone marrow;
- Immunotherapy⁶, which is based on the modulation and improvement of the body's immune response against cancer (such as: immune checkpoint inhibitors, T-cell transfer therapy, vaccines). However, it is limited by the poor availability of tumour-specific antigens and the inability to predict the efficacy and the patient response;
- Targeted therapy⁷, that uses drugs or compounds which target directly the specific molecules responsible for tumour growth, progression and sustainment (such as: hormone therapies, apoptosis inducers, angiogenesis inhibitors, signal transduction inhibitors). However, the limitation is that the tumour could develop resistance and find new pathways to develop.

New promising approaches⁸ include:

- Gene therapy, that consists in the insertion of a foreign gene sequence into the patient's cells (delivery of a nucleic acid sequence to replace a mutated gene, to silence it, to stimulate the immune system, or to directly kill cancer cells);
- Cell therapy, which is based on the injection of cells to replace the immune system cells or to directly find and kill cancer cells (such as CAR T-cell therapy, where the patient's T cells are engineered in the laboratory to better recognize and attack the tumour).

As far as gene therapy and delivery of sequence of foreign DNA inside the body are concerned, it is of vital importance to find carriers able to protect and transport the cargos and efficiently target them to the right place at the right time. The ones used in gene therapy are usually viral carriers or non-viral carriers in form of nanoparticles (such as lipid-based vectors or cationic polymers that can interact with nucleic acid through electrostatic forces). Nanoparticles are used not only in gene therapy, but also for the delivery of chemotherapeutic agents. In fact, nanotechnology is a versatile field⁹ that deals with the design, the synthesis and the characterization of nanomaterials, such as nanoparticles, which can constitute smart and effective drug delivery systems. The use of nanoparticles to carry and deliver small molecular weight compounds brings a lot of advantages, compared to the use of free anti-cancer drugs: they increase treatment selectivity, maximize treatment efficacy and minimize undesired side effects. Nanoparticles are multifunctional devices, able to carry one or more therapeutic agents (therapy) or contrast agents (imaging, diagnosis). They can rely on two main ways to reach the tumour site: passive targeting and active targeting. The first is based on the enhanced permeability and retention effect, that often characterizes the tumours¹⁰: the hyper-permeability of the tumour blood vessels and the immaturity of the lymph drainage system are responsible for the accumulation of small nanoparticles (generally characterized by sizes below 200-300 nm) inside the tumour site. For the EPR effect, nanoparticles are required to have long blood residence time and efficient particle evasion from the clearing organs (e.g.: liver): after reaching the tumour, they undergo cellular internalization to release their cargo in the cytoplasmic and/or nuclear targets. This mechanism works well in solid tumours and inflamed tissues where the leaky vasculature is preponderant, but the problem with this type of targeting is that not all the tumours are characterized by high permeability (such as pancreatic cancer and melanoma). Various studies^{11,12} have demonstrated the efficacy of some vascular modulator (such as nitric oxide, NO), able to augment vascular permeability via vasodilation. The second type of targeting, the active targeting, relies on specific recognition between a ligand (attached to the surface of the nanoparticle) and its receptor on the target site. It requires the functionalization of the surface of the drug delivery system with specific targeting agents, able to be recognized actively by the tumours. In this way, the vehicle would be much more selective towards the tumour tissue, preventing the drug from being released in the wrong place (such as in healthy cells, where it could also produce deleterious side effects). These ligands include antibodies, fragments of antibodies, peptides and aptamers, which

are DNA or RNA structures characterized by better site specificity and less immunogenicity than antibodies¹³. Furthermore, it is possible to modify the surface of the nanoparticles with polyethylene oxide (PEO) or polyethylene glycol (PEG), which are antifouling polymers¹⁴ that prevent proteins absorption and make the particle “invisible” to the immune cells, such as macrophages. It is known that every foreign body is recognized and eliminated by the immune system, so that it cannot reach the desired site of action. For this reason, it is fundamental for the nanoparticles to escape the immune recognition, prolong their blood residence time and be able to reach the tumour site without being phagocytized first. The PEG chains can be found in two main conformations, brush and mushroom¹⁵. The former is the most resistant one and it prevents more effectively the attack of the immune cells and the absorption of the protein thanks to the steric activity of the chain. It is preferable to have high density and length of the chain, so that they can cover the entire surface of the nanoparticles.

Therefore, drug delivery systems play a vital role in nanomedicine: they protect the cargo from our immune system and from degradation, allow a controlled release in space and time offering a specific and selective targeting and are able to overcome biological barriers. However, the nanoparticles could have some drawbacks: a non-specific uptake by phagocytic cells and poor control over intracellular internalization¹⁶. The final purpose would be to deliver to the target the optimal amount of drug with appropriate kinetics without inducing deleterious side effects on healthy tissues. For this reason, it is extremely important to modulate the physical and chemical properties of the nanoparticles (e.g.: shape, size, charge, ligand density, elasticity), since they strongly affect the efficacy of the system. The pharmacokinetics, vascular transport and cellular uptake are strongly controlled by the size of the nanoparticle; the blood circulation and internalization by the cells depend on the shape; the charge can determine electrostatic interaction with the cargos or functionalization of the carrier; the ligand density influences the biodistribution and the cellular uptake; and different elasticity of the vehicle determines the level of phagocytosis and endocytosis. For these reasons, it is fundamental to modulate and choose the optimal features of the nanoparticles so that it is possible to direct the system to the desired responses.

Having understood the great potential of nanoparticles in the treatment of cancer, this research project is focused on improving the formulation of a novel β -tubulin

polymerization inhibitor, CCI-001, which demonstrated to be even more efficient and cytotoxic than paclitaxel, being characterized by a stronger anti-tumour activity (even in those tumours which are paclitaxel-resistant) and selectivity. Moreover, it can be used synergistically with gemcitabine, an antimetabolite, producing an even robust effect. The drug delivery system investigated is constituted by CCI-001-loaded albumin nanoparticles. The idea comes from the already FDA approved (2005) Abraxane[®], paclitaxel-loaded albumin nanoparticles, used for metastatic breast cancer, non small cell lung cancer, metastatic adenocarcinoma of the pancreas, bladder cancer, gastric cancer. The strategies investigated are nab-technology, a desolvation method and a modified version of desolvation, based on an incubation process.

Proteins are natural molecules that share the advantages of synthetic polymers, plus the biodegradability and low toxicity. The reasons for choosing albumin, as will be explained in the next chapters, are its great potential and wide range of applications: it is one of the most abundant proteins in blood plasma and it is a versatile carrier. It can bind both hydrophilic and hydrophobic drugs with high affinity, it is not rejected by the immune system being an endogenous substance, and it can actively deliver the drug to the tumour site in a specific and selective manner (active targeting through gp60/SPARC pathway).

From the idea of nab-paclitaxel, the purpose of this work was to investigate, design, and generate a new formulation, consisting on CCI-001-loaded albumin nanoparticles, analyse its characteristics and determine its efficacy on cancer cell lines.

1.2 Microtubules and tubulin

1.2.1 Main components of the cytoskeleton

The cytoskeleton is the structure that provides shape, stability, internal organization and mechanical support to eukaryotic cells. It is composed of three types of protein, very different in size and composition:

1. Actin filaments. They are the smallest type, with diameters of 6 nm and they are composed of a globular protein called actin, which polymerizes to form long polar filaments. Each actin monomer (globular G actin) is composed of 375 amino acids and has head-to-tail interactions with two other actin monomers, creating filaments (filamentous F actin). The filaments are double-stranded helix because

each monomer is rotated by 166° in the filaments. Actin polymerization is reversible and there is always equilibrium between actin monomers and filaments¹⁷. Actin has been extensively studied in muscle cells: here, besides the thin actin filaments, it is possible to find some thick filaments formed by a protein called myosin. These two types of filaments, organized in a structure called sarcomere, are responsible for the mechanism of muscle contraction. In non-muscle cells, actin forms a network of filaments which determines cell shape, mechanical support and cellular movements¹⁸.

2. Intermediate filaments. They are thicker than actin filaments, but thinner than microtubules, with diameters of about 10 nm¹⁹. They share a common tripartite structure, composed of a highly conserved central α -helical rod domain, a variable N-terminal head and a C-terminal tail domain²⁰. They are less dynamic than actin filaments or microtubules (in particular, they are extremely compliant at small deformation but stiffen at larger stretch) and their main function is to provide integrity, strength and support to the fragile tubulin structures²¹. Unlike actin or tubulin, intermediate filaments are not polar. Cells in different tissues of the body have different types of intermediate filaments (e.g.: keratins in epithelial cells, desmin filaments in muscle cells, neurofilaments in neurons), which possess particular functional characteristics, determining the function of the cell.

3. Microtubules. They are rigid hollow rods with internal diameter of around 14 nm and external diameter of 25 nm and they are composed of a single type of globular protein, tubulin. Tubulin is a dimer consisting of two 55-kDa polypeptides called α -tubulin and β -tubulin²², which polymerize to form microtubules, made of 13 parallel protofilaments assembled around a

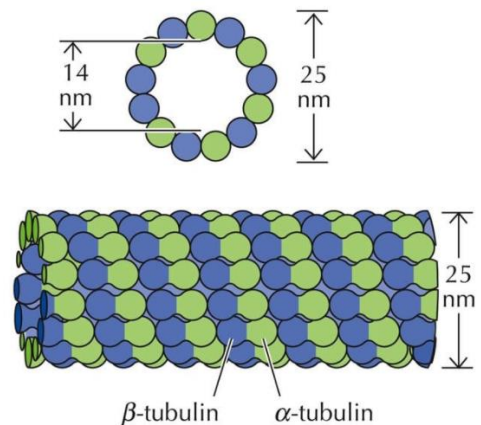


Figure 1: Microtubule. From THE CELL, Fourth Edition, Figure 12.42.

hollow core. The α -tubulin and β -tubulin are approximately 40% identical at the sequence level. A third type of tubulin, γ -tubulin, is found in the centrosome, which plays a vital role in the microtubule assembly. Microtubules, like actin filaments, have a polarity and furthermore, they are ever-changing, constantly adding and subtracting tubulin dimers at both ends of the filament. There is a

discrepancy in the growth rate between the end that possesses an exposed β -tubulin (faster extension, plus end), compared to the end that exposes an α -tubulin (slower extension, minus end). They influence cell shape, cell movements, the intracellular transport of organelles and the separation of chromosomes during cell mitosis²³.

1.2.2 Microtubule dynamic instability

The reversible polymerization and depolymerization of tubulin dimers show that microtubules can undergo rapid cycles of assembly and disassembly, in a process called dynamic instability²⁴. Both α -tubulin and β -tubulin bind GTP: the GTP bound to β -tubulin is hydrolyzed to GDP and this hydrolysis weakens the binding affinity of tubulin with the nearby molecules, stimulating the depolymerization of microtubules²⁵. It is the comparison between the rate of tubulin addition and the rate of GTP hydrolysis that determine the growth (rescue) or shrinkage (catastrophe) of microtubules²⁶: if the GTP-bound tubulin is added more rapidly than GTP is hydrolyzed, the microtubule grows, whereas if the tubulin addition is slower, the GTP bound to the tubulin is hydrolyzed to GDP resulting in the dissociation of the GTP-bound tubulin from the growing microtubule²⁷. Stabilization of the whole microtubule structure is normally afforded by the binding of a GTP cap at the end of the microtubule, which shields the terminal β -tubulin from a conformation change that induces its dissociation. The onset of microtubule assembly is critically dependent on a number of factors, including temperature range, local concentration of tubulin and supply of biochemical energy in the form of GTP. This mechanism of continuous turnover is vital in many cellular functions, such as mitosis²⁸: during prophase, chromosomes have been condensed and form an identical copy, called sister chromatids. Centrosome consists of two centrioles from where spindle formation originated. The centrosomes move to opposite direction to generate spindle pole. At metaphase, polymerization of microtubules occurs and pushes the sister chromatids from pole towards the centre (equator). Mitotic spindles

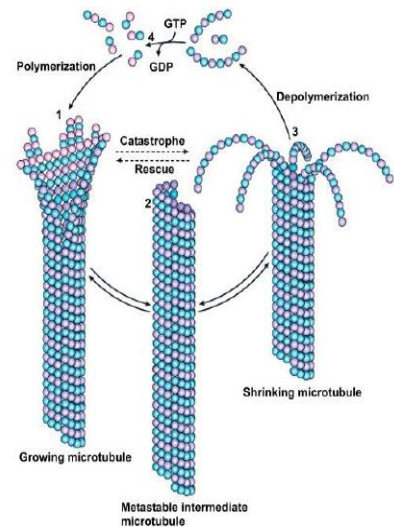


Figure 2: Dynamic instability. From ref[24] with permission.

attach to centromeres of sister chromatids through the kinetochore and are then called kinetochore spindles. At anaphase, mitotic spindles contract, leading to the pulling of sister chromatids towards opposite poles and separation of chromosome. At telophase, mitotic spindles disappear and chromosomes are encapsulated inside the nuclear envelope. Therefore, during the mitosis, the dynamics of microtubule assembly and disassembly change drastically: the rate of microtubule disassembly and the number of microtubules emanating from the centrosome increase. Because of their vital importance in the mechanisms of cell division and proliferation, microtubules are appealing targets in pharmacological applications: it is possible to use drugs that affect the polymerization and depolymerization of microtubules, changing the mitosis process and, therefore, leading cells (e.g.: cancer cells) to apoptosis.

1.2.3 The tubulin code

1.2.3.1 Tubulin isotypes

As already highlighted, microtubules play various roles, modulating cell shape, division, motility and differentiation²⁹. Being constituted by heterodimers of α -tubulin and β -tubulin, one of the questions that may arise is how the microtubules can adapt to a huge variety of functions, behaviours and properties. The first thing to consider is that microtubules can interact with many microtubule-associated proteins (MAPs), able to modulate the MT dynamics, promoting their assembly/disassembly, and connect them to cell structures (membranes or cytoskeletal components)³⁰. Moreover, microtubules features and functions are determined by the “tubulin code”, a combination of tubulin variants, called isotypes, and post-translational modifications of tubulin (PTMs). Tubulin isotypes have homologous amino acid sequences that appear to have diverged as a result of accumulated mutations (which arise from the altered genetic expression of tubulin) and they differ from species to species: in human, both α -tubulin and β -tubulin are encoded by nine genes, whereas in yeast, α -tubulin is encoded by two genes and β -tubulin by one. The incorporation of different tubulin isotypes in a microtubule can have two main functions: first, it can affect the primary structure of tubulin dimers and thus the dynamic assembly and disassembly, stability and also physical properties of MTs, and secondly it can affect the interaction of MTs with the MAPs. Several isotypes of α -tubulin and β -tubulin were discovered, but much more information regards β -tubulin, which is a more suitable target for many antimitotic drugs (less is known about α -tubulin, which shows

higher conservation). In fact, one of the main disadvantages of the tubulin-binding drugs is that they bind tubulin indiscriminately, leading to death of both cancer and healthy cells. However, the broad cellular distribution of several tubulin isotypes provides a platform upon which to construct novel chemotherapeutic drugs that could differentiate between different cell types, decreasing the harmful side effects linked to the current chemotherapeutic treatments. Therefore, drugs with increased specificity for tubulin within cancerous cells are required to provide effective tools in the treatment of cancer. In particular, ten different β -tubulin isotypes have been investigated: β I (TUBB), β IIA (TUBB2A), β IIB (TUBB2B), β III (TUBB3), β IVA (TUBB4), β IVB (TUBB2C), β V (TUBB6), β VI (TUBB1), β VII, β VIII, expressed by different types of cells³¹. In healthy normal cells, the most expressed types are β I, β IVB and β V. In the brain, β IIA, β IIB, β III, β IVA, whereas in the hematopoietic cells, β VI. The β III tubulin is overexpressed in tumour tissues, compared to healthy ones: therefore, it is the most appealing isotype for the development of antimetabolic drugs³². The importance of the tubulin isotypes becomes apparent, since the ultimate goal of cancer research is to develop compounds that will target only cancer cells. That is the reason why researchers are focusing their attention on obtaining data for drug binding to each β -tubulin isotype. This would permit the formulation of individualized treatment regimens for any given cancer cell type, reducing the side effects that are normally linked to current chemotherapeutic treatments.

1.2.3.2 Tubulin PTMs

The second component of the tubulin code is constituted by the post-translational modifications, which are catalysed by a range of enzymes and label distinct microtubule subpopulations in cells, programming these microtubules to specific functions³³. Some of the most investigated PTMs of tubulin are: deetyrosination-tyrosination, polyglutamylation and polyglycylation, acetylation, methylation and phosphorylation. Most of the PTMs are localized in the C-terminal tails of α -tubulin and β -tubulin³⁴, exposed to the outer surface of assembled microtubules, and enzymes catalysing these PTMs usually modify microtubules over soluble tubulin dimers. The tubulin code can influence the structural and mechanical features of microtubules. For example, depending on the tubulin isotypes and the PTMs present, the microtubule formed can be constituted by 11, 13, 14 or even 15 protofilaments, which determine different MT functions. Furthermore, the microtubule flexibility is modulated by the different tubulin isotypes

present: the right mechanical assembly of microtubules is determined by the slide of adjacent protofilaments one against each other, a movement that is allowed by specific non-covalent interactions between tubulin molecules. Not only the tubulin isotypes influence the microtubule mechanics, but also the PTMs are known to have an effect on it: for example, the acetylation of α -tubulin has been demonstrated to promote the mechanical ageing, in which the microtubules lose their flexural rigidity, preventing microtubule breakage. The tubulin PTMs also affect the microtubule dynamics: some of the post-translational modifications, such as phosphorylation and acetylation, prevent the tubulin dimers to assemble, downregulating the microtubule polymerization, whereas others, such as polyamination, have the opposite role, preventing the depolymerization. The interactions between microtubules and the microtubules-associated proteins can be modulated by both the tubulin isotypes and the tubulin PTMs³⁵: several studies have identified the precise site of communication between MAPs and tubulin and have realized the major influence of the tubulin sequence in the interactions with the proteins. The unfolded C-terminal tubulin tail is involved in various MAP interactions and a single amino acid difference, such as a lysine residue in the tail of β III-tubulin, reduces the run length of kinesin-1 on microtubules. Moreover, the tyrosination state of microtubules affects the nature of the interactions between microtubules and MAPs: detyrosination is able to reduce the binding of the cytoplasmic linker protein CLIP170 to the microtubules, affecting negatively the MT growth and resistance. Many modifying and demodifying enzymes (that catalyze the post-translational modifications) are able to control the intracellular distribution of MAPs and organelles. Therefore, microtubule functions and transport processes in cells are influenced by a combined effect and crosstalk of PTMs and/or tubulin isotypes, so that the tubulin code can help microtubules adapt to changing physiological requirements and reach homeostasis. The tubulin code plays vital cellular and physiological roles in cilia and flagella, in neurons, in muscles and in cell cycle and centrosomes.

1.2.3.3 The tubulin code in cell division

As stated above, microtubules are fundamental in many cellular functions, such as mitosis, where they give rise to the mitotic spindles and are responsible for the separation of chromosomes. The different tubulin isotypes affect the behaviour of mitotic spindles: each isotype, regardless of the similarity with the others, confers specific properties to the

mitotic spindles and modification of the tubulin code can have devastating consequences. Furthermore, various PTMs are found on spindle microtubules: for example, mitosis is characterized by increased polyglutamylation, increased polyglutamylase activity, detyrosinated tubulin³⁶ in spindle microtubules that point to cell equator and tyrosinated tubulin in astral microtubules. Polyglutamylation is enriched on the centrioles, cylindrical arrays of 9 microtubules that compose the centrosomes, the microtubule-organizing centres and this PTM plays a vital role in centriole maintenance and function, and, consequently, in cell division.

1.3 Microtubule-targeting agents

1.3.1 Mechanisms of action

Microtubules are highly dynamic and sensitive to therapeutic inhibitors. For this reason, several drugs targeting the tubulin have been used in order to alter microtubules polymerization and dynamics³⁷: in particular, these compounds are mainly antimetabolic agents which bind to microtubules and, suppressing the microtubule dynamics during the vulnerable mitotic phase of the cell cycle, prevent the cells from proliferating and induce the tumour cell death. The tubulin-targeting drugs can be classified into two groups: they can either work leading to an enhanced polymerization (microtubule-stabilizing agents) or, on the other hand, to an enhanced depolymerization (microtubule-destabilizing agents)³⁸. The first group induces the lengthening of microtubules, whereas the second induces their shortening. As a result, no microtubules are available to produce mitotic spindles for cell division. Examples of the first class include the taxanes (paclitaxel and docetaxel), the epothilones (ixabepilone and patupilone), the discodermolides, eleutherobins, sarcodictyins, dictyostatin, peloruside, cyclostreptin, laulimalide and rhazinilam. They usually bind to the same or to an overlapping taxoid-binding site on β -tubulin, placed in the inside surface of the microtubule. Examples of the second class are the vinca-site binders (which bind in the vinca domain of tubulin), such as the vinca alkaloids (vinblastine, vinorelbine, vinflunine, vincristine, vindesine), the cryptophycins and the dolastins (tasidotin, eribulin, maytansinoids, spongistatin, rhizoxin). Other microtubule destabilizing agents are the colchicine-site binders (which bind tubulin in its colchicine domain), that include colchicine and its analogues, podophyllotoxin, combretastatins, CI-980, 2-methoxyoestradiol, phenylahistins, steganacins and curacins.

Both groups of drugs, the microtubule-stabilizing agents and the microtubule-destabilizing agents, despite the opposite mechanisms of action, work towards the same goal: they inhibit microtubule dynamics and block mitosis. An interesting fact to consider is that components of the two families, for example taxanes and vinca alkaloids, can be used simultaneously with no antagonistic effect. On the contrary, combination of the drugs have shown synergism and higher activity *in vitro*. It is preferable to use low drug concentrations for prolonged periods of time (also known as “metronomic chemotherapy”), instead of peaks of high intracellular drug concentration. Studies demonstrate that tumours have a greater fraction of actively dividing cells than healthy normal tissues³⁹. That is the reason why microtubules, playing vital roles in the mitosis, represent appealing targets for the treatment of cancer. Microtubule-targeting agents-induced disruption of the microtubule dynamics causes mitotic arrest in cancer cells *in vitro* within 8-24 hours, due to the incapability to properly segregate chromosome to daughter cells, leading to apoptosis⁴⁰. Usually, the effects and the activity of these compounds are investigated *in vitro* using cancer cell lines that have the characteristic of proliferating rapidly, with doubling time of 24-48 hours. In xenograft and animal models, cancer cells divide every 10-12 days. In patients, cancer cells do not divide as rapidly as they do in preclinical models: the rate of cell division is around 150-300 days. This fact provides evidence that mitosis in human solid tumours is not as frequent as *in vitro* and the antimitotic activity, even though predominant, is not likely to be the only anticancer mechanism of microtubule-targeting agents. It has been proven that tubulin-binding drugs can initiate apoptosis independently of mitosis: one of their most important dose-limiting toxicities is the initiation of peripheral neuropathy, a condition characterized by the damage of non-dividing neuronal cells that carry messages to and from the brain from and to the rest of the body. Neuronal survival and development rely on the axonal transport processes, which require the action of intact microtubules⁴¹. Microtubule-targeting agents inhibit the transport of proteins and other components within neurons. Peripheral nerves are thought to be more sensitive to these compounds-induced damage, because of the longer length of their axons that rely on the efficient microtubule-depending trafficking. Furthermore, sensory peripheral neurons are more affected to the drugs effects than central neurons, because of the different permeability of blood-nerve and blood-brain barriers. Recent studies have demonstrated that microtubule-targeting agents have effects also on tumour vasculature, as another proof that their action is much more complex than initially speculated⁴². The growth of new blood vessels towards

tumours and tumour cell migration towards metastatic sites are two important factors in anticancer treatments. The tumour blood vessels are appealing therapeutic targets, because usually the tumour cells die if they are not constantly supplied with nutrients from the blood. It is possible to target the tumour blood vasculature in two main ways: using angiogenesis-inhibiting agents (AIAs), which inhibit the formation of new blood vessels, or using vascular-disrupting agents (VDAs), which damage the already existing vasculature. AIAs and VDAs differ in their physiologic target, in the type of disease to treat and the treatment scheduling. The administration of the former ones consists in chronic exposure, necessary to restrain revascularization after the initial blockage, leading to the stabilization of the condition, rather than tumour shrinkage. The latter ones, instead, have a more immediate effect and are administered through acute exposure. The consequences of the activity of vascular-disrupting agents are increased vascular permeability, reduction in blood vessel diameter, decreased blood flow (with resulting ischemia), increased interstitial pressure leading to plasma leakage and, at the end, shutdown of the blood vessels. This approach has significant potential when applied in particular to the vasculature of solid tumours, due to its differences with the one of healthy tissues⁴³. The normal tissues are characterized by an efficient and hierarchically organized vascular network, modulated by the balance of pro-angiogenic and anti-angiogenic molecular factors and a lymphatic system that drains the waste products from the interstitium. On the other hand, tumour vasculature is characterized by a disorganized, non-hierarchical, tortuous and immature network of blood vessels, due to the incontrollable growth and overexpression of neoplastic cells and pro-angiogenic factors. In the same way, the lymphatic system is leaky and inefficient, compared to the one of the healthy tissues. Tumor vessels are thought to be more permeable than normal ones, they have irregular diameters, abnormal basement membranes and impaired blood flow. Tumour neovascularization⁴⁴ consists of different steps: degradation of the blood vessel membrane, migration of endothelial cells out of a pre-existing vessel, proliferation of endothelial cells, organization of the cells into tube-like structures. Angiogenesis-inhibiting agents have the capability to interfere in one or more steps of this process, such as inhibiting the proliferation and migration of endothelial cells (at concentrations that are 100-fold lower than those required to produce cell toxicity), targeting the vascular endothelial growth factor (VEGF) and its receptor (VEGFR), leading to the disruption of tumour vasculature. Furthermore, these compounds act also on the focal adhesions and adherens junctions of endothelial cells. Focal adhesions are adhesive contacts between

the cells and extracellular matrix, through the interaction of the integrins with their extracellular ligands⁴⁵. In endothelial cells, microtubule-targeting agents cause decreased focal adhesion formation and defective focal adhesion assembly. Adherens junctions in endothelial cells are intercellular protein structures that maintain endothelial integrity and, consequently, regulate vasculature permeability⁴⁶. They both regulate adhesion between cells and support the local concentration of signaling molecules. VE-cadherins are the main components of the endothelial adherens junctions. Microtubule-destabilizing agents are known to disrupt VE-cadherin engagement, leading to rounding up of endothelial cells and to an increased vasculature permeability.

1.3.2 Mechanisms of resistance

In order to develop more efficient compounds, it is extremely important to understand the mechanisms of resistance to tubulin-targeting drugs⁴⁷. Some tumour cells do not respond to microtubule-binding agents, such as renal cell carcinomas, which are thought to have microtubule-independent trafficking of key oncogenic proteins. Cancer cells possess several types of mechanisms of resistance to tubulin-targeting compounds. One of the most important mechanisms through which cells overcome the effects of microtubule-targeting chemotherapeutic agents is their resistance to enter the apoptotic pathway. The inhibition of proteins with anti-apoptotic effect may therefore improve the effect of anti-microtubule drugs. There are two types of resistance to anticancer drugs: the “intrinsic” resistance is the one that tumour cells have without the exposure to anticancer drugs and it may be caused by factors such as genetic mutation and tumour microenvironment. The “acquired resistance”, on the other hand, is not an intrinsic feature of the tumour, but it is generated by high exposure to cytotoxic drugs. The most investigated mechanisms of resistance with known clinical significance are:

- Activation of transmembrane proteins effluxing the chemical compounds in and out of the cells (ABC transporters);
- Activation of the enzymes of the glutathione detoxification system;
- Alterations of the genes and the proteins involved into the modulation of apoptosis (p53 and Bcl-2);
- Mutations and overexpression of specific tubulin isotypes.

1.3.2.1 ABC transporters

The main resistance mechanism is constituted by the ATP binding cassette (ABC) membrane transporters, which modulate the flux of substances, including drugs, in and out of the cells, by using energy produced by the hydrolysis of ATP⁴⁸. It was calculated that there are 49 ABCs and they are classified into seven subfamilies (ABCA-ABCG), according to the similarity of their amino acid sequences. They are potent transmembrane regulatory proteins and their presence modulates the drug concentration inside the cells. An overexpression of ABCs, linked to gene amplification, transcriptional and epigenetic changes, can lead to multi-drug resistance in cancer (MDR), the phenomenon in which cancer cells show resistance to various anticancer drugs, structurally and functionally different⁴⁹. Having the role of catalyzing the ATP-dependent transport of diverse compounds across cellular membranes, ABC transporters are vital elements for the cells in the protection against chemicals which are present in the environment. For this reason, people possessing defected ABC genes have higher vulnerability to specific diseases⁵⁰. The ABCs are composed of two domains, the first is the cytosolic nucleotide (ATP) binding domain (NBD) and the second is the transmembrane domain (TMD). Each NBD contains three main elements: Walker-A, Walker-B, and C or ABC signature motifs. The Walker-A and Walker-B are separated by 120 amino acids, while the third motif, the C, is unique for each ABC and it is critical for the interactions between the Walker-A and the Walker-B, that form the “ATP-sandwich” and allow the ATP hydrolysis. The TMD spans the membrane, produces channels and determines the characteristics of the transported substrates. Furthermore, some ABCs co-transport several substances at the same time: this fact provides evidence that there must be two binding sites with different affinities in each ABCs pump, responsible for the co-transport. One of the most famous ABC transporters is P-glycoprotein (P-gp), belonging to the ABCB family. Up to now, P-gp has been proven to interact with more than 200 compounds, both substrates and modulators. In fact, it possesses a large flexible drug-binding pocket characterized by low specificity. This feature can be used to develop inhibitors/modulators, capable of binding and blocking the transport function of the transporter, reversing the multi-drug resistance⁵¹. In fact, P-gp can be inhibited in three main ways. The first is by blocking of the drug binding site competitively, non competitively or allosterically, the second is by interfering with ATP hydrolysis and the third is by altering the integrity of the cell membrane lipids⁵². Depending on their specificity, affinity and toxicity, P-gp modulators

can be classified in three generations. Examples of the first generation P-gp inhibitors are Verapamil, which could overcome drug resistance in leukemia cells, but caused harmful side effects, Cyclosporine A, Reserpine, Quinidine, Yohimbine, Tamoxifen and Toremifena. Due to their potential toxicity, their non-selective and low binding affinity, they were replaced by a second generation of inhibitors, which were optimized to be more potent, specific and less toxic. Examples are Dexverapamil, Valspodar, Dexniguldipine and Dofequidar fumarate. They possessed greater affinity for P-gp, but they caused the inhibition of more ABC transporters, leading to complicating pharmacokinetic alterations. For this reason, third generation inhibitors are under clinical trials and show higher specificity and lower toxicity than the previous ones. Examples include Cyclopropyldibenzosuberane zosuquidar, Laniquidar, Mitotane, Biricodar, Elacridar, ONT-093, Tariquidar and HM30181. They are very potent, around 200-fold more effective than the previous inhibitors and they can be used at very low concentrations (25-80 nM). Even natural compounds, such as plant extracts, have been studied for their ability to inhibit P-gp, exhibiting less cytotoxicity and better bioavailability. Another possible approach would be to use monoclonal antibodies⁵³, such as MRK16, MRK17, C219, JSB-1, HYB-241, UIC2, 4E3, 7G4, 17F9 and Mab57, against P-gp in multi drug resistance⁵⁴. MRK16 and MRK17 were first proven to inhibit the growth of human multi drug resistant tumours transplanted into nude mice. MRK16 enhanced the antibody-dependent cellular cytotoxicity and induced regression of the resistant tumour when administered after the tumour became palpable. Also MRK17 showed direct inhibition of tumour grown in vitro, but its efficacy and activity were inferior than the ones of MRK16. Monoclonal antibodies, especially used in conjugation with P-gp reversing agents, can offer efficient anti-cancer activity.

1.3.2.2 Glutathione detoxification system

Besides the ABC transporters, the second mechanism involved in multi-drug resistance is constituted by glutathione and its associated enzymes. Glutathione (GSH) and glutathione S-transferases (GST) have been widely investigated and linked to the existence of a multi-drug resistance in cancer cells. It has been demonstrated that GSTs are important determinant of drug response for some (but not all) anticancer drugs⁵⁵. Like P-glycoprotein, GST-mediated detoxification system is able to recognize various chemical compounds and to mediate their transports in and out of the cells. In particular,

GSH and its associated enzymes have the fundamental role to protect the cells: GSH is the most abundant antioxidant found in living organisms and it is also the most abundant non-protein thiol present in the cells. When GSH binds to a compound, either spontaneously or catalyzed by GST, it has the capability to make that compound less toxic and more hydrophilic, which means that it makes it more easily cleared from the body. In fact, the metabolism of drugs is composed of two main phases: phase I, where P-450 isozyme family makes small changes to the drugs (for example, by producing reactive sites which can covalently interact with other molecules) and phase II, cytoprotective, where GST isozyme family makes the drugs more hydrophilic and less toxic. GSH has various functions in the cells, including preserving cellular redox homeostasis. By both detoxifying the body from xenobiotics and promoting therapeutic resistance in cancer cells, it plays both beneficial and pathogenic roles in various diseases⁵⁶. In cells, metabolic processes such as respiration and oxidative stress are linked to the formation of reactive oxygen species (ROS)⁵⁷, whose level increases with any kind of fluctuation in environmental stress factors. They include superoxide, hydrogen peroxide, nitric oxide, peroxynitrite, hypochlorous acid and hydroxyl radical⁵⁸. ROS can be very harmful to cells and they may be associated with DNA damage that leads to different diseases, dysfunctions and ageing processes. Glutathione may provide defence not only against ROS, but also against their toxic products. In particular, GSH provides a first line of defence against ROS, by scavenging free radicals and reducing H₂O₂. By contrast, glutathione-dependent enzymes represent a second line of defense, by detoxifying the products generated by ROS and preventing the propagation of free radicals⁵⁹. ROS production is dramatically higher in cancer cells because of the particular microenvironment characteristics, such as mitochondrial dysfunction, genetic mutations and abnormal metabolism. For this reason, cancer cells take advantage of various ROS-scavenging molecules, such as glutathione, which act as detoxifying agents. In particular, GSH is responsible for detoxification of xenobiotics, maturation of iron-sulfur clusters of proteins, maintenance of cysteine pools and regulation of transcription factors linked to redox signaling. In cancer initiation and progression, GSH and ROS play a dual role, having both a tumour promoting and a tumour suppressing functions⁶⁰: firstly, moderate ROS levels can stimulate the survival and proliferation of tumour cells by activating signaling pathways that help the cancer to grow in stressful environment. However, high levels of ROS, which are often found in cancer, can cause damage to the cells, provoking cell death. Therefore, tumours have the necessity to modulate ROS and antioxidants (such

as GSH), maintaining a balance in order to survive. GSH is vital in the removal of carcinogens and alterations of GSH levels may have profound effects on cell survival. However, elevated levels of GSH are involved in the protection of tumour cells, by conferring resistance to several chemotherapeutic drugs. Furthermore, elevated levels of GSH have been demonstrated to promote metastasis in both melanoma and liver cancer. The complexes formed by GSH-GST-drug obtained are effluxed out of the cell through multiple resistance-associated protein transporters (MRP1). In fact, drug-resistant tumours are often characterized by high levels of GST and MRP1. Therefore, even though GSH provides a first line of defence against ROS and glutathione-dependent enzymes provide a second line of defence, it has been demonstrated that GST and MRP are both required to be balanced and co-ordinately regulated in order to be able to protect the cells against the ROS. In fact, an overexpression of GST alone, without an increased capacity to transport conjugates out of the cells, would not be sufficient to produce resistance to oxidative and chemical stress⁶¹. Reversal of drug resistance may be achieved by the use of molecules capable of inhibiting GSTs, due to the overexpression and accumulation of specific GSTs in different cancers. For this reason, various compounds characterized by this ability have been discovered and others have been synthesized⁶². Most of these compounds are GST substrates or GSH analogues and they help to overcome drug resistance in different ways.

1.3.2.3 p53 and Bcl-2 proteins

p53 protein is constituted by 393 amino acids and characterized by a molecular weight of 53 kDa. p53 gene (the “guardian of genome”) is a tumour suppressor gene⁶³, which has the function to block the formation of tumours. Mutations in p53 gene leads to the complex network of events characterizing the formation of a tumour and it can be linked to various cancer types: p53 is known to be mutated in approximately 50% of human cancers⁶⁴. In particular, p53 protein, located in the nucleus of cells throughout the body, works by binding DNA, which in turn promotes the production of a protein, p21, that interacts with cdk2, a cell-division-stimulating protein. When p21 and cdk2 are bound, the cell cannot go through the next stage of cell division. On the other hand, if p53 is not able to target the DNA, the protein p21 is not produced and it does not provide the “stop signal” for cell division, leading to an uncontrollable proliferation of cells and formation of tumours. Increase of p53 levels has three main functions: growth arrest, DNA repair

and apoptosis. In fact, as a result of DNA damage, in order to preserve the integrity of the germ line, p53 protein has the capability to trigger programmed cell death, a permanent cell-cycle-arrest response to harm⁶⁵. On the other hand, under condition of low-level stress and reparable damage, p53 protein can respond with protective and pro-survival measures, temporary cell-cycle arrest, antioxidants production and DNA repair, in order to maintain the viability of cells. For this reason, the concentration of p53 must be precisely regulated. The main regulator is MDM2, which is able to stimulate the degradation of p53 via the ubiquitin system. Therefore, protein p53 constantly undergoes processes of production and degradation. After cellular stress stimuli, such as DNA damage, MDM2's activity is decreased, leading to p53 stabilization. The resulting enhancement of p53 activity leads to an upregulation of MDM2 activity, which, in turn, determines the degradation of p53, in a continuous loop (MDM2 downregulates p53 and p53 upregulates MDM2). If the p53 gene is altered or damaged (and, consequently, the conformation of p53 protein is changed), for example by the actions of chemicals, radiations or viruses, the balance between p53 and MDM2 is altered too and the tumour suppression is exponentially reduced, leading to uncontrollable division of cells⁶⁶. Furthermore, overexpression of mutated p53, which can lead to the loss of p53 functions, has often been linked to resistance to standard medications⁶⁷. Tumour cells hosting wild-type p53 are usually sensitive to antitumour drugs, but they become resistant to therapy when wild-type p53 is inactivated⁶⁸. As already highlighted, p53 protein is able to mediate apoptosis⁶⁹: in particular, the protein is responsible for both transcription-dependent and transcription-independent apoptosis. The first one is characterized by an extrinsic and an intrinsic pathways. In the extrinsic pathway, p53 promotes the transcription of death receptors of the tumour necrosis factor receptor family, leading to the formation of death-inducing signaling complexes which stimulate DNA fragmentation. The intrinsic pathway, on the other hand, is represented by DNA damage mechanisms which involve mitochondrial apoptotic events, coordinated by the Bcl-2 family of proteins. p53 activates the pro-apoptotic genes Noxa, PUMA, Bid and Bax, which can homo-multimerize or hetero-multimerize with Bak, leading to DNA fragmentation. In the transcription-independent mechanism, instead, p53 protein reaches the mitochondria and interacts directly with the anti-apoptotic protein BCL-2, in order to stimulate the homo or hetero-multimerization of Bak and Bax, which change conformation, form oligomers and permeabilize the mitochondrial outer membrane (MOMP)⁷⁰. In this way, p53 allows the release of pro-apoptotic factors inside the cytoplasm. The Bcl-2 (B-cell lymphoma-2)

family of proteins has been widely studied and owes its importance to the modulation of the apoptotic response, tumorigenesis and cellular responses to anti-cancer therapy⁷¹. It is constituted by anti-apoptotic proteins (BCL-2, BCL-X_L, BCL-W, MCL-1, BFL-1/A1), pro-apoptotic proteins pore-formers (BAX, BAK, BOK), also known as effectors, and pro-apoptotic BH3-only proteins (BAD, BID, BIK, BIM, BMF, HRK, NOXA, PUMA, etc), also known as activators, which interact with one another⁷². In fact, the proteins (for example, Bax and Bak), as already mentioned above, can aggregate to form homo or heterocomplexes⁷³. These proteins are characterized by various domains: the first two domains, BH-1 and BH-2, are necessary for BCL-2 and BCL-X_L to interact with Bax and Bak, in order to inhibit apoptosis. The third domain, BH-3, is sufficient but not required for the pro-apoptotic proteins, such as Bax, Bak or Bad, in order to bind BCL-2 or BCL-X_L and trigger apoptosis. The last domain, BH-4, is responsible for conferring the anti-apoptotic capacity. In fact, mutated BCL-2 proteins, which lack their BH-4 domain, lose their anti-apoptotic effect and behave like killer proteins. This provides evidence of a competition model for apoptotic regulation: the ratio of anti-apoptotic to pro-apoptotic molecules, such as BCL-2:Bax, determines the cell response to apoptotic signal. Defects and mutations in the mitochondrial apoptotic pathway are strongly linked to the development of diseases, such as cancer and autoimmunity⁷⁴. Overexpression of anti-apoptotic BCL-2 proteins and loss of some of the pro-apoptotic proteins accelerate tumorigenesis, by keeping cells alive long enough to acquire oncogenic mutations that drive their neoplastic progression⁷⁵. It is well known that a hallmark of cancer cells is their ability to ignore and evade apoptosis and this ability is fundamental for the uncontrollable growth of cancer and for the development of resistance to therapy. Therefore, tumour cells may become dependent on BCL-2 anti-apoptotic activity for survival under stressful conditions, overexpressing the protein, which sequesters and disactivates the pro-apoptotic activity of the activators and effectors. This overexpression of anti-apoptotic BCL-2 family member in cancer cells confers the ability to resist to various classes of anticancer drugs, such as DNA-damaging and antimicrotubule agents, glucocorticoids, nucleoside analogues and immunotherapy⁷⁶. As highlighted in this paragraph, the activity of BCL-2 anti-apoptotic proteins and the mutations of p53 proteins are regarded as an obstacle in cancer therapy, due to their ability to confer chemotherapeutic resistance. Therefore, a wide range of small molecules targeting Bcl-2 family members and mutant p53 have been investigated and developed, in order to reverse the resistance. By using small molecules that are able to bind to mutated p53, restore its

active form and its tumour suppression function, it is possible to induce apoptosis again. One of the most effective ways for improving cancer therapy is the ablation of mutant p53 in cancer, by promoting its degradation. The second strategy for targeting mutant p53 is to restore the mutant p53 to a wild-type resembling conformation. Furthermore, BCL-2 inhibition has been demonstrated to be a promising strategy for improving cancer treatments⁷⁷. Possible compounds used to inhibit BCL-2 proteins are oligonucleotides, antibodies, peptides or small molecule inhibitors⁷⁷. One of the most appealing alternatives is constituted by the use of BH-3 domain-mimicking peptides, due to the small size and the high binding affinity. In fact, mimicking the BH-3 domain, they are able to bind with high specificity the hydrophobic region present on anti-apoptotic BCL-2 proteins, working as competitive inhibitors⁷⁸, and induce apoptosis. However, the hydrophobic groove of the anti-apoptotic proteins to which the BH-3 domain binds is very challenging to target⁷⁹ and it is of vital importance to find compounds able to bind BCL-2 family members with high affinity, as the BH-3 domain-mimicking peptides do. An alternative would be to target the regulation of another anti-apoptotic protein, MCL-1, which has been proven to be easier than developing an effective BH-3 mimetic⁸⁰. MCL-1 is essential for the development and survival of acute myelogenous leukemia cells. This is the reason why selective MCL-1 inhibitors have been investigated with great interest. Furthermore, some anti-cancer drugs, such as anti-tubulin compounds, are able to reduce the levels of MCL-1, promoting apoptosis⁸¹.

1.3.2.4 Mutations and overexpressions of tubulin isotypes

Another contribution to the resistance to MTAs is given by alterations in the target of these compounds, the tubulin-microtubule complex⁴⁷. Three are the main mechanisms investigated: the first is the overexpression of specific tubulin isotypes, in particular of β -III tubulin, a multifunctional protein characterized by a key role in the pathobiology and aggressiveness of the tumour; the second is the occurrence of tubulin mutations that can influence the microtubule stability and dynamics; and the third is the development of tubulin mutations that lead to impaired ligand binding⁸². In fact, as stated above, tubulin heterogeneity, caused by the existence of different tubulin isotypes and post-translational modifications, contributes to microtubule diversity. In many studies^{83,84}, it has been demonstrated that enhanced levels of β -III tubulin are linked to reduced response to taxanes and some vinca alkaloids in a variety of tumours, such as lung, breast, ovarian

and gastric cancer. In particular, the presence of this tubulin isotype has been proven to inhibit the drugs' ability to affect microtubules dynamics. Furthermore, microtubules composed of the β -III tubulin isotypes show more dynamicity than the microtubules formed by the β -II or β -IV isotypes. This provides evidence that the different compositions of tubulin isotypes can modulate the dynamicity of microtubules. Considering the fundamental role that microtubules play in cells, any modification in the expression levels of the tubulin isotypes can alter the overall microtubule function. In particular, there are two main reasons for the introduction of different tubulin isotypes into the protofilament: first, as already mentioned, alterations in the structured core of the tubulin isotypes can affect the physical properties, the assembly kinetics and the stability of microtubules; second, modifications in the sequence of the C-terminal tail, which is one of the preferential binding sites for a variety of MAPs, can alter the interactions between MAPs and the microtubules. β -III tubulin is not only involved in drug resistance, but it also thought to act as a survival factor in many tumours, by increasing the development and progression of cancer, regardless of the treatment. Its potential role as survival factor is demonstrated by the fact that β -III tubulin levels are augmented in conditions of stress like hypoxia, glucose deprivation and ischaemic necrosis, where the protein is overexpressed. Therefore, it protects the cells against genotoxic stress caused by cytotoxic compounds. In this way, when targeted and suppressed, it makes cells more vulnerable to chemotherapy, both of MTAs and DNA-damaging agents, via enhanced apoptosis induction and reduced tumorigenesis⁸⁵. That is the reason why the design of drugs and compounds which target specifically β -III tubulin would be an effective strategy to fight cancer and overcome the multi-drug resistance that many tumours possess. Apart from the overexpression of certain tubulin isotypes, alterations in tubulin-binding sites or microtubule dynamics may play a vital role in the mechanism of resistance to taxanes and vinca alkaloids, leading to an intrinsic insensitivity to antimetabolic drugs. Microtubule-polymer levels and dynamics, tubulin protein folding, tubulin dimer sequestration and regulatory pathways are mainly regulated by factors that are likely to affect sensitivity to microtubule-targeting agents, such as post-translational modifications of tubulin and regulatory proteins like microtubule-associated protein 2 (MAP2), tau, γ -actin, MAP4, stathmin, MAP6 and survivin⁸⁶. These proteins are able to bind to microtubules and their increased expression is linked to resistance or enhanced sensitivity to microtubules-targeting agents. Other factors, such as tumour microenvironment and signalling proteins, are responsible for the modulation of microtubule stability.

Transforming growth factor- β induced (TGFBI) can stimulate microtubule stabilization and make cancer cells more vulnerable to paclitaxel and its suppression can induce resistance to paclitaxel. As far as the tumour microenvironment is concerned, further investigation is needed in order to fully understand its influence on the mechanisms of action of MTAs and microtubule dynamics. Tubulin molecules are also subjected to several post-translational modifications, which are responsible for the modulation of the rate of assembly into microtubules: alterations in the PTMs of microtubules have been observed in many types of cancer. Furthermore, it is possible that PTMs could alter the interaction with MAPs, regulating microtubule dynamics and leading to drug resistance. Another important line of defence of cancer cells is their capability to “camouflage” the target, the microtubules, so that MTAs cannot recognize and bind them anymore⁸⁷. Some of the mutations acquired after exposure to taxanes or epothilones are found in the taxane binding site and they influence drug binding through differences in Van der Waals or hydrophobic interactions. Also mutations within the β -tubulin genes have been observed in cell lines resistant to microtubule-targeting agents⁸⁸, but they are not thought to result in changes to drug binding affinity.

1.3.3 Main classes of microtubule-targeting agents

Microtubule-targeting agents are unique among the anti-cancer compounds, not only because of their original mechanisms of action, but also because of their extreme structural diversity.

1.3.3.1 Vinca domain-binding agents

Vinca alkaloids, such as vincristine, vinblastine, vindesine and vinorelbine, discovered in the 1950's by Canadian scientists, Robert Noble and Charles Beer⁸⁹, are the oldest of the clinically used anti-tubulin agents and they belong to the family of microtubule-destabilizing agents. They are drugs extracted from the pink periwinkle plant *Catharanthus roseus* and they possess cytotoxic and hypoglycemic effects. They have been investigated and used for the treatment of diabetes, high blood pressure and cancer and they have been into the clinic for 40 years. At the beginning, they were considered “wonder drugs”, due to their chemotherapeutic success in childhood leukaemia. In fact, they became popular as single-agent treatment of childhood haematological and solid malignancies and then for adult haematological malignancies too. Tubulin and

microtubules are the main targets of the vinca alkaloids, which depolymerize microtubules and destroy mitotic spindles at high concentrations, inhibiting the microtubule dynamics and leaving the dividing cancer cells blocked in the mitosis with condensed chromosomes. Initial studies^{90,91} on the biochemical effects of vinca alkaloids revealed disruption of microtubules and elevated oxidised glutathione, whereas they demonstrated to have no influence on cellular respiration, glycolysis, nucleic acid or protein synthesis. Furthermore, their hydrophobic nature allows them to partition into lipid bilayers⁹² when uncharged, leading to alteration in the structure and function of cellular membranes. They usually bind to a region known as vinca-binding domain, at the inter-dimer interface between two longitudinally aligned tubulin dimers⁹³, in a rapid and reversible way. In particular, vinca alkaloids have two distinct binding sites on microtubules: they bind with high affinity to tubulin at the microtubule ends, but with low affinity to tubulin along the sides of microtubule surface⁹⁴. Furthermore, they possess the ability to enhance the affinity of tubulin for themselves, leading to the production of spiral aggregates. The vinca site is composed of a core zone, defined by interactions of vinca alkaloids, and a pocket which extends towards the exchangeable guanosine nucleotide site on β -tubulin. The suppression of the microtubule dynamics has two effects on the spindles: it prevents the correct assembly of the mitotic spindles and it reduces the tension at the kinetochores of the chromosomes. The transition from metaphase into anaphase is blocked and the cells die by apoptosis. Examples of this class of compounds are vinblastine, vinorelbine, vincristine, vindesine, vinflunine, dolastatins, maytansine, halichondrin B, spongistatin-1, Rhizoxin⁹⁵. Usually, the vinca alkaloids are administered via intravenous bolus, but they can also be administered for prolonged periods of time, as longer infusion, leading, however, to worse side effects. Different agents possess various dose limiting toxicities: vincristine is neurotoxic, vinblastine is myelosuppressive, vindesine is both neurotoxic and myelosuppressive. Vinorelbine is the best tolerated, showing granulocytopenia and leucopenia as harmful consequences. Moreover, it was the first to be administered orally, showing the same pharmacokinetic profile of the IV administration. In conclusion, vinca alkaloids are anti-cancer drugs that cause microtubule depolymerization, suppress treadmilling and dynamic instability, inhibit mitotic progression and lead to cell death by apoptosis. However, their harmful side effects limit their applications. In order to overcome the limitations and drawbacks that characterize the majority of these compounds, drug delivery systems and combination therapy are smart and appealing solutions that have been investigated in the last years⁹⁶.

1.3.3.2 Taxol domain-binding agents

Taxanes, such as paclitaxel (Taxol), docetaxel (Taxotere) and cabazitaxel (Jevtana), were among the most investigated anti-cancer compounds during the last century and they belong to the family of microtubule-stabilizing agents, also known as depolymerizing inhibitors⁹⁷. In 1995, their clinical use was approved and since then, they have been successfully adopted for the treatment of solid tumours, both as single agents and in combination with other chemotherapeutic or targeted agents. The taxanes possess low binding affinity to soluble tubulin, but high affinity to tubulin assembled into microtubules. They bind in a region called taxane-site, which is located in a pocket of β -subunit, precisely on the inside surface of the microtubule and the compounds form both hydrophobic and polar interactions with several of the secondary structural elements⁹⁸. Paclitaxel generally gains access to its binding sites by diffusing through small openings in the microtubule. The conjugation between these compounds and the microtubules leads to stabilization of the microtubules, increased polymerization and suppression of their dynamics, causing cell cycle arrest in the G₂/M phase and apoptosis. Examples of this group of compounds are paclitaxel, docetaxel, cabazitaxel, epothilones, ixabepilone, dictyostatin, eleutherobin, cyclostreptin and zampanolide. As with vinca alkaloids, researchers have focused their attention on improving formulations and investigating smart drug delivery systems⁹⁹ and combination therapies, in order to overcome the limitations imposed by the previously described compounds. One of the most used and investigated drug delivery systems for the transport of a taxane is nab-paclitaxel[®], albumin-based nanoparticles encapsulating paclitaxel, which will be discussed in details later.

1.3.3.3 Colchicine domain-binding agents

Colchicine is an ancient compound, a major alkaloid isolated in 1820 from the seeds and bulbs of *Colchicum autumnale* and *Gloriosa superba*, that has exhibited a wide range of therapeutic

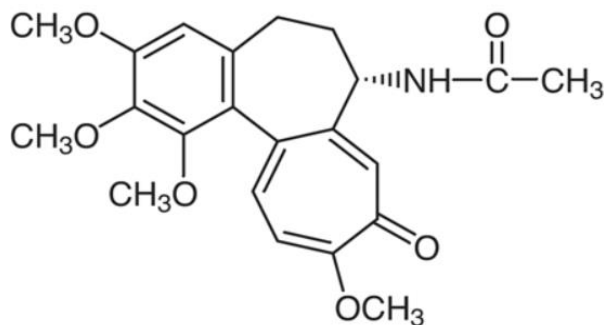


Figure 3: Chemical structure of colchicine.

effects¹⁰⁰. Its summary formula is $C_{22}H_{25}NO_6$ and its molecular weight is 399.44. The main structure of the compound is composed of three rings¹⁰¹ (Figure 3). The ring A is a trimethoxy benzene ring, that is essential for tubulin affinity in conjunction with ring C and fundamental for anti-tubulin activity¹⁰². The 1-methoxy group is important in setting the correct conformation of the molecule, whereas the 3-methoxy group is important for binding ability: replacing it with bulky groups results in great reduction of the affinity. The ring B is a seven-membered ring characterized by an acetamido group at C7 position, which may influence the conformation of colchicine analogues and their tubulin binding properties like the on-rate, off-rate, activation energy reversibility and quantum yield of the drug-tubulin complex. Therefore, modification on ring B is aimed at modulating the kinetic properties of the compounds. It has been proven that the introduction of a double bond in ring B enhances the binding ability with tubulin. The ring C is a methoxy tropolone ring, crucial for colchicine-tubulin interactions. It can be affected by photochemical decomposition, transforming into a fused four or five-membered ring having carbonyl and methoxy substituents and reducing its binding ability. Methoxy and carbonyl group can exchange positions, producing isocolchicine and the 10-methoxy group can be substituted with halogen, alkyl, alkoxy or amino groups without altering the tubulin binding affinity. Moreover, modifications of the seven-membered tropolone into aromatic phenol does not influence the affinity with tubulin. In fact, allocolchicine is also a tubulin inhibitor. The ring A and C of colchicine are thought to bind to β -tubulin, whereas the side chain of ring B interacts with α -tubulin¹⁰³. It is popular for the treatment of various inflammatory diseases and gout disease, a common type of arthritis that causes intense pain, swelling and stiffness in a joint. It has also been used to treat Behcet's disease, dermatitis herpetiformis, pericarditis, biliary and hepatic cirrhosis, Paget's disease, familial Mediterranean fever and amyloidosis¹⁰⁴. In fact, in 2009 it was FDA approved for the treatment of gout and Mediterranean fever. More recent studies investigated its antiproliferative activity and antimetabolic effect, related to the formation of a colchicine-tubulin complex, which prevents microtubule polymerization, due to a conformational inflexibility that makes tubulin dimers unable to lead to microtubule assembly, by inhibiting the elongation of microtubules. Cancer cells are more effectively killed by colchicine than the normal cells, since they undergo mitosis at higher rates, but this compound is characterized by low therapeutic index and high toxicity, including neutropenia, gastrointestinal upset, bone marrow damage and anaemia¹⁰⁵. That is the reason why various colchicine analogues have been produced. Although colchicine has

been used as a therapeutic agent for years, its mechanism of action remained unknown until 1968, when tubulin was recognized as its main target¹⁰⁶. In 2004, colchicine-binding site was identified as a deep pocket located at the interface of the α - β tubulin heterodimer, whereas the principal interaction zone is located on the β subunit. Colchicine interacts with tubulin through hydrogen bonding and hydrophobic interactions. The binding of colchicine to tubulin causes important structural changes within the tubulin subunits, shifting from a straight to a curved conformation, which prevents the tubulin dimer assembly into microtubules, inducing their depolymerization. Furthermore, in the 1930s, colchicine was found to have damaging effects on tumour vasculature¹⁰⁷, causing haemorrhage and extensive necrosis in both animal and human tumours. Colchicine domain-binding agents can prevent new blood vessels formation by outgrowth from pre-existing ones (angiogenesis inhibitors) or destroy the existing tumour vasculature (vasculature disrupting agents). Another advantage of this family of compounds is that most of these drugs have no multi-drug resistance issues. As already highlighted, one of the major limitations of the application of microtubule-targeting agents is the innate and acquired drug resistance, due to the presence of P-glycoprotein, mutations in tubulin and overexpression of β III-tubulin isoform, which is an indicator of resistance to microtubule-targeting agents, such as paclitaxel and vinorelbine. Therefore, some colchicine domain-binding agents were identified as appealing anti-tumour agents due to their ability to overcome P-gp/ β III-tubulin mediated drug resistance and their anti-vascular effect. Furthermore, they possess chemically-modifiable structures, providing the possibility to improve pharmacokinetics properties, efficacy and reduce toxicity of the pre-existing compounds. In fact, researchers developed some colchicine derivatives¹⁰⁸, able to overcome further the P-gp-mediated resistance and to maintain similar level of cytotoxic activity in cancer cells¹⁰⁹. In order to do it, they introduced modifications on B and C rings and evaluated the compounds obtained. It is known that colchicine interacts with P-gp through hydrophobic interactions, causing conformational changes in the transmembrane helical domains and enhancing the transport of other ligands as well as colchicine itself. In order to reduce the P-gp efflux liability, polar substituents were introduced to decrease the hydrophobic interactions. In particular, the addition of amino groups at C-10 position showed increased cytotoxicity, no P-gp efflux due to the loss of hydrophobic interactions and gain of hydrogen bindings and ionic interactions, increased expression of pro-apoptotic protein p21, good pharmacokinetic profile and excellent physicochemical properties (solubility and lipophilicity). Therefore, the derivatives were

even less vulnerable to the efflux of the hydrophobic transmembrane domain of P-gp, compared to colchicine¹¹⁰. For all these reasons, colchicine-site ligands are probably the most studied class of microtubule-targeting agents. Since the first atomic investigation of colchicine-binding to tubulin in 2004, a wide range of structurally diverse natural and synthetic colchicine-site ligands in complex with tubulin have been characterized by X-ray crystallography to medium and high resolution. A variety of colchicine-binding site drugs are natural products, obtained from natural sources such as plants, animals and microorganisms, which constitute excellent sources for drug discovery and development. Through chemical modifications of their structures, some derivatives and synthetic analogues of these natural compounds have been produced in the lab. Another way to overcome the limitations imposed by the side effects and cytotoxicity of colchicine is to use smart drug delivery systems. In fact, colchicine is known to have low therapeutic index and poor oral bioavailability. At first, colchicine was usually administered through the oral route, but it was associated with gastrointestinal side effects, such as abdominal cramps and pain, nausea, vomiting and diarrhea, in the 80% of patients. Colchicine was also administered through intravenous route, but it caused severe side effects like tissue necrosis, cytopenias, intravascular coagulation and even death. For this reason, in 2008, the intravenous route was banned by the FDA. One of the greatest limitations of the colchicine-binding site agents is their high hydrophobicity, which results in the reduced absorption of the drug. Moreover, the rapid elimination can lead to short biological half-life and need for frequent drug used, and non-specific drug distribution lowers the drug levels at the site of action and enhances the harmful side effects. To overcome these issues, two possible solutions have been found: the use of chemical modifications of the compounds (creation of prodrugs) and the use of advanced drug delivery systems. The prodrug may possess a better solubility, absorption, improved stability and it may convert to the parent drug at the site of action. Carriers to transport the drugs may increase the solubility, increase or reduce drug dissolution, increase permeability and absorption, reduce drug elimination by increasing the biological half-life and reduce the off-target drug distribution. Table 1 shows the principal colchicine drug delivery systems that have been investigated so far to improve its therapeutic efficiency.

Table 1: Summary of the nano-delivery systems of colchicine.

Formulation	Size/MW	Route of administration	<i>In vitro</i> / <i>In vivo</i> results	References
Gelatin biodegradable microspheres, crosslinked with glutaraldehyde	70-300 μm	Intravascular delivery	Zero-order release observed for the entrapped anticancer drug. Diffusion of the drug from the matrix, followed by slow degradation of the matrix. Cytotoxicity on MCF-7 breast cancer cell line depended on the compositions of the microspheres. Sustained release of colchicine from gelatin microspheres exhibited a prolonged and higher cytotoxic effect in the MCF-7 breast cancer cell-line, compared to the free drug.	[111]
Niosomes	-	-	The release rate of the drug from niosomes was evaluated <i>in vitro</i> and it was much slower, compared to the one of the free drug. After 12 hours, 64% of colchicine was released from the free solution, compared to only 12% from the niosomes.	[112]
Thermoresponsive poly(<i>N</i>-isopropylacrylamide) co-polymer films	-	Local delivery vehicle to vascular smooth muscle (intravascular delivery)	It was demonstrated that the drug was taken up by BASMC and could target its intracellular site of action. The cellular uptake was maximal by 24 hours. The colchicine released was able to inhibit proliferation and migration of BASMC.	[113]
Poly(phosphazenes)	1.1-1.8 x 10 ⁶	Intra-articular administration (local delivery to joints)	Release of colchicine was consistent with the degradation of the polymers. The faster the degradation, the faster the release rate. Release occurred through degradation and diffusion. <i>In vitro</i> dose-response studies measuring osteoblast cell growth showed that cell growth on matrices containing colchicine was significantly inhibited in contrast to growth on tissue culture polystyrene (TCPS) and EG-PPHOS matrix without drug.	[114]
PEG-coated biodegradable poly(lactic acid)/poly(ϵ-caprolactone) microspheres	3-6 μm	Local delivery vehicle to vascular smooth muscle (intravascular delivery)	Zero-order <i>in vitro</i> release profile of colchicine. Large local concentration of drug in the target tissue, with least systemic side effects. The studies suggested that inhibition of restenosis was dose-dependent. Release follows a diffusion-based model through pores, rather than a polymer erosion-based model. Release of	[115]

			the drug was sustained over four weeks <i>in vitro</i> .	
Eugenol-based nanoemulsion	41.2 ± 7.2 nm	Oral delivery	The transport of colchicine across a rat intestinal membrane was studied <i>in vitro</i> with a diffusion chamber. The intestinal absorption of colchicine was enhanced significantly by eugenol in the tested nanoemulsion. Furthermore, the effect of eugenol on the absorption of colchicine was examined by <i>in vivo</i> absorption studies. The results showed an increase in the AUC and C _{max} of colchicine after oral administration.	[116]
Theranostic oil-core PLA nanocapsules	200 nm	Intravascular delivery	Approximately constant release rate of the drug observed <i>in vitro</i> . The results of the <i>in vitro</i> experiments revealed that the free Cou-6 was less effectively taken up by all the studied cells, in comparison to the encapsulated dye molecules. Moreover, free dye molecules could also be absorbed <i>in vivo</i> by healthy cells surrounding the target tissue. For this reason, encapsulation of fluorescent markers offers much advantage. In all the tested cancer cell lines, the nanoencapsulation process enhanced the antitumour activity of colchicine.	[117]
Elastic liposomes	100-200 nm	Transdermal delivery	The <i>in vitro</i> skin permeation studies conducted on excised rat abdominal skin showed 10.2-fold higher flux of drug from elastic liposomal formulation, compared to free drug. <i>In vivo</i> performance aimed at evaluating the anti-gout efficacy of the compound. Edema, a typical feature of inflammation, was measured in terms of exudate volumes and the results obtained from elastic liposomes showed 5-fold higher reduction in terms of exudate volumes and leukocytes present.	[118]
Transethosomal gels	85.4-169.9 nm	Transdermal delivery	The <i>ex vivo</i> skin permeation studies revealed that the transethosomal gels had superior skin permeation properties in comparison with a simple colchicine gel formula, due to the presence of ethanol, phospholipids and surfactants, which worked in synergy to improve the permeation of colchicine through the skin.	[119]

Lipid bilayer-coated mesoporous silica nanoparticles	100 nm	Intravascular delivery	The <i>in vitro</i> experiments strongly demonstrated the potential of the formulation as drug delivery system and its stability. After 120 min, the delivery of colchicine through the lipid bilayer into HuH7 liver cancer cells was achieved and the microtubule filaments could hardly be recognized.	[120]
Folic acid and chitosan-glycine complex coated mesoporous silica nanoparticles functionalized with phosphonate groups	330 ± 22.2 nm	Intravascular delivery	The <i>in vitro</i> experiments showed that anticancer activity depended on the cell line and delivery method. Full inhibition of HCT116 colon cancer cells was observed. A weaker activity was reported in HepG2 liver and PC3 prostate cancer cells. This formulation showed almost no cytotoxicity in healthy cells, compared to free colchicine. The nanoparticles conferred higher apoptotic activity than the free drug.	[121]
Cubosomes	35.6 ± 3.09 – 328.2 ± 7.92 nm	Transdermal delivery	<i>Ex vivo</i> permeation studies conducted on animal skin models demonstrated that after 24 hours, the amounts of drug deposited in the skin were 2-fold higher if released from the cubosomes, compared to the free drug. <i>In vivo</i> absorption study showed that C_{max} of the drug after oral administration was much lower than C_{max} observed after transdermal delivery from the cubosomes, indicating slower release.	[122]
Colchicine-gadolinium tubulin nanoparticles	45 nm	Intravascular delivery	The <i>in vitro</i> experiments showed that the formulation had specific killing effect on tumour cells rather than on normal cells. The nanoparticles exhibited excellent MRI contrast capability and long circulation time (12 hours). The effect of the nanoparticles on growth of tumours was explored using GL261 subcutaneous tumour-bearing mice model and they showed a prolonged circulation time, useful for the passive targeting.	[123]

Another smart carrier for the delivery of colchicine would be albumin, the most abundant protein in plasma, which is known for its capability to transport both hydrophobic and hydrophilic compounds. The interaction between colchicine and human serum albumin was investigated by fluorescence and UV-vis absorption spectroscopy. The results

exhibited the formation of colchicine-HSA complexes, where Van der Waals interactions and hydrogen bonds played a vital role in the stability of the complex¹²⁴. In particular, the binding site for colchicine on human serum albumin is located in sub-domain IIA (Trp²¹⁴). However, there are still no formulations based on albumin-colchicine complexes on the market.

1.4 Novel derivatives and CCI-001

As highlighted above, there are many drugs and compounds in the market that target microtubules for the treatment of cancer. However, they often lack specificity, they are characterized by harmful side effects or they have to face chemotherapeutic resistance. Colchicine has been investigated and studied in detail, primarily for the treatment of gout, but also to treat

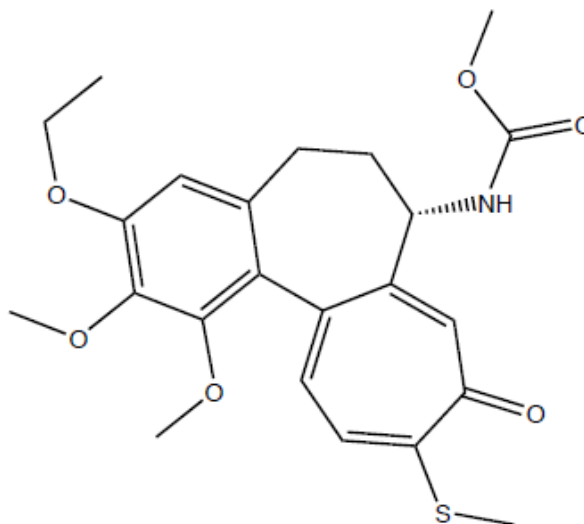


Figure 4: Chemical structure of CCI-001.

conditions such as leukemia, prostate cancer, Behcet's disease, acute and recurrent pericarditis, heart diseases, atrial fibrillation and diabetic nephropathy. However, its applications have been limited by a high toxicity profile and a low therapeutic index¹²⁵. In fact, colchicine, when administered at low doses, causes cardiac and renal toxicity and gastrointestinal side effects, and, when administered at high doses, it causes systemic toxicity and high mortality rate. In order to overcome the existing limitations, Dr Jack Tuszynski and his co-workers (Allard Chair, Division of Experimental Oncology, Cross Cancer Institute and University of Alberta, Edmonton, Canada) designed and synthesized CCI-001, also known as CR-42-024, JD-101, D33 or Compound 24, a novel colchicine derivative characterized by reduced general toxicity and increased cancer specificity and selectivity, in order to target the desired site in a more precise way¹²⁶. CCI-001 (C₂₃H₂₇NO₆S, molecular weight: 445.5, Figure 4) possesses an increased binding affinity for the β -III tubulin isotype, which is an excellent target since it is overexpressed in many cancer cells, almost absent in healthy cells and constitutes a clinical marker of poor prognosis. CCI-001's LogP is of 2.58 and its solubility in water at pH=7.4 is of 0.007

mg/mL¹²⁷. Researchers initially focused their attention on colchicine, which was known to bind to β -tubulin, generating tubulin-colchicine complexes and inhibit microtubule dynamics, showing anti-proliferative and anti-neoplastic properties. The harmful side effects and toxicities of colchicine are due to the fact that its primary target is the β -IV tubulin isotype, which is highly expressed in healthy cells. Therefore, it is not the most suitable isotype for the specific targeting of cancer. β -III tubulin, on the other hand, would be the most promising target, since it is highly expressed in a variety of tumours, such as breast, ovarian and gastric cancer. It is always present in the most aggressive and metastatic cancer cells, it is overexpressed in taxol resistant tumours, it is not found in normal tissues and if silenced, it makes cancer cells more vulnerable to chemotherapy. The reason why β -III tubulin binds poorly to drugs, compared to the other isotypes, has been investigated and studied, in particular in the case of colchicine. Colchicine, as already stated, interacts with tubulin in two steps: firstly, there is the binding, and secondly, as a consequence of the binding, the tubulin molecule undergoes a conformational change. In β -III tubulin, the second step is slower, since it possesses a much more rigid conformation than the other isotypes¹²⁸. Many colchicine derivatives have been evaluated during the past 7 years and Dr Tuszynski and co-workers, having understood the potential of β -III tubulin as a target, have tried to synthesize β -III tubulin-specific colchicine derivatives, which offer higher tumour specificity and selectivity, without causing harm to healthy tissues. Among the identified agents that demonstrated to possess an improved capability to kill cancer cells, the compound CCI-001 proved to have increased cytotoxic effects in cancer cells, reduced side effects on normal cells and increased binding affinity for β -III tubulin, compared to colchicine. For these reasons, it was proposed as a new and appealing candidate drug for preclinical and clinical development, and its efficacy and synergistic activity with other chemotherapeutics were demonstrated using *in vitro* and *in vivo* assays. In particular, 70 compounds were synthesized in two series, CH and CR-42, and their efficacy and cytotoxicity were evaluated both *in vitro* and *in vivo*. The colchicine derivatives with bulkier hydrocarbon groups at the R2 position have been proven to be the most potent, characterized by smaller IC₅₀s. The most effective ones were: CH-35, CR-42-017, CR-42-018, CR-42-023 and CCI-001. Of the first series, CH-35 showed to be more effective than Taxol against human breast tumour and, furthermore, was more specific towards β III-tubulin isotype. Compared to colchicine, it showed higher toxicity to cancer cells and lower toxicity to healthy cells. Of the second series, the only ones that resulted to be patentable were CR-

42-023 and CCI-001, and the latter was superior in terms of ADMET profile. Therefore, CCI-001 was considered to be the lead compound, on which specific experiments have been performed. First, the binding free energies for different tubulin isotypes were predicted through high-quality computational models at University of Alberta, Edmonton, AB (2011-2012). The compound was then successfully synthesized, with 95% purity. The cytotoxicity of the lead compound was evaluated, through MTS and MTT assays to evaluate the cytotoxic effects on various cancer cell lines and healthy cell lines, revealing much higher efficacy than the parent compound, colchicine. CCI-001 was active on bladder, colorectal, skin, breast, pancreatic and kidney cancer cells with IC₅₀ values in the nanomolar range (0.8-10 nM) on every cell line tested¹²⁹. It was most potent on the prostate cell line LnCap with an IC₅₀ of 0.9 nM and least potent on the metastatic kidney cancer cell line Caki-1 with an IC₅₀ of 10.5 nM. It was more effective than paclitaxel, with the exception of 786-0 kidney cancer cell line and it was only marginally cytotoxic to healthy GM38 fibroblast cells. It had higher efficacy on every cell line, compared to gemcitabine. In particular, it was proven to be effective against the T24 bladder cancer cell line, constituting a successful therapy for this disease. In order to confirm this evidence, CCI-001 was tested on a panel of bladder cancer cell lines (T24, 253J, UM-UC-3, UM-UC-14) and its activity was compared to gemcitabine and cisplatin. Dr Tuszynski's lead compound showed higher performance than both single agents gemcitabine and cisplatin and combination gemcitabine/cisplatin treatment. Furthermore, it had low nanomolar IC₅₀ values, ranging from 10 nM to 1.9 nM. CCI-001 has the same mechanism of action of colchicine, acting by inducing microtubules depolymerization and G₂/M phase arrest, leading cells to death. Cells treated with the lead compound showed a strong reduction in cell migration and, in particular, CCI-001 exhibited a variety of advantages: it inhibited migration in primary endothelial cells, leading to anti-metastatic action, it selectively induced cytotoxicity in rapidly dividing cells and it caused anti-angiogenic effects in mouse models. After having demonstrated its efficacy *in vitro*, CCI-001 activity was examined also *in vivo* on bladder cancer. T24 xenografted mice were administered both CR42-024 (3 mg/kg or 6 mg/kg) and vehicle control every second day for 18 days (10 injections, Figure 5). The lead compound was able to suppress tumour growth of T24 xenografts *in vivo*, without any excessive toxicities, evaluated by measuring the change in body weight and was able to prevent tumour growth at a dose of 3 mg/kg. Furthermore, CCI-001 was also tested on a patient-derived xenograft model and

it was demonstrated the compound had the ability to treat larger tumours *in vivo*, making it a useful compound for the treatment of bladder cancer¹²⁶.

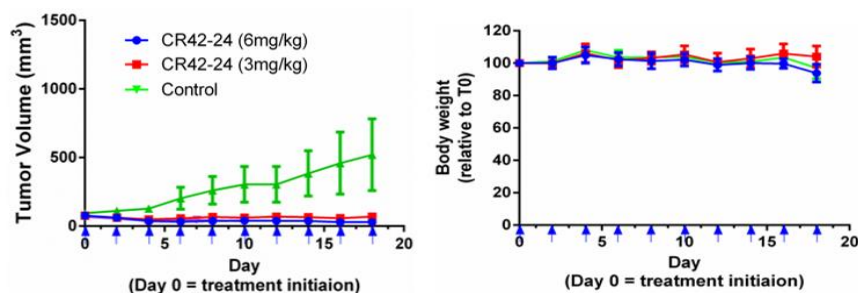


Figure 5: Comparison between the activity of control, CCI-001 (6 mg/kg) and CCI-001 (3 mg/kg) on T24 cell line xenografts *in vivo*. From ref [126] with permission.

Moreover, the activity of CR42-024 was also compared to the combination of gemcitabine/cisplatin¹²⁶. In particular, mice bearing T24 xenografts were administered CR42-024 (3 mg/kg), gemcitabine/cisplatin (40 and 3 mg/kg respectively) and vehicle control (10.5% DMSO in PBS), as shown in Figure 6. The results showed that CCI-001 had the same effect as gemcitabine/cisplatin and was able to inhibit the tumour growth. No significant difference in tumour volume was reported between CCI-001 and the combination gemcitabine/cisplatin, whereas there was a significant difference between control and CCI-001 and between control and gemcitabine/cisplatin. The mice were weighed once a week during the administration of the drugs and no toxicity was reported, suggesting that a dose of 3 mg/kg of lead compound did not lead to toxicity in mice.

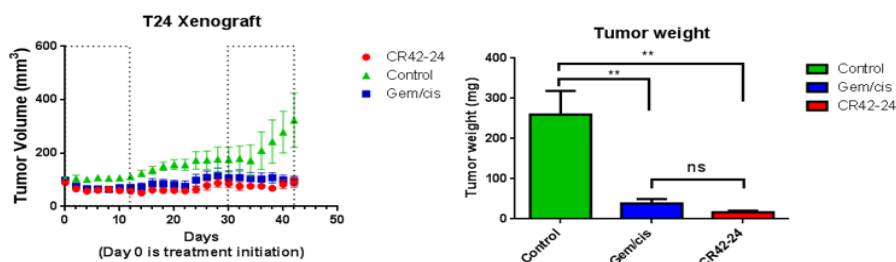


Figure 6: Comparison between the activity of CCI-001 and gemcitabine/cisplatin on T24 xenografts *in vivo*. From ref [126] with permission.

CCI-001 was then tested and compared with all the other major microtubules-targeting agents, such as paclitaxel, vinblastine, combretastatin, laulimalide and taccalonolide, in

order to evaluate its effects on taxol-resistant breast cancer cells. The lead compound was more potent and effective, but cell viability was still present at high concentrations. In fact, paclitaxel-resistant cell lines were found to be around 6-fold more resistant to CCI-001, most likely due to P-gp activity. In order to overcome this limitation, a combination of CCI-001 and 3-bromo pyruvate (3BP) was tested and showed successful results. The effects of the combination of the two compounds (2 nM CCI-001 and 20 μ M 3BP) were observed on breast cancer cell lines, such as SK-BR-3 and paclitaxel-resistant SK-BR-3, and exhibited promising synergistic activity. The viability of the SK-BR-3 cells was 14.8% when CCI-001 alone was used, whereas it decreased to 6.1% when the combination of CCI-001 and 3BP was used. The viability of the paclitaxel-resistant SK-BR-3 cells was 27.9% when CCI-001 was used, whereas it decreased to 2.1% when the combination of the two compounds was used. This fact provides evidence that the synergy of CCI-001 and 3BP could constitute a promising solution, especially if applied with a time delay, with 3BP preceding the administration of the lead compound by 3 hours.

It has been shown that CCI-001 is a weak substrate for P-glycoprotein, in fact it interacts with the protein many times less compared to the parent compound colchicine, and this fact could contribute to drug resistance in a cell line-dependent manner. In the studies conducted on different cell lines, PC3, U87 and CAPAN-1 were found to be insensitive to CCI-001 and these cell lines were thought to possess increased expression of MDR-1, conferring resistance to the lead compound. When incubated with both CCI-001 and cyclosporine A, which is a competitive inhibitor of MDR-1, Hela and UM-UC-14 cells became much more sensitive to CCI-001 killing, exhibiting a much more rapid reduction in cell viability when the lead compound was combined with CyA, as compared to CCI-001 alone. On the other hand, CAPAN-1 and PC3 cells incubated with CyA did not become more vulnerable to the drug. Therefore, it is possible to conclude that the resistance to the chemotherapeutic is most likely cell line-dependent and there are other mechanisms of resistance that may be responsible for the insensitivity to CCI-001 as well. Researchers have also examined whether CCI-001 could be used in combination with current therapies for bladder cancer, such as gemcitabine and cisplatin and to do so, they tested the drugs in a sequential manner. The results reported that the lead compound was synergistic with both cisplatin and gemcitabine when given sequentially. In particular, synergy was observed when cells were pre-treated with CCI-001 and followed by cisplatin, and when they were pre-treated with gemcitabine and followed with CCI-001.

On the other hand, pre-treatment with CCI-001 followed by gemcitabine did not show synergy and pre-treating the cells did not make them more sensitive to gemcitabine, compared to non-pre-treated cells. In the same way, cells pre-treated with cisplatin and followed by CCI-001 did not show synergy either. Therefore, the lead compound can successfully be used in combination with other chemotherapeutics, but the synergy is only observed if the administration occurs in a specific sequential manner. Furthermore, it was demonstrated that high concentrations of colchicine and its derivatives permeabilize cell membranes, which may contribute to the still unknown cytotoxic effects of these compounds. CCI-001 was also demonstrated to possess less negative side effects on the immune systems of cancer patients, compared to colchicine. To summarize, various experiments conducted *in vitro* and *in vivo* has demonstrated that CCI-001 could constitute a new promising and appealing alternative to the chemotherapeutic approach for the treatment of cancer. In fact, the compound is not only highly effective against a variety of cancers in general, but also against those ones that are resistant to standard therapies. Moreover, CCI-001's synergy with other agents make it even more interesting for a broad spectrum treatment of bladder cancer. The limitations imposed by the poor water solubility of the compound can be overcome by the use of drug delivery systems. Up to now, the only formulation in the market is the micellar formulation¹³⁰ of CCI-001. The micelles were prepared by solvent evaporation method, using PEO-PBCL in acetone. The size of the micelles was of 58.01 ± 0.2829 nm and the PDI was 0.16 ± 0.014 . The encapsulation efficiency of the drug was 94.5%.

1.5 Albumin

1.5.1 Characteristics and features of albumin

Albumin is one of the most abundant proteins in blood plasma, constituting approximately 60% of all the proteins in the blood (around 35-50 mg/mL)¹³¹. It is a highly water-soluble small globular protein, characterized by a molecular weight of 67 kDa and an average half-life of 19 days. Albumin has a pI in the range of 4.7-5.5. It shows stability for a pH range of 4-9 and it can be heated for 10

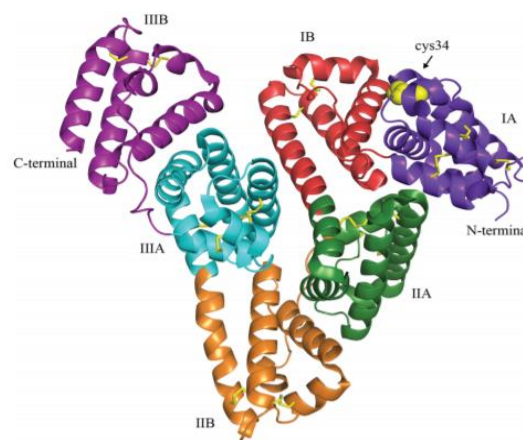


Figure 7: Structure of albumin. From ref [131] with permission.

hours at 60°C. It is made of a single chain of 585 amino acids; its secondary structure, highly flexible, is characterized by 67% α helix and there are 17 disulphide bridges with 6 turns. The disulphide bridges act as crosslinkers for the three homologous domains that characterize albumin (domains I, II, III) and each one of the three domains is comprised of a pair of subdomains (A,B)¹³², as Figure 7 shows. IA is composed of the amino acids 1-112, IB by amino acids 113-195, IIA by amino acids 196-303, IIB by amino acids 304-383, IIIA by amino acids 384-500 and IIIB by amino acids 501-582. Albumin can be extracted from many sources including human serum (human serum albumin, HSA), bovine serum (bovine serum albumin, BSA), rat serum (rat serum albumin, RSA) and egg white (ovalbumin, OVA), but the two most used types are HSA and BSA. Albumin is a perfect candidate for drug delivery¹³³ and it has attracted attention for its characteristics and abilities, such as high loading capacities of both hydrophobic and hydrophilic drugs, specific targeting, as well as virtually non-toxicity and non-immunogenicity. It is biocompatible, biodegradable and it is a versatile carrier with great potential and applications. A huge number of different molecules can be encapsulated/entrapped inside the albumin vehicle in many different ways or they can be chemically conjugated to the protein. Moreover, the surface of albumin nanoparticles can also be functionalized with ligands due to the presence of functional groups to which different types of linkers or spacers can be attached. The high lipophilicity of many existing drugs represents one of the main limitations of their applications. Hence, finding a non-toxic, widely available

and efficient vehicle which is able to improve the solubilization and the transport of therapeutics is of fundamental importance. The most important albumin binding sites for hydrophobic compounds (especially neutrally and negatively-charged hydrophobic drugs) are domains IIA and IIIA, highly elongated hydrophobic pockets with positively-charged lysine and arginine residues¹³⁴. In this way, various therapeutics, such as paclitaxel and docetaxel, can be bound and subsequently delivered effectively to the tumour site.

1.5.1.1 Human serum albumin

Human serum albumin is a protein produced by hepatocytes in the liver, at a rate of 9-12 g/day¹³⁵. Despite albumin's plasmatic abundance, the majority of albumin is not found in blood circulation, since 60% is stored in the interstitial space. In fact, even though its half-life is of 17-19 days, it only lasts 16-18 hours in circulation¹³⁶. The transcapillary movement of albumin is reversible, as it can return inside the plasma through the lymphatics in order to maintain constant the plasma protein concentrations. Its production is modulated by the body's needs. In particular, the synthesis is stimulated by insulin, thyroxine and cortisol or conditions like hypoalbuminemia, whereas it is hindered by potassium and exposition of hepatocytes to excessive osmotic pressure. Furthermore, an adequate supply of nutrients is fundamental to correctly regulate albumin production. In fact, poor adsorption of nutrients reduces the liver's ability to produce the protein. Degradation of albumin can take place in any tissues, but it occurs mainly in the liver and kidney. The balance between albumin production, degradation and movement between intravascular and interstitial spaces determines the effective albumin plasma concentration. Albumin is responsible for the maintenance of the colloid osmotic pressure (which keeps fluid from leaking out of the blood vessels), nourishes tissues, transports hormones, vitamins, drugs and divalent cations, like calcium and zinc, through the body, acts as a free radical scavenger in inflammatory conditions and it is involved in processes like coagulation and wound healing¹³⁷. Furthermore, it possesses antioxidant properties and has a heparin-like activity, by enhancing the effects of antithrombin III: in fact, hypoalbuminemia can cause coagulopathy¹³⁸. The compounds that bind to albumin can be classified as endogenous and exogenous. The first class includes all the substances that are already found in the body, such as bilirubin, fatty acids, cations, free radicals, vitamins and hormones. The second one consists of the drugs that are introduced in the body from

the outside, such as antibiotics, anticoagulants, anti-inflammatory drugs, anticonvulsants, cardiovascular and renal drugs, central nervous system drugs and hypoglycemic agents¹³⁹. Albumin molecules carry many charged amino acid residues and have a net charge of -17 at physiological pH. For this reason, sodium ions, and other cations, are strongly attracted by it. As a consequence of sodium attraction to albumin, water is dragged into the blood vessels (1 gram of albumin can retain 18 ml of water within the blood vessels). When conditions interfere with its production by the liver, levels of albumin may decrease, protein breakdown may increase, the protein loss via the kidneys may be augmented and the volume of the liquid portion of blood (plasma) may be expanded, diluting the blood. Examples of the conditions that can alter albumin concentration are severe liver disease and kidney disease¹⁴⁰. In fact, since albumin is produced by the liver, a loss of liver function can provoke a decrease in the levels of albumin. One of the main roles of the kidneys is to maintain the plasma proteins, preventing them from being eliminated in urine with waste products. If the kidneys are damaged, for example in diabetes, hypertension or with nephrotic syndrome, they lose their ability to maintain the concentrations of the plasma proteins and levels of albumin decrease.

1.5.1.2 Serum albumin from other species

Bovine serum albumin is derived from bovine serum and it is very similar to HSA. Its molecular weight is 69.323 kDa and it has a pI of 4.7 in water (25°C), which makes it negatively charged at neutral pH and positively charged under acidic conditions¹⁴¹. The presence of both negatively charged and positively charged amino acids can result in the binding of both positively and negatively charged substances. Because it is widely available at low cost and easy to purify and control, it has been extensively used as a drug delivery carrier. Furthermore, it has high loading capability, it is water soluble and can bind both hydrophilic and hydrophobic drugs, making it a very versatile carrier. The only downside could be a possible immunogenic response *in vivo* in humans¹⁴², but also in mice¹⁴³. HSA and BSA share 80% sequence homology, their molecular weights differ by less than 1% and their isoelectric points are similar. One important difference is the number of tryptophan (Trp) residues. HSA has one Trp, whereas BSA has two. The advantage of HSA is that it is not recognized as a “foreign body” by the human organism since it is already present in our blood in high quantities, making it highly biocompatible, hence it will not be attacked and rejected by the immune system. That is the reason why

bovine serum albumin could be substituted by human serum albumin, in order to overcome these limitations. The antibody response to BSA exposure has been explored in animal models and this protein has been used as a model protein to investigate the immune response to proteins. In 2005, a quantitative radioimmunoassay was developed to measure anti-BSA IgG antibodies in healthy subjects and in cancer patients¹⁴⁴. Western blot analysis confirmed the presence of anti-BSA antibodies after human exposure to BSA, but elevated levels of anti-BSA antibodies were not associated with any clinical events in either healthy or cancer patients. In another study, bovine serum albumin was administered to three strains of rabbits¹⁴⁵. The results highlighted the fact that the immunogenicity of BSA varied considerably in the different strains of rabbits and that some rabbits even failed to respond to the stimulation. This lack of response may be genetic or related to the nature of the antigen. Furthermore, it was demonstrated that immunogenicity of BSA is linked to its molecular state. BSA can be present partly as a monomer and partly in aggregated form, which is able to induce an antibody response. Another fact to consider is that the non-immunogenicity of BSA in some rabbits might be due to its close similarity with rabbit serum albumin, which present some structural homologies with BSA. Ovalbumin (OVA) is the main protein found in the egg white, representing the 55% of the total protein contents¹⁴⁶. Its function is still unknown, but it is thought to be a storage protein. It belongs to the serpin family, it is a globular, acidic glycoprotein, characterized by a molecular weight of 42-47 kDa and it is composed by a single polypeptide chain of 386 amino acids¹⁴⁷. Its isoelectric point is of 4.8, similar to that of human and bovine serum albumins. However, OVA is often chosen as one of the most popular model antigen, due to its immunogenicity. Rat serum albumin (RSA) possesses 608 amino acids and has a different size than its homolog-human: it has a molecular weight of 69 kDa. Furthermore, its isoelectric point is of 5.7. Comparing the amino acid composition of RSA with that of HSA, the first presents more tyrosine and less lysine, cystine and leucine¹⁴⁸. However, it is much more immunogenic than the other types of albumin.

1.5.1.3 Roles of albumin in drug delivery

Albumin plays different roles and functions in improving the transport of therapeutics to the tumour, avoiding the healthy tissues. Firstly, it protects the drugs from being degraded before reaching the desired site of action and it allows them to selectively act in a specific

place (through active targeting). Secondly, it is the vehicle that permits the suspension of the hydrophobic drugs in the aqueous phase, making them able to be efficiently transported inside the blood. The drugs bind to the binding sites of albumin and this formulation allows to avoid the use of organic solvents or surfactants that would otherwise be needed. Lastly, albumin serves as the stabilizer. At physiological pH, albumin shows a negative zeta potential. This negative charge stabilizes the suspension because of the electrostatic repulsive forces between the nanoparticles during the formulation, preventing the formation of aggregates. Furthermore, albumin nanoparticles can be crosslinked or not. Crosslinked nanoparticles usually allow longer and more sustained release profiles, whereas the non-crosslinked ones can be quickly taken up by tumours. Albumin can bind drug molecules in two main ways¹⁴⁹, either by covalent or non-covalent bonding. As described before, the reversible non-covalent one is based on electrostatic/hydrophobic interactions (weaker than covalent bonding) between albumin and the compound and it is usually preferred because it allows the faster availability and release of the drug where and when needed. Since the structure of albumin is characterized by both hydrophobic and hydrophilic domains and abundant charged amino acids, it possesses the ability to load different payloads with different physiochemical properties by electrostatic or hydrophobic interactions. Drugs can also bind to albumin by covalent conjugations: they can directly link to albumin amino acid residues or *via* linker. In fact, albumin has lysine residues that can form an amide bond with the drug, or cysteine residues that can attach to a maleimide group. If a linker is used, it is possible to connect a drug to a linker with a maleimide group that can then be attached to the Cys-34 residue of albumin, allowing the covalent attachment of protein and cargo¹⁵⁰. Being complexed with albumin, both by physical and chemical bonds, the compounds are sterically protected from degradation and from renal clearance. In particular, the use of reversible, non-covalent binding with albumin allows for the promptly release of the therapeutic, promoting its interaction with the target site, its faster penetration and diffusion into regions that would not allow the entrance to larger molecules.

1.5.2 The unique properties of albumin in tumour targeting

1.5.2.1 Passive targeting

The enhanced permeation and retention (EPR) effect, characterized by the hyper-permeability of the tumour blood vessels and the impaired lymph drainage, has been

proposed as responsible for the passive targeting of many nano-carriers in cancer in solid tumours¹⁵¹. However, the defining role of EPR effect has been extensively questioned recently¹⁵². The reason for the importance of EPR effect lies in the belief that there is an anatomical difference between normal and tumoral tissues, responsible for the selective delivery of the therapeutics to the desired location. Although it constitutes a paradigm in cancer nanomedicine, Chan et al demonstrated that 97% of the nanoparticles are delivered into solid tumours by endothelial cells through an active process of transcytosis and that the interendothelial gaps, which characterize the EPR effect, are not responsible for the transport of nanoparticles into solid tumours, since the frequency of the gaps is too low to account for the accumulation of nanoparticles into tumours. Furthermore, the rate of leakage from the vessels is slow and there is the chance that the drug gets metabolized during the time it takes for the accumulation to reach therapeutic levels¹⁵³. Several studies, including a study from Japan¹⁵⁴, suggested the use of vascular mediators, such as nitric oxide (NO), which could augment vascular permeability via vasodilation, increasing the EPR effect to overcome problems of insufficient accumulation of drugs inside the tumour site. Nitric oxide has very short blood residence time and this creates a limitation for its usage. For this reason, a NO drug delivery system, S-nitrosated human serum albumin dimer (SNO-HSA dimer), which proved to deliver efficiently NO to the tumour site, was developed to overcome this limitation.

1.5.2.2 Active targeting and albumin receptors

One of the unique features that makes albumin such a versatile and interesting drug carrier is that it binds to receptors, which are overexpressed by tumours. This active targeting¹³ allows the drug to enter only the tumour cells, without heading towards healthy cells (where it could also be toxic and cause some deleterious side effects). The main pathway that albumin relies on for the internalization inside the tumours is the receptor-mediated endothelial transcytosis. Albumin binds with high affinity to the gp60 receptor, a 60 kDa glycoprotein (albodin)¹⁵⁵. This receptor is found on the surface of endothelial cells of the tumours and, after the interaction with albumin, it binds to caveolin-1, an intracellular protein which gives rise to an invagination of the cell membrane leading to the formation of transcytosis vesicles (caveolae) transporting albumin inside the tumour. Moreover, SPARC (secreted protein acidic rich in cysteine), also known as antiadhesin, osteonectin, BM-40 and 43K protein, which is overexpressed by many types of tumour and absent in

normal tissues, attracts albumin and contributes to its accumulation inside the tumour. These two main mechanisms allow the protein to be actively internalized in the cancer site. Among the albumin receptors, apart from gp60, there are also gp18 and gp30, which are cell surface glycoproteins characterized by molecular weight of 18 and 30 kDa, respectively¹⁵⁶. They are expressed in endothelial cell membranes of liver and peritoneal macrophages. They are scavenger receptors characterized by high affinity for damaged albumin. In fact, modified BSA shows 1000-fold higher tendency of interactions for gp18 and gp30, compared to native BSA¹³¹. These two receptors are involved in the endo-lysosomal sequestration and catabolism of this protein, probably as a safety mechanism to degrade old, damaged or altered albumin (for example, generated by oxidation from inflammation or hyperglycation in diabetes). On the other hand, native albumin does not have high affinity for gp18 and gp30 receptors, but binds mainly to the previously described gp60, which is involved in the transcytosis of albumin through the endothelium. Another receptor which takes part in albumin homeostasis is FcRn, the neonatal Fc receptor, also known as the Brambell receptor. It is a transmembrane heterodimeric protein, consisting of a MHC-class I-like heavy chain, characterized by three extracellular domains ($\alpha 1$, $\alpha 2$, $\alpha 3$), which is non-covalently associated to a β_2 -microglobulin light chain, necessary for the function of the receptor¹⁵⁷. It is found in many tissues including vascular endothelium, gut, lungs and kidney¹⁵⁸. This receptor can determine a different fate for albumin nanoparticles after internalization, playing a vital role in maintaining high levels of the protein. Usually, as already pointed out, HSA is non-immunogenic and it is not recognized as a foreign substance, but, if altered or damaged, it is immediately targeted by the immune system and degraded. However, the protein is well known for its prolonged half-time, which makes it a useful carrier in drug delivery. The exceptionally long half-life of albumin is due to the rescue from intracellular degradation by FcRn receptor, which recycles internalized albumin back to the blood stream through a pH-dependent mechanism¹⁵⁹. In conclusion, in drug delivery, it is gp60 that allows albumin to specifically target the cancer cells, since it mediates albumin-based drug delivery systems transport over two biological barrier, epithelial and endothelial, and it is overexpressed in cancer cells, functioning as a targetable molecule. Furthermore, SPARC, whose expression is associated with pathophysiological conditions that involve extracellular matrix remodelling, such as cancer and neo-angiogenesis processes, is used as a prognostic tool, and its high levels are linked to the efficacy of the albumin-based drug delivery systems in inhibiting cancer proliferation. An additional step to enhance

even more the targeting capability of albumin would be to functionalize (through covalent or non-covalent bonding) its surface with specific targeting agents, able to actively recognize the tumour (ligand-receptor interactions)¹⁶⁰. These molecules could include antibodies or fragments of antibodies, peptides, folic acid¹⁶¹ and also aptamers, which are short DNA or RNA structures characterized by better site specificity and less immunogenicity than antibodies¹⁶².

1.5.2.3 Stealth nanoparticles

Another useful modification of albumin nanoparticles involves the addition on the surface of the nanoparticles of polyethylene oxide (PEO) or polyethylene glycol (PEG), which are antifouling polymers able to make the particle “invisible” to the immune cells, such as macrophages. As stated above, every foreign body is recognized and eliminated by the immune system¹⁶³, so that it cannot reach the desired site of action. Therefore, it is of vital importance for the nanoparticle to be able to escape the immune system, prolonging their blood residence time and acquiring stability and longevity, so that they have the time needed to reach the tumour site without being phagocytized (constituting the so called “stealth nanoparticles”). It is important that the PEG chains cover the whole surface of the nanoparticle (high density) and it is preferable to have long chains. The PEGylation, which is the chemical coupling of polyethylene glycol (PEG) to the surface of nanoparticles, prolongs their circulation half-life, making them less immunogenic, promoting their accumulation in tumours and reducing their accumulation in the liver, by “escaping” the reticuloendothelial system (the RES usually removes nanoparticles from the circulation, preventing them to reach their target site). Furthermore, the PEGylation decreases the attraction between the nanoparticles, by augmenting the steric distance between them¹⁶⁴. Even though the use of PEG has various advantages, it still has some drawbacks that limit its applications. The toxicity of PEG is low, but sometimes it can be toxic with frequency inversely proportional to the molecular weight of the layer. PEG can be degraded by light, heat or sheer stress, leading to fragmentation of the layer. Alternatives to this polymer have been investigated, and they are mainly constituted by PEG hybrids, chitosan, dextran, polyvinyl pyrrolidone (PVP), polyvinyl alcohol (PVA) and polyacrylic acid (PAA).

1.5.3 ABI-007 (Abraxane[®])

Already introduced in the previous chapter, paclitaxel is an antimetabolic drug, belonging to the family of taxanes, which are microtubule-stabilizing agents. Paclitaxel summary formula is $C_{47}H_{51}NO_{14}$ and its molecular weight is of 853,91 g/mol¹⁶⁵. It is hydrophobic, and its melting temperature is 216-217°C. Its toxicity limits its applications: that is the reason why many drug delivery systems have been investigated. Nab-paclitaxel (Abraxane[®] for Injectable Suspension, ABI-007 manufactured by Abraxis Bioscience) is a formulation constituted by paclitaxel-loaded albumin nanoparticles, obtained through nab-technology¹⁶⁶. This technology was FDA approved in 2005 and it has been commercialized with the aim of increasing the efficiency and targeting while reducing the side effects due to the solvent-based formulations previously discussed. It is currently used for the treatment of metastatic breast cancer, non-small cell lung cancer, metastatic adenocarcinoma of the pancreas (in this case, combination of nab-paclitaxel with gemcitabine, an antimetabolite, shows optimal results), bladder cancer, gastric cancer (in Japan). The formulation is composed of three-dimensional nanoparticles (size of approximately 130 nm) of paclitaxel encapsulated, in an amorphous state, in human serum albumin, through non-covalent hydrophobic interactions. It is free of any toxic solvents/surfactants and its zeta potential is of -31 mV, which shows the stability in aqueous phase.

1.5.3.1 Advantages of ABI-007 over Taxol

It has already been outlined how important the vehicle of a formulation is and how much it influences the efficacy and the specificity of a drug delivery system. The Taxol formulation, using cremophor (hydrogenated castor oil) and ethanol as solvents to make the drug soluble and adaptable to intravenous injection, results in more side effects than advantages. CrEL-paclitaxel is responsible for hypersensitivity reactions and development of neuropathy¹⁶⁷. Therefore, its clinical use requires premedication with corticosteroids and antihistamines (even with the use of premedication, 40% of the patients still have minor reactions, such as flushing and rash, and 3% have life-threatening reactions)¹⁶⁸. To overcome these limitations, various solvent-free formulations such as liposomal encapsulated paclitaxel, paclitaxel-vitamin E emulsion and polymer microsphere formulation of paclitaxel have been investigated, but they had limited success. Instead, a successful outcome was obtained by nab-paclitaxel, which can be

injected, after being reconstituted in saline, at concentrations of 2-10 mg/mL, compared to the 0.3-1.2 mg/mL of CrEL-paclitaxel. For this reason, the volume and infusion time of CrEL-paclitaxel is higher (3-24h compared to 30 min for nab-paclitaxel), making the formulation time-consuming. The maximum tolerated dose for Taxol is 175 mg/m² whereas for nab-paclitaxel is 300 mg/m² for an every-3-weeks regimen, and it is 80 mg/m² for Taxol versus 150 mg/m² for nab-paclitaxel in a weekly regimen. Furthermore, conventional infusion equipment (PVC bags) cannot be used with CrEL-paclitaxel because of the danger of leaching plasticizers, bringing an enormous economic burden to the manufacturer¹⁶⁹. Nab-paclitaxel shows a distinct linear pharmacokinetics, characterized by rapid tissue distribution, increased distribution volume and a higher rate of clearance¹⁷⁰. Nab-paclitaxel resulted to be more effective than Taxol, with an IC₅₀ (in a hepatocellular carcinoma cell line) being 15-fold lower than that of paclitaxel alone¹⁷¹. The non-covalent bond between albumin and paclitaxel and the presence of the drug in a non-crystallized amorphous state allow the ready bioavailability of the drug to the target site. The cellular uptake is higher, because it mainly relies on endothelial transcytosis due to the presence of albumin¹⁷². At equal doses, intra-tumoral paclitaxel accumulation was found to be 33% higher for nab-paclitaxel. In human umbilical vascular endothelial cells (HUVEC), binding and transport across the endothelial layer was higher (respectively 9.9 and 4.2 fold) with nab-paclitaxel, but this difference was inhibited by methyl β -cyclodextrin, an inhibitor of the endothelial gp60 receptor and caveolar-mediated transport¹⁷³. A key factor is that the tumour itself requires albumin: the protein is highly accumulated in tumours and inflamed tissues, because it plays a vital role in their proliferation and sustainment, functioning as a nutrient source. On the other hand, Taxol showed nonlinear pharmacokinetics, slower tissue distribution, reduced activity and efficacy as well as increased toxicity. Overall, the preclinical and clinical studies conducted on Paclitaxel demonstrate that properties of the drug are widely influenced by the composition of the pharmaceutical preparation¹⁷⁴. To sum up the evidence, the potential advantages of Abraxane over Taxol are higher tolerated dose and greater efficacy, longer drug residence in the tumour as a result of nanoparticles formulation, reduced infusion time, reduced risk of hypersensitivity and no required premedication, more rapid distribution of Paclitaxel to the tissues based on pharmacokinetics data. Apart from paclitaxel, albumin was used as a carrier for many different compounds. Table 2 summarizes the existing drugs, other than paclitaxel, that are used in albumin-based formulations.

Table 2: Other drugs combined with HSA in albumin-based formulations.

Drug	Formulation	Binding strategy	Indication	Studies performed	References
Paclitaxel	1. PEGylated PTX-HSA NPs	1. Physical encapsulation	Metastatic breast cancer, non-small lung cancer, pancreatic cancer, gastric cancer	1. <i>In vitro</i> and <i>in vivo</i> 2. <i>In vitro</i> 3. <i>In vitro</i> and <i>in vivo</i> 4. <i>In vitro</i> and <i>in vivo</i> 5. <i>In vitro</i> and <i>in vivo</i> 6. <i>In vitro</i> and <i>in vivo</i>	[13,165,175,176,177,178,179,180]
	2. PTX/HSA NPs encapsulated in PEGylated liposomes containing Curcumin	2. Physical encapsulation			
	3. Co-loaded PTX-Pirarubicin HSA NPs	3. Physical encapsulation			
	4. CREKA and LyP-1-decorated PTX/HSA NPs	4. Physical encapsulation and chemical conjugation with peptide on the surface of NPs			
	5. Trastuzumab-decorated PTX/HSA NPs	5. Physical encapsulation with chemical conjugation with antibody			
	6. PTX/HSAF (albumin fragments) NPs	6. Physical encapsulation			
Docetaxel	1. DTX-HSA NPs	1. Physical encapsulation	Non-small cell lung cancer, gastric, breast, pancreatic and ovarian cancers	1. <i>In vitro</i> and <i>in vivo</i> 2. <i>In vitro</i> and <i>in vivo</i>	[181,182,163,183,184,185]
	2. DTX-HSA + quercetin NPs	2. Nanoparticle			
	3. Biotin-decorated DTX-BSA	3. Physical encapsulation with chemical conjugation with biotin on the surface			
Doxorubicin	1. DOX-HSA NPs	1. Physical encapsulation	Breast cancer, soft-tissue sarcomas, esophageal carcinomas and osteosarcoma	1. <i>In vitro</i> and <i>in vivo</i> 2. <i>In vitro</i> and <i>in vivo</i> 3. <i>In vitro</i>	[186,187,188,189,190,191,192,193,194,]
	2. PEI-coated DOX-HSA NPs	2. Nanoparticle			
	3. Co-loaded DOX and Curcumin NPs	3. Physical encapsulation			
	4. Co-loaded DOX and Cyclopamine NPs	4. Physical encapsulation			
Cabazitaxel	Jevtana	Physical encapsulation	Metastatic castration-resistant prostate cancer	<i>In vitro</i> and <i>in vivo</i>	[195,196,197]
All-trans-retinoic acid	HA-decorated cationic ATRA-loaded HSA NPs	Physical encapsulation	Targeting of cancer stem cells	<i>In vitro</i> and <i>in vivo</i>	[198,199,200]
Methotrexate	1. MTX-HSA	1. Covalent conjugates	Breast cancer, lung cancer, lymphoma, leukemia, inflammatory conditions, autoimmune disorders	1. <i>In vitro</i> and <i>in vivo</i> 2. <i>In vitro</i> 3. <i>In vitro</i> and <i>in vivo</i> 4. <i>In vitro</i>	[201,202,203,204,205,206,207,208,209]
	2. LHRH-decorated MTX-HSA	2. Covalent conjugates			
	3. Biotin-decorated MTX-HSA	3. Covalent conjugates			
	4. Transtuzumab-decorated MTX-HSA	4. Covalent conjugates			
Atorvastatin	Atorvastatin calcium-loaded HSA NPs	Physical encapsulation	Decrease cholesterol level and prevent	<i>In vitro</i>	[210]

			cardiovascular diseases		
Kolliphor HS15 + THP	THP-HSA complexes	Physical encapsulation	Antimetastasis activity	<i>In vitro</i> and <i>in vivo</i>	[211]
Ruxolitinib	Ruxolitinib-HSA complexes	Physical encapsulation	Philadelphia-negative myeloproliferative neoplasms	<i>In vitro</i>	[212,213]
Natural products (Piceatannol)	PIC-HSA NPs	Physical encapsulation	Colorectal cancer	<i>In vitro</i> and <i>in vivo</i>	[214,215]

1.5.4 Albumin: more than a carrier for anticancer drugs

Albumin has acquired great importance as a drug delivery carrier for drugs in the treatment of cancer, but it can also mediate the transport of drugs for the treatment of different diseases. For example, some types of diseases that have seen the use of albumin as a carrier are type II diabetes, postherpetic neuralgia, neutropenia, haemophilia B and A, chronic hepatitis C, cocaine addiction and inflammatory diseases, bacterial infections and rheumatoid arthritis. Table 3 provides a summary of the existing albumin-based formulations used in the treatment of diseases, other than cancer.

Table 3: Albumin-based formulations in other diseases.

Disease	Formulation	Active therapeutic ingredient	Preparation strategy	References
Diabetes	1. Albiglutide 2. CYC-1134-PC 3. Victoza 4. CJC-1131	1. DDP-IV-resistant GLP-1 2. Exedin-4 3. Liraglutide 4. DDP-IV-resistant GLP-1(7-36)	1. Fusion protein 2. Covalent 3. Non-covalent 4. Covalent	[216,217,218,219,220,221,222]
Postherpetic neuralgia	CJC-1008	Modified Dyn A	Covalent	[223]
Neutropenia	Balugrastim	G-CSF	Fusion protein	[224,225]
Haemophilia B	rIX-FP	Factor IX	Fusion protein	[226,227]
Haemophilia A	rVIIa-FP	Factor VIIa	Fusion protein	[228]

Chronic hepatitis C	Albuferon	Interferon alpha2b	Fusion protein	[229]
Cocaine toxicity	1. AlbuBChE 2. HSA-fused CocH1 protein	1. C-terminus CocH1 2. N-terminus CocH1	1. Fusion protein 2. Fusion protein	[230]
Inflammatory conditions	-	Acetyldiflunisal	Non covalent	[231,232]
HIV-1	PC-1505	Maleimido-C34 analogue	Covalent	[233,234]
Bacterial infections	1. – 2. RH01 (Safety Technology)	1. Lysostaphin 2. Myr FARKALRQ	1. Protein fusion 2. Non covalent	[235,236]
Rheumatoid arthritis	1. ALX-0061 2. ATN-013	1. IL-6R 2. TNF- α inhibitor	3. Nanobody 4. Nanobody	[237]

1.5.5 Future perspectives

The great potential of albumin has been widely demonstrated by various studies *in vitro* and *in vivo*. While gp60 and SPARC have been proven to play a vital role in the active internalization of the protein inside tumours and inflamed tissues, more studies on the involvement of gp30 and gp18 and their interactions with albumin nano-vectors need to be performed, in order to investigate in depth their specific roles and to understand how receptors influence albumin-based therapeutic at cancer sites. Furthermore, it is important to clarify how binding of ligands to albumin affects receptor binding. The methods of preparation of albumin and their mechanisms of loading should be analysed further and the differences in the usage of different crosslinking agents should be discussed more. It would be equally important to examine the biological impact that albumin-based formulations have on the whole organism. It is known that tumours are able to trap plasma proteins and use their degradation products for proliferation and development²³⁸. In fact, albumin nanoparticles take advantage of the active targeting to enter and accumulate in the solid tumours and the inflamed joints, which have a strong “desire” for albumin, an essential protein for the sustainment and growth of the tumours. As in cancer patients, people affected by rheumatoid arthritis often develop hypoalbuminemia²³⁹, caused by the high albumin consumption in the sites of inflammation. It would be interesting to investigate the long-term effects on the whole organism of albumin accumulation. A deep understanding of the intracellular pathways and of the effects of albumin distribution

would be an important requirement for optimizing the existing drug delivery approaches and for further development of albumin-based therapeutics in drug delivery. Moreover, studies conducted on mice bearing syngeneic ovarian and mammary carcinomas suggested that nab-paclitaxel acts as a radiosensitizer, improving the effect of radiotherapy if used in combination with radiation (in particular, if administered before radiation)²⁴⁰. In contrast to the strong enhancement of tumour radioresponse, there was a complete lack of modification of healthy tissue radioresponse. Therefore, nab-paclitaxel showed antitumor effect when administered as a single agent and it enhanced the antitumor activity of radiotherapy in a supra-additive manner. Its efficacy in increasing therapeutic gain of radiotherapy is an interesting feature that could be investigated further in the future.

2 Aim of the work

This chapter describes the aim and purpose of the research project (unluckily reduced in time due to the covid19) which consisted in the investigation, realization and characterization of a drug-loaded albumin-based formulation. In particular, the formulation consisted of CCI-001 (colchicine derivative)-loaded albumin nanoparticles, and this specific carrier was chosen to improve the solubility of the drug, its stability, its release, the cellular uptake and toxicity, while reducing its side effects.

The purpose of this study was to develop a smart and efficient drug delivery system to improve the characteristics, reduce the side effects, protect from degradation and help the transport of the β -tubulin polymerization inhibitor, CCI-001 (one of the colchicine derivatives synthesized and patented in the Department of Oncology, University of Alberta, Edmonton, Canada) in its path towards the target site, the tumour. Already used in free form and in micellar formulation, this extremely potent compound had never been used with other drug delivery systems, such as proteins. Therefore, there was the need to find other valid alternatives for its transport inside the body. The necessity for drug delivery systems to carry it comes from the need to reduce the toxicity of the compound, which could also affect healthy cells. For this reason, albumin has been used to potentially protect the drug during the transportation, to prolong its blood residence time, to improve the specificity and selectivity of the drug and to reduce the off-target side effects. Furthermore, the main advantages that make albumin unique are the fact that this protein is found inside the body, as one of the most abundant proteins in blood plasma, and it is naturally able to provide both passive and active targeting, without the use of external ligands, since it is recognized by receptors, such as gp60, overexpressed in tumours. That is the reason why researchers at Department of Oncology, University of Alberta, thought about trying to design an albumin-based formulation for their compound. As stated above, CCI-001 has already been extensively tested against numerous cancer cell lines providing very encouraging results, and its IC_{50} resulted to be very low (in the concentration range of nM) compared to other anti-cancer agents used for the same purposes, which makes it an even more appealing candidate for the treatment of various types of cancer. Albumin had already been used as a carrier for many compounds and drugs, especially lipophilic drug, for its high ability to interact with hydrophobic compounds through a particular pocket in its structure. This way, the protein allows the transportation in the blood

circulation of these compounds, which otherwise, due to their poor water solubility, would not be able to travel in the systemic circulation and would require the use of organic solvents, such as cremophor EL or tween 80, that could cause severe hypersensitivity reactions. Therefore, it can constitute a possible solution to the problems raised by the solvent-based formulations. Taxol[®] (Cremophor-ethanol based paclitaxel) and Taxotere[®] (Polysorbate 80-ethanol based docetaxel) have shown acute toxicity, including neuropathy, and hypersensitivity reactions. These formulations require the administration of premedication to prevent the deleterious side effects and, as a consequence, the maximum tolerated dose of the drug would be decreased. Another reason why nanoparticle formulations are superior is that solvents, such as cremophor, can leach plasticizers from PVC bags, which are commonly used infusion system. This provides strong evidence that the choice of the vehicle is extremely important during the formulation of a drug delivery system. Abraxane (a nano-formulated paclitaxel molecule encapsulated in albumin) is an albumin-bound form of paclitaxel, characterized by a mean particle size of 130 nm. The non-crosslinked formulation is not stable in circulation and after intravenous administration, the nanoparticles can rapidly disintegrate in blood, forcing the drug to bind to endogenous albumin, which is able to interact with the albumin receptors and mediate the transcytosis inside the tumour vasculature. It was FDA approved in 2005 and has been successfully applied for many types of tumour. Paclitaxel is a lipophilic drug, characterized by high affinity for albumin, which is able to interact with the compound thanks to the presence of special pockets in its structure. This study aimed at using a similar method to try to formulate a new drug delivery system for the compound CCI-001. After the design and realization, the formulation was characterized and tested on different cell lines, in order to compare its effect with the free drug. There are various methods of preparation of albumin nanoparticles: they are classified in chemical-based methods, which use chemical compounds, such as ethanol, cottonseed oil or β -mercaptoethanol, and physical-based methods, which take advantage of physical factors, such as heat or pressure, in order to generate the nanoparticles. Among the chemical-based methods, it is possible to find desolvation, emulsification and self-assembly processes, leading to nanoparticle formation. Nano-spray drying, thermal gelation and nab-technology[®] belong to physical techniques. Reproducibility is a key feature which has to be achieved and every process should aim at producing nanoparticles characterized by predictable and reproducible properties¹⁵¹.

The main challenge of the project was associated with the difficulty to find an effective way to encapsulate the drug inside the carrier: it has been shown that the development of around 40% of the discovered compounds fails because of their poor bioavailability, often linked to poor aqueous solubility²⁴¹. In fact, only 5 out of 5000 investigated drugs are able to reach the clinical trials, and only 1 of the chosen 5 will be approved for the use in human. Despite the discovery of a certain number of techniques available for poorly water soluble compounds, there is still the need to optimize the approaches, in order to improve the delivery of these agents and avoid the use of organic solvents. CCI-001, besides being an extremely lipophilic compound (much more than the parent drug, colchicine, showing a water solubility of 0.007 mg/mL, compared to the 7 mg/mL of colchicine), possesses very low affinity for albumin, which makes the task even harder. Therefore, as opposed to paclitaxel, CCI-001 has a very low interaction with the binding pockets of the protein and the realization of the drug delivery system is made even more challenging.

After having found the best technique to obtain the nanoparticles and after having designed and synthesized them, their characteristics were analysed, the encapsulation efficiency and loading amount were measured for the various trials performed, release studies were performed, in different conditions, and the formulations produced were tested on two cell lines and its activity was compared with the one of the free drug and the carrier alone, not loaded with the drug (blank nanoparticles). Furthermore, the experiments were performed with both bovine serum albumin and human serum albumin.

3 Materials and methods

This chapter deals with all the reagents used, the various techniques adopted for the realization of the nanoparticles and the different methods of characterization used for the analysis and investigation of the formulations.

3.1 Materials

3.1.1 Chemicals and cell lines

For the production of the drug-loaded albumin nanoparticles, the following materials have been used:

The compound CCI-001 ($C_{23}H_{27}NO_6S$, 3.937 g) was provided by the Department of Oncology, University of Alberta, Edmonton, Canada. As already stated in the previous paragraphs, it is a colchicine derivative, a very potent compound which has shown its efficacy in various types of cancer. It is an appealing anti-cancer agent, due to its potency and its extremely low IC_{50} on the majority of the cell lines investigated, which makes it incredibly effective even at the lowest concentrations. However, because of its toxicity, it would be preferable to develop drug delivery systems to transport it to the tumours. HSA (human serum albumin, lyophilized powder >96%, agarose gel electrophoresis, 5 g) was obtained by Sigma Aldrich (Canada). As described above, it is the most abundant protein in blood plasma. Due to its characteristics and features, it is a perfect candidate for the transport of CCI-001, since it possesses the ability to carry even highly lipophilic compounds. BSA (bovine serum albumin, lyophilized powder, 100 g) was purchased by Tocris Bioscience. It is obtained from bovine source and it shares most of the properties and characteristics of human serum albumin. Since it derives from animals and not from humans, it is more immunogenic than human serum albumin, and it should be recognized as an external substance by the human immune system. Glutaraldehyde ($OHC(CH_2)_3CHO$, grade II, 25% in H_2O , 100 mL), also known as pentanedial, glutaral and 1,5-pentanedial, was provided by Sigma Aldrich (Canada). In its pure form, it is an unstable compound. Therefore, it is usually found and sold in a solution mixed with water. It is often employed to disinfect equipment that cannot be subject to heat sterilization. It is a homobifunctional reagent and it is one of the most used crosslinking agents, due to its ability to unselectively react with amino groups of proteins, forming pH-sensitive

Schiff base groups (C=N) between the two carbonyl ends of glutaraldehyde and positively charged amino groups on the surface of the protein. Often, the functional groups of the protein that reacts with glutaraldehyde are the amino groups of the lysine side chains. Sodium hydroxide (NaOH, pellets), also known as caustic soda, was obtained from Sigma Aldrich (Canada). It is a water-soluble inorganic base, used commonly in laboratory work as a buffer solution (to adjust the pH). All the other chemicals used in this study were analytical or high-performance liquid chromatography (HPLC) grade. HCT-116 and SW-620, colorectal cancer cell lines, were obtained as a generous gift from the laboratory of Dr Michael Weinfeld, Katz Group Centre, University of Alberta, Edmonton (Canada). The medium used for supporting the growth and development of the SW-620 was the DMEM + F12 (Dulbecco's Modified Eagle Medium, provided by Thermo Fisher Scientific), which is a mixture of DMEM and Ham's F-12, combining high concentrations of glucose, amino acids and vitamins with F-12's wide variety of components. 10% fetal bovine serum and 1% antibiotic penicillin-streptomycin were added to the medium. The medium used for the culture of HCT-116 was the DMEM media (provided by Thermo Fisher Scientific), enriched with 10% fetal bovine serum and 1% penicillin-streptomycin. Trypsin was used to sub-culture the cell lines, in order to detach the cells from the flasks. DMSO was used to freeze the cells, in order to avoid any damage due to the formation of sharp crystals of ice.

3.1.2 Instruments

For the production of the BSA/HSA solution, a magnetic stirrer (Corning PC-353 Stirrer) and glass vials (28.0 x 57 mm, Fisherbrand[®], Fisher Scientific) were used. A peristaltic pump, a syringe or a 1 mL micropipette were used for the addition of the drug solution (or the desolvating agent) to the BSA/HSA solution, for the production of the crude emulsion. A probe sonicator (Sonicator[®] XL Ultrasonic Liquid Processor, Heat Systems), a hand homogenizer (Grainger, PRO250 Hand-Held Homogenizer) and a high-pressure homogenizer (Nano DeBEE Laboratory Homogenizer) were utilised in nab-technology for the formation of the final emulsion. A rotary evaporator (Buchi Rotavapor[®] and Buchi 461 Water Bath) was needed for the solvent evaporation in nab-technology. A water bath (VwR Shaking Water Bath) was used for the incubation overnight of the drug solution with the already formed crosslinked albumin nanoparticles in the modified version of desolvation. A centrifuge (Sorvall[™] Legend[™] Micro 21 R Microcentrifuge, Thermo

Scientific) was used for the precipitation of the nanoparticles and the removal of unreacted albumin, glutaraldehyde and drug. A water bath sonicator (Cole-Parmer 8852 Ultrasonic Cleaner) was used to stimulate and increase the entrapment of the drug in the nanoparticles and to reduce the particle size. Another centrifuge (Mistral 2000, MSE) was used in cell culture work, a shaker (Titer Plate Shaker, Thermo Scientific) was used for mixing properly the contents of the wells in the 96-wells plates used in cell culture work and a microscope (Leitz Diavert Inverted Tissue Culture Workhorse Microscope with Phase Contrast) was used to analyse the confluency and vitality of the cells. A Zetasizer (Malvern Instruments Ltd, Malvern, UK) was used for the analysis of the size and zeta potential of the nanoparticles, a UV-Vis spectrophotometer (UV-2600i UV-Vis spectrophotometer, Shimadzu, Mandel) was used for the measurement of the drug concentration for the analysis of the encapsulation efficiency and loading amount of the drug, a plate reader (Synergy H1 Hybrid Multi-Mode Reader, Biotek) was utilised for the evaluation of the cell toxicity and determination of the IC₅₀, a freeze-dryer (VirTis, SP Scientific) was used for the lyophilization of the nanoparticles and an HPLC machine (Varian ProStar 210 HPLC System) was used for the precise measurement of the drug concentration for the analysis of encapsulation efficiency, loading amount and release studies. A field emission scanning electron microscope (ZEISS GeminiSEM) was used to study the morphology of the nanoparticles.

3.2 Methods

3.2.1 Preparation of CCI-001-loaded albumin nanoparticles

During this research project, a considerable amount of time was spent trying to find the most effective and reproducible technique that allowed to encapsulate the drug in the protein carrier, hard task due to the poor water solubility of the drug and the extremely low interaction between the compound and the protein. Because of the very lipophilic nature of the drug and the low binding affinity between the compound and albumin, various methods of preparation of the CCI-001-loaded albumin nanoparticles have been investigated and tested. The main techniques adopted were the nab-technology[®] (by analysing and comparing the effects of sonication and high-pressure homogenization), the desolvation process and a modified version of the desolvation process, based on incubation. The same techniques were tested, used and repeated multiple times, in order

to optimize the processes and find the best set of parameters and variables that allowed the achievement of the best formulation. In particular, all the methods were used both for BSA and HSA.

3.2.1.1 First strategy: Nab-technology®

Nab-technology® is one of the most popular techniques used to generate drug-loaded albumin nanoparticles. It is a nanotechnology-based method that takes advantage of the intrinsic properties of albumin to obtain a selective and efficient delivery of hydrophobic drugs and compounds to a tumour site, without using toxic solvents. The process relies on an emulsion-based method. As shown in Figure 8, the steps of the process are the following:

1. An oil phase (the drug solution) is added dropwise to an aqueous phase (the human/bovine serum albumin solution).
2. The mixture is subjected to mild homogenization at low rpm, in order to generate a crude emulsion.
3. The final emulsion is obtained by using a high-pressure homogenization.
4. By transferring the mixture in a rotary evaporator, the solvent is removed and the nanosuspension is produced. It should be a translucent system and the drug-loaded albumin nanoparticles should have a diameter of hundreds of nm (generally <200 nm).
5. A 0.22 µm filter is used to control the size of the nanoparticles and to sterilize the formulation, filtering out the impurity and bacteria.
6. After that, the nanoparticles are eventually lyophilized to provide stability to the formulation (without adding any cryoprotectant).

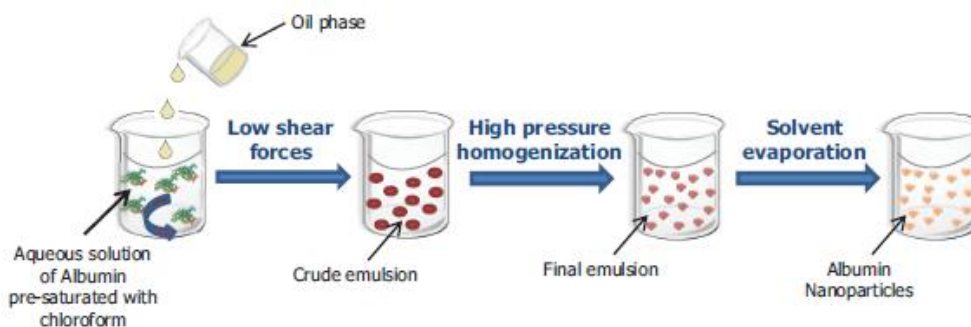


Figure 8: Nab-technology process. From ref [149] with permission.

In the present study, BSA nanoparticles were produced using a method inspired from nab-technology, adopting two experimental techniques: sonication and high-pressure homogenization, which are two high (mechanical)-energy emulsification methods, widely spread for the generation of emulsions, thermodynamically unstable systems. In fact, emulsions, characterized by dispersions of insoluble liquids, require a form of energy to disperse one of the liquid phases (dispersed phase) into the other (continuous phase), in the form of droplets. If the size of the droplets is in the nanometer range, the emulsions are called nano-emulsions. An emulsion is considered a highly dispersed and stabilized emulsion if the droplets are disrupted and stabilized. First, sonication was used, and its effect and influence were studied in both high and low volumes. After that, the same experiments were repeated with the use of high-pressure homogenizer, in order to compare the two approaches. Hosseinifar et al²⁴² used both of the methods, in order to compare the effects of the two and evaluate the differences. As they found out, the effect of the sonicator was not comparable to the high-pressure homogenizer for the creation of stable and effective nanoparticles and the latter was much more reliable and effective.

- Sonication: the first nab-technology trials were carried out using sonication, due to the lack of high pressure homogenizers in the lab. Sonication is one of the methods of choice for the creation of nano-emulsions and nanoparticles, even if, as opposed to high-pressure homogenization, is not adaptable for use on an industrial scale. In sonication, the process of acoustic cavitation is involved in the droplets disruption and stabilization. Cavitation is a phenomenon characterized by the formation of bubbles or cavities in areas of low pressure of a liquid. These microbubbles then collapse and generate huge amount of energy, free radicals and local turbulence. The acoustic cavitation, characterized by the presence of sound waves, responsible for the pressure changes in the liquid, sees the formation of OH· and H·, which give rise to H₂ and H₂O₂ and are able to act as crosslinking agents in the protein, triggering the formation of disulfide bonds and stimulating the nanoparticles formation. Furthermore, the turbulence generated helps to transform the primary oil droplets into smaller ones, generating finely dispersed nano-emulsions and nanoparticles. The effect of the sonicator has also been combined with the use of a hand homogenizer, to try and optimize the process. Different organic solvents were used to dissolve the lipophilic drug: first, ethanol and chloroform, then acetonitrile, used in various ratios and volumes. Both water

and PBS were tested for the dissolution of the bovine serum albumin. Different energies and power of the sonicator were used and their influence on the creation of the nanoparticles was evaluated. The effects of centrifugation and filtration on the obtained formulations were evaluated.

- High-pressure homogenization: the last performed nab-technology trials involved the use of a high pressure homogenizer (Nano DeBEE Laboratory Homogenizer, Department of Agricultural, Food & Nutritional Sciences, University of Alberta, Edmonton, Canada), which was provided by another faculty at the University of Alberta, once it became available for use. Here, as opposed to sonication, it is the process of hydrodynamic cavitation that is responsible for the droplets disruption and stabilization. In this type of cavitation, the pressure variations are caused by the passage of a liquid through a constriction. When the liquid passes through a small orifice, its kinetic energy increases and the pressure decreases. As a consequence, microbubbles and cavities are produced. Their collapse produces a high amount of free radicals and a state of turbulence, which, as already stated above, trigger the formation of nano-emulsion and nanoparticles. As for the sonication, high-pressure homogenization takes advantage of the mechanical force to transform the oil droplets into uniform dispersions and provokes some conformational changes of the protein, which, consequently, encapsulate the oil droplets. The high shear forces involved in this process may determine the modification and disruption of the tertiary and quaternary structure of globular proteins (by altering the hydrogen bonds and hydrophobic and electrostatic interactions inside the protein), without influencing the secondary structure. Furthermore, the high shear forces characterizing the high pressure homogenization process increase the reactivity of SH groups, determining the formation of new disulfide bonds. As a consequence, the protein should create a coating, encapsulating the hydrophobic compound and, furthermore, albumin becomes a stabilizer in the formulation, due to its the isoelectric point, which makes the nanoparticles negatively charged at physiological pH and, therefore, determines the formation of repulsion forces between them. This way, they should not aggregate and they should be sterically stabilized in the formulation. In particular, the hydrodynamic cavitation, that characterizes the high-pressure homogenization, possesses some advantages over the acoustic cavitation, which is involved in sonication: the equipment required is cheaper, more efficient and

can be used at much larger scale of operation. These are some of the reasons why high-pressure homogenization is preferred over sonication for the production of nanoparticles in the nab-technology process.

In particular, different trials have been performed, using both the sonication method and the high-pressure homogenization method. Unfortunately, access to the high-pressure homogenizer has been given from another faculty almost at the end of the research project, due to covid19, and there was not enough time to optimize the process. Briefly, a bovine serum albumin solution was prepared, by dissolving albumin in water (1% w/v) on a magnetic stirrer. A drug solution, generated by adding the drug to a mixture of chloroform and ethanol (ratio 9:1), was added to the BSA solution drop by drop. The system obtained was then sonicated to produce, in theory, very fine particles (100-200 nm) and obtain an emulsion. The resulting formulation was transferred to a rotary evaporator for 30 minutes, and the organic solvents were removed at 40°C at reduced pressure. The system was then centrifuged at about 5000 rpm for 5 minutes, to separate the non-loaded drug and precipitate the micro/macro particles from the nanoparticles. The upper phase was filtered through a 0.22 µm filter (Acrodisc Syringe Filter 0.22 µm Nylon Membrane), in order to separate the smaller nanoparticles from the bigger ones. Different amounts of drug, organic solvents and albumin have been tested and the differences were evaluated. Different energies and powers of the sonicator have been used (25% of the allowable power, 50% of the allowable power and 100% of the allowable power). The effects of the usage of a hand homogenizer for mixing the water and the oil phase was investigated. The organic solvents ethanol and chloroform were then replaced with another organic solvent, acetonitrile, in order to see if any different result was obtained. In the first trials, BSA was dissolved first in water, and then PBS was tested. Later on, instead of a single centrifugation followed by filtration, the effects of two centrifugation (the first one at 7000 rpm for 5 minutes and the second one at 14500 rpm for 10 minutes) were analysed. When access to the high-pressure homogenizer was provided, a new protocol was followed. Briefly, a BSA solution was generated by dissolving BSA in water. A drug solution, composed of drug dissolved in chloroform and ethanol (in a ratio 9:1), was added to the water phase drop by drop, on a magnetic stirrer. This time, the system was transferred to a high-speed homogenizer (around 10000 rpm), to obtain a crude emulsion. Then, the pre-mixed emulsion was transferred to a high-pressure homogenizer (at 20000 psi, for 6 cycles) to form the nanoparticles. After that, the organic

solvents were evaporated at 40-45°C for 30 minutes in a rotary evaporator and the effects of centrifugation (both a single one at 4500 rpm for 5 minutes and two centrifugations, the first one at 4000 rpm for 5 minutes and the second at 14500 for 20 minutes) and filtration were observed. Table 4 shows the different batches obtained with nab-technology, characterized by different volumes and amounts of ingredients.

Table 4: Formulations prepared with nab-technology.

Batch	Organic solvents	Ratio drug/BSA	Sonicator energy
1	Ethanol and chloroform	0.11	50% of allowable power
2	Ethanol and chloroform	0.1	100% of allowable power
3	Acetonitrile	0.1	50% of allowable power
4	Ethanol and chloroform	0.05	25% of allowable power
5	Acetonitrile (and PBS instead of H ₂ O)	0.025	50% of allowable power
6	Ethanol and chloroform	0.025	50% of allowable power
7	Acetonitrile	0.025	100% of allowable power
8	Ethanol and chloroform	0.1	- High-speed and high-pressure homogenizer

3.2.1.2 *Second strategy: Desolvation*

Desolvation is one of the most known and used techniques to produce albumin nanoparticles. It involves the following steps, as shown in Figure 9:

1. The constant addition, drop by drop, of a desolvating agent, such as acetone or ethanol (plus drug, in case of the production of drug-loaded nanoparticles), to an aqueous solution of albumin under continuous stirring, until turbidity of the

solution is reached. The desolvating agent, added gradually, works by changing the tertiary structure of albumin, leading to phase separation and aggregation of the protein. In this way, the homogeneous solution separates in two phases, one of which is constituted mainly of solvent and the other of solute, albumin, that forms aggregates.

2. Most of the time, the obtained nanoparticles are not stable enough and a crosslinker, such as glutaraldehyde, is required to further preserve and stabilize the morphology of the resulted formulation. In fact, the crosslinking agent (in this case, glutaraldehyde) triggers the solidification, by a condensation reaction, of the amino moieties in lysine residues and the arginine moieties in guanidine side chains of albumin with the aldehyde-group of glutaraldehyde.

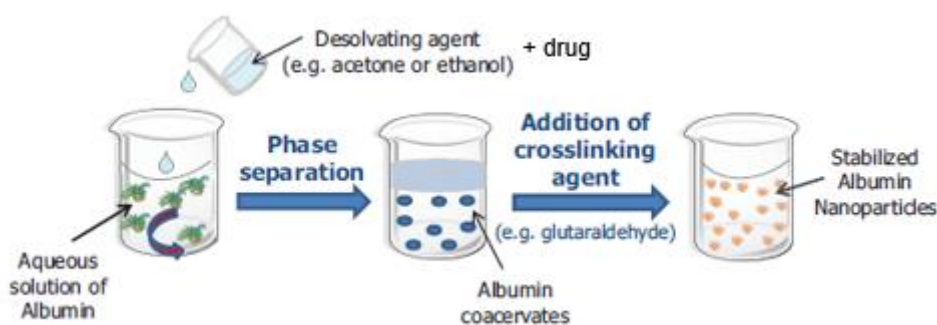


Figure 9: Desolvation process. From ref [149] with permission.

In the desolvation, carefully controlling the flow rate of the desolvating agent is vital for the achievement of optimal nanoparticles. Therefore, during the experiments, the effects of the manual addition of ethanol (by pipette) and the automatic addition of ethanol (by a simple apparatus designed for modulating the rate of flow) were compared. The properties of the resulting system depend on the conditions of the process, such as pH, protein concentration, crosslinker concentration, desolvating agent concentration, ionic strength and stirring speed. As stated above, due to the carcinogen nature of glutaraldehyde, it is fundamental to remove it completely after the formation of the nanoparticles and before injection in human. The concentration of the desolvating agent was varied systematically and its influence on the characteristics of the formulation, such as particles size and size distribution, was analysed. Furthermore, the influence of pH on the nanoparticle size was investigated. Since desolvation is applied to stirred protein

solution, shear stress may affect the particle preparation process and characteristics. Therefore, another parameter taken into consideration was the different stirring speed adopted during the desolvation process and the pre-stirring period of the protein solution, prior to protein desolvation. The ratio of antisolvent/solvent was studied for its influence on particle size.

Even in this second strategy, various trials, some of them unsuccessful and some of them successful, have been performed, in order to find the best set of parameters and variables that could allow the achievement of the formulation. First, a traditional desolvation process was adopted. Then, due to the nature of CCI-001, very lipophilic and characterized by low affinity for albumin, this technique was slightly changed into a modified version of desolvation, which resulted to be the most effective method. In the traditional desolvation, a BSA (/HSA) solution was generated by dissolving the albumin in water on the magnetic stirrer and the pH of the solution was adjusted by the addition of NaOH. A drug solution, prepared by dissolving the drug in the desolvating agent, was added drop by drop to the BSA (/HSA) solution, at a rate of 1 mL/min. After 30 minutes, a glutaraldehyde 8% solution (1.172, 0.588 and 0.235 $\mu\text{L}/\text{mg}$ albumin) was added to the system for crosslinking the nanoparticles and left overnight stirring. The day after, the system obtained was centrifuged at 14000 rpm for 20 minutes and washed three times (to remove the glutaraldehyde unreacted, fundamental step due to the toxicity of the crosslinking agent). At the end, the nanoparticles were collected in the pellet. Different concentrations of BSA solution and drug solution were tested, different desolvating agents have been used, the influence of different pH of the BSA solution was analysed, different stirring speed and concentrations of glutaraldehyde were investigated.. Table 5 shows the different batches obtained with the desolvation method, characterized by the use of different desolvating agents, pH of the BSA solution and ratio of drug/BSA.

Table 5: Formulations prepared with desolvation.

Batch	Desolvating agent	pH	Ratio drug/BSA
1	Ethanol	8	1/4
2	Ethanol	8	1/10
3	Acetone	8	1/10
4	Ethanol	5.5	1/10
5	Ethanol	8	1/20

3.2.1.3 Modified version of desolvation

In order to improve the process, the method was then modified and adapted to the nature of the drug. A first attempt was made by encapsulating the drug into already formed, but not crosslinked, albumin nanoparticles, instead of adding it to the desolvating agent when forming the nanoparticles, as shown in Figure 10. A second attempt, optimized, was performed by making the drug enter into the already formed and crosslinked nanoparticles. An albumin solution was prepared by dissolving BSA (/HSA) in water on the magnetic stirrer and the pH of the solution was adjusted by adding NaOH. After 30 minutes, ethanol, the desolvating agent, was added drop by drop to the BSA (/HSA) solution, to form blank albumin nanoparticles. 30 minutes later, the glutaraldehyde 8% solution (1.172, 0.588 and 0.235 $\mu\text{L}/\text{mg}$ albumin) was added to the system, to stabilize and crosslink the albumin nanoparticles. The system was left overnight, stirring. The day after, the formulation was centrifuged at 14000 rpm for 30 minutes and washed three times to remove the unreacted glutaraldehyde. At the end, the blank albumin nanoparticles were collected in the precipitate. After that, a drug solution, obtained by dissolving the drug in specific ratios of ethanol and water, was added to the previously obtained albumin nanoparticles. In particular, the drug solution was generated by adding water drop by drop to the ethanolic solution of the drug, while vortexing, in order to avoid any precipitate, due to the very lipophilic nature of the drug. The formulation was placed

in the water bath sonicator for 30 minutes, to help and stimulate the encapsulation of the drug, and then transferred to the water bath and left there overnight, shaking at 75-100 rpm, 37°C. The day after, the system was centrifuged at 14500 rpm for 45 minutes, in order to collect the drug-loaded albumin nanoparticles in the pellet. Different volumes of water and oil phase have been tested, the ratio of water and ethanol in the drug solution has been optimized, the amount of BSA was varied to obtain the best loading amount, different methods of shaking inside the incubator were analysed and also different sizes of glass vials were tested, in order to reduce the evaporation of the ethanol. Different types of vials used during centrifugation have been utilized. Furthermore, the effects of different concentrations of glutaraldehyde (1.175, 0.588 and 0.235 $\mu\text{L}/\text{mg}$ albumin) have been evaluated.

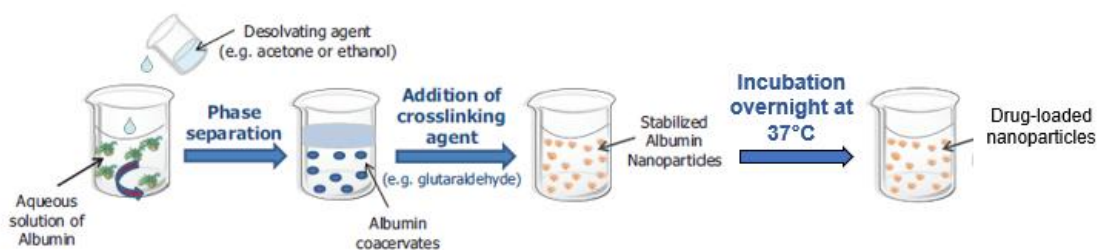


Figure 10: Modified version of desolvation process. Adapted from ref [149] with permission.

The same methods and experiments were performed both for bovine serum albumin and human serum albumin, and the differences between the two were investigated. In particular, after finding the best set of process conditions and parameters (such as pH and ratio drug/albumin), they were directly adopted for the preparation of HSA nanoparticles, preferred over BSA nanoparticles. Table 6 shows the different batches obtained with the modified version of desolvation method, characterized by the use of different pH of the BSA solution, ratios of drug/BSA and ratios of EtOH/H₂O in the drug solution.

Table 6: Formulations prepared with a modified version of desolvation.

Batch	Type of albumin	Crosslinked or not	Ratio drug/albumin	Ratio EtOH/H₂O in drug solution	Volume NaOH added
1	BSA	Yes	1/50	1/9	25 μ L
2	BSA	Yes	1/50	1/4	Not added
3	BSA	Yes	1/50	1/4	25 μ L
4	BSA	Yes	1/25	1/4	25 μ L
5	BSA	Yes	1/15	1/4	25 μ L
<u>6</u>	BSA	Yes	1/10	1/4	25 μ L
7	HSA	Yes	1/10	1/4	25 μ L
<u>8</u>	HSA	Yes	1/10	1/4	50 μ L

3.2.2 Freeze-drying

Freeze-drying is a commonly used process for drying drug nanosuspensions²⁴³. It removes water from a frozen sample through sublimation. It consists of freezing, primary drying (ice sublimation) and secondary drying (desorption of unfrozen water). To protect nanoparticles from stress and aggregation, a cryoprotectant is generally used. When a cryoprotectant is present, water freezes into ice crystals while excluding solutes and particles into a cryo-concentrated liquid phase. The formulation obtained (BSA nanoparticles, HSA nanoparticles, CCI-001-loaded BSA nanoparticles and CCI-001 HSA nanoparticles) were freeze-dried, in order to improve their long-term stability and to be able to store them for long periods of time. After obtaining the fresh nanoparticles, the formulation was transferred to the -80°C freezer and stored there overnight. The day after, the frozen formulation was placed in the freeze-drying machine for at least 48 hours. By

lyophilizing the formulation, solid powder, which can be easily reconstituted to the original dispersion by addition of water or saline, was obtained. The influence of a cryoprotectant was evaluated: the nanoparticles were lyophilized both in the presence of trehalose (2.5% w/v) and without it and the differences between the two versions were investigated. Trehalose is a naturally derived sugar which protects the protein from cryopreservation damage²⁴⁴. The coating of trehalose, which “entraps” the protein, slows down the water molecules directly adjacent to the protein, preventing ice crystallization in its immediate vicinity. The role of trehalose is fundamental, since the interaction between water and the protein dramatically affects the protein structure, dynamics and functionality. The same analysis performed on the fresh nanoparticles were carried out also on the lyophilized ones, in order to compare the characteristics and the behaviours of the different formulations.

3.2.3 Characterization of CCI-001-loaded albumin nanoparticles

3.2.3.1 Size and zeta potential

The hydrodynamic diameter, polydispersity index (PDI) and zeta potential of BSA nanoparticles, HSA nanoparticles, CCI-001-loaded BSA nanoparticles and CCI-001-loaded HSA nanoparticles, obtained by the different techniques adopted, were evaluated by dynamic light scattering (DLS) measurement at 25°C: the nanoparticles were dispersed in water, diluted (usually 1:10, or 1:100), vortexed and characterized by the Zeta-Sizer Nano (Malvern Instruments Ltd, Malvern, UK), a high performance instrument for the detection of aggregates and measurement of small or diluted samples. The analysis was performed at a scattering angle of 173° at 25°C. For the measurement of the size, 0.5 mL of sample were analysed, using low volume disposable cuvettes. For the measurement of the zeta potential, 0.8 mL of sample were analysed, using the zeta dip cell with a quartz cuvette. Any air bubble present in the sample was removed before starting the zeta potential evaluation. The measurement of the hydrodynamic size and zeta potential was performed for both the fresh nanoparticles and the nanoparticles redispersed in water after lyophilization (when the freeze-drying was adopted), in order to evaluate the stability of the formulations.

3.2.3.2 Nanoparticles morphology

The morphologies of CCI-001-loaded BSA nanoparticles and CCI-001-loaded HSA nanoparticles were evaluated by SEM images (Field Emission Scanning Electron Microscope, Zeiss, GeminiSEM). 0.1 mL of nanoparticle dispersion was placed on a glass substrate and allowed to dry overnight. After drying, the nanoparticles were placed on a metal support and coated with gold (Denton Sputtering System), to render them electrically conductive and examined under the microscope. Electron microscopy was performed using an accelerating voltage of 5 kV and a working distance of 5 mm. Pictures were taken at 45000 and 16000-fold magnification using secondary electron detection mode.

3.2.3.3 Yield

The yield of a formulation measures the weight of the formulation produced referred to the amount of components used to generate the formulation. For the calculation of the yield, it is necessary to consider the lyophilized formulation (obtained after freeze-drying), which allows to obtain the drug-loaded albumin nanoparticles in form of solid powder. After 48 hours of freeze-drying, the nanoparticles were collected and weighed. The weight of the solid formulation was compared with the weight of the components used for the achievement of the solid powders.

$$Y \% = \frac{\text{Weight of the formulation (mg)}}{\text{Sum of the weight of all the components (mg)}} * 100$$

3.2.3.4 Drug entrapment efficiency and drug loading

The drug encapsulation efficiency was defined as the percentage of CCI-001 actually loaded relating to the initial amount of drug supplied. On the other hand, the drug loading was calculated as the ratio between the amount of CCI-001 in the nanoparticles (in µg) and the albumin present in the formulation (in mg). The two parameters were calculated by UV-Vis spectrophotometer (UV-2600i, UV-Vis Spectrophotometer, Shimadzu, Mandel). First, the λ_{max} (the maximum wavelength at which to make the analysis) of CCI-001 was evaluated. After that, different standards of CCI-001 were prepared (various solutions of CCI-001 in ethanol, at different known concentrations), and their absorbance measurements at the chosen λ_{max} were performed, in order to generate a standard graph

(a calibration curve), which displays absorbance values against concentrations values. It is fundamental to have the calibration curve of the compound used, in order to be able to calculate the concentrations of any unknown sample. Moreover, the absorbance of the supernatant, obtained from the centrifugation of the samples, was measured, in order to perform a mass balance. Another technique adopted for the measurement of the drug concentration in the formulations, to confirm the values obtained by UV-vis, was HPLC (High Performance Liquid Chromatography), more precise and reliable due to the very low drug concentrations of the formulations. In particular, it was vital to find an effective way of extracting the drug from the nanoparticles, to be able to measure the exact amount of drug which was encapsulated in the formulation. In this research project, two slightly different ways have been utilised and compared: in the first one, the albumin-drug nanoparticles were re-dispersed directly in 1 mL ethanol, vortexed, transferred to the water bath sonicator for 1 hour and then centrifuged at 14500 rpm for 30 minutes, in order to collect the drug in the upper phase; in the second one, the albumin-drug nanoparticles were re-dispersed first in 100 μ L water and transferred to another vial; at this point, 1 mL ethanol was added on top. After that, again, the system was vortexed, transferred to the water bath sonicator for 1 hour and then centrifuged at 14500 rpm for 30 minutes, in order to collect the drug in the upper phase. This second approach was adopted when it was noticed that often the drug, being extremely lipophilic and possessing low affinity for albumin, was prone to adsorption to the vials during centrifugation, trying to “escape” from the carrier and the aqueous solvent. Therefore, in order to obtain a more reliable and real estimate of the amount of encapsulated drug, it was chosen to move the formulation to another vial after centrifugation, to measure just the drug present in the nanoparticles and avoid to detect the quantity of the drug stuck to the walls of the vials.

$$EE \% = \frac{\text{Amount of drug in nanoparticles } (\mu\text{g})}{\text{Amount of drug supplied } (\mu\text{g})} * 100$$

$$DL \left(\frac{\mu\text{g}}{\text{mL}} \right) = \frac{\text{Amount of drug in nanoparticles } (\mu\text{g})}{\text{Amount of albumin in nanoparticles } (\text{mg})}$$

3.2.4 *In vitro* drug release studies

Release of CCI-001 from the albumin nanoparticles was evaluated using equilibrium dialysis method, in PBS 1X (pH 7.4). Different *in vitro* release studies were performed, in order to evaluate the release profile of CCI-001 from CCI-001-loaded BSA

nanoparticles and CCI-001-loaded HSA nanoparticles, both for the fresh nanoparticles and the lyophilized nanoparticles. Furthermore, as a control, the release of free CCI-001 was also investigated. Both the fresh nanoparticles and the lyophilized ones were re-dispersed in water: 0.1 mL water was added to each pellet of fresh nanoparticles obtained after centrifugation and vortexed: around 20 pellets re dispersed in water were used in each release study (obtaining a total volume of around 2.5 mL for the release study). On the other hand, the lyophilized nanoparticles, around 160 mg, were re dispersed in 2.5 mL of water and used for the release studies. For the release of the free drug, the optimal formulation needed to be designed and the main substances used for the formulations were ethanol, PBS and tween 80. The effects of different ratios of the constituents were investigated. The release studies were carried out in different release media: first, in phosphate buffer saline (PBS, pH=7.4) + tween 80, and then, after figuring out how to optimize the study, in only PBS. CCI-001-albumin nanoparticles and free CCI-001, with the same drug content, were transferred into a dialysis bag (Spectrapor, MW cutoff 3500 Da) and the system was placed into 450 mL of dissolution medium (PBS) under shaking at 50 rpm, 37°C. The volume of the dissolution media was chosen according to the sink condition, which is the ability of the dissolution media to dissolve at least 3 times the amount of drug present in the dosage form. The dialysis bag was sealed at both ends. At selected time points, 0.1 mL of sample was removed from inside the dialysis bag and replaced with 0.1 mL double distilled water (or, in the case of the free drug, with the solvents used in the formulation, in the same ratios). At first, the release study was performed by taking the samples out from the release medium, outside of the bag, but the results were not optimal and the concentrations were not detected, since they were very low. For this reason, the next studies were carried out by taking the samples from inside the membrane, in order to make the detection of the concentrations easier. The samples were stored in the freezer, to maintain the stability and prevent the absorption of the drug on the plastic vials (a recurrent problem during the research project) as much as possible. After having collected the 0.1 mL samples and having taken them out of the freezer, 0.2 mL of ethanol was added on top. They were vortexed and placed in the water bath sonicator for around 1 hour and, after that, centrifuged for 30 minutes at 14500 rpm, in order to extract the drug and precipitate the rest of the formulation. The upper phases were analysed by HPLC or plate reader for determining the amount of CCI-001 present. The remaining concentration obtained at t_i was subtracted from the initial concentration of CCI-001 at t_0 and used to plot the cumulative drug release (%) versus time. The

extraction procedure and the release studies were repeated at least three times for each formulation, and average and standard deviation were calculated. The release profiles were compared using similarity factor, f_2 , and the profiles were considered different if f_2 was < 50 .

$$f_2 = 50 \times \log_{10} \left[\frac{100}{\sqrt{1 + \frac{\sum_{t=1}^n (R_t - T_t)^2}{n}}} \right]$$

Where n is the sampling number, R_t and T_t are the percent released of the reference and test formulations at each time point t .

3.2.5 HPLC analysis of CCI-001

A Varian Prostar 210 HPLC system was used for the quantification of CCI-001 in the samples. Mobile phase was an isocratic mixture of water and acetonitrile (70:30), containing 0.1% trifluoroacetic acid, and the separation was obtained by a Microsorb-MV 5 μm C18-100 Å column (4.6 x 250 mm). The flow rate was set at 1 mL/min, at room temperature and the detection wavelength was 386 nm (Varian Inc., Palo Alto, CA, USA). The retention time was 3.7 min. The assay was found linear over the examined range of 6.25-1000 $\mu\text{g/mL}$ in the mobile phase, with a calibration curve of $y = 1.0451x - 1.6946$ and a correlation coefficient of 0.999. The concentrations of CCI-001 in the samples were determined from the aforementioned regression equation. The lowest limit of quantification was set at 6.25 $\mu\text{g/mL}$. The inter- and intra-day variations were less than 10% for all concentrations. No interfering peak was observed.

3.2.6 Cell culture

The cell culture studies were performed on two different cell lines: HCT-116 (doubling time: 18-21 hours) and SW-620 (doubling time: 26 hours), colorectal cancer cell lines. The cell lines, belonging to other laboratories, had to go through a mycoplasma test in order to detect any possible contaminations. It is vital to identify and treat contaminated cells, since contaminations are very widespread and can compromise the cell physiology, and, therefore, the outcomes of the experiments²⁴⁵. Mycoplasmas, belonging to over 100 species, are small, round or filamentous prokaryotic organisms. Due to their very small size and their ability to deform, they can be difficult to recognize and detect in the

traditional cell culture works, since they can pass through the filter used for sterilization. After having resulted negative to the mycoplasma test, the cell lines, which had been retained in quarantine, could be transferred and stored in a humidified incubator at 37°C, 5% CO₂. The SW-620 cell line was cultured in DMEM + F12 (1:1) (1X) medium, containing L-glutamine, 15 mM HEPES, 10% fetal bovine serum and 1% penicillin/streptomycin antibiotic. The HCT-116 cell line was cultured in DMEM (1X) medium, enriched with 10% fetal bovine serum and 1% penicillin/streptomycin antibiotic.

3.2.6.1 Cell freezing

Once the cell lines were obtained and brought to the laboratory, they had to be stored: in fact, cryopreservation is vital to long-term maintenance of cells. From the 75 cm² flasks in which the cells were contained, the exhausted media was removed and thrown away. The cells were then washed twice with 2 mL of PBS. 3 mL of trypsin were added to the cells and the flask was left in the incubator for 3-4 minutes, in order to allow them to be detached from the bottom of the flask. After checking the occurred detachment with the microscope, 5 mL of fresh media were inserted in the flask and homogenized, in order to inactivate the trypsin. The content of the flask (cells, trypsin and media) was centrifuged at 200-250 G for 5 minutes. The supernatant obtained from the centrifugation was discarded and 10 mL of a solution of DMSO (5%) in media was added to the pellet and homogenized, to resuspend the cells. The cell concentration was measured by haemocytometer: trypan blue-stained cells (obtained by mixing 15 µL cells solution and 15 µL trypan blue dye) were counted with a haemocytometer to estimate the cell concentration (cells/mL). After that, the cells were stored in various tubes (around 2 million cells/tube) and they were placed in isopropanol and kept in the -80°C freezer overnight, to allow them to freeze very gradually and slowly (otherwise, a quick freezing would result in a high damage of the cells). The day after, the cryovials were transferred to the liquid N₂ tank.

3.2.6.2 Cells thawing

Before starting any cell culture, the first thing to do was thawing the particular frozen cell line needed. As already stated, to achieve the greatest cell viability, it is fundamental to freeze cell slowly. For the thawing, the opposite is true: it is necessary to thaw them

quickly. As described in the previous paragraph, cell lines are stored with dimethyl sulfoxide (DMSO), used as cryoprotectant. When added to the media, DMSO prevents intracellular and extracellular sharp crystals from forming in cells during the freezing process. Otherwise, without DMSO, cells would be damaged by the ice crystals during the freezing process. However, during the thawing of the frozen cell lines, it is vital to remove quickly the DMSO, due to its toxicity to the cells. First, the cells were removed from the liquid N₂ tank and immediately placed in a 37°C water bath, in order to allow them to reach the liquid form, until just the tiniest ice crystal was left in the vial (usually, 5 mL frozen cells). Once the cells were thawed, a test tube was filled with 9 mL of fresh media (+ FBS and P/S) and the volume of cells just thawed. This step needed to be performed very carefully, since the cells had just been defrost and they were very fragile at this point. Once the cells were re dispersed in the media and homogenized, forming an homogeneous solution, the content of the test tube (composed of cells, media and DMSO) was centrifuged at 300 G for 5 minutes. The supernatant, containing media and DMSO, was discarded, whereas 10 mL of fresh media was added to the pellet of cells and homogenized, in order to generate a clear solution. The solution of cells and fresh media was placed in a 75 cm² flask with 10 mL of extra fresh media, up to reaching 20 mL of total volume. The content of the flask was then homogenized and the flask was placed into a humidified incubator, at 37°C, 5% CO₂.

3.2.6.3 *Sub-culture*

All the cell lines were cultured until they reached approximately 80-90% confluency, at which point they were sub-cultured, based on cell growth rates (that is the reason why it is very important to always know the doubling times of the various cell lines in question). In particular, the cells were cultured in 75 cm² flasks. First, the exhausted media was removed from the cell flask with a 10 mL tip: it is important not to touch the bottom of the flask, since the cells are attached on it, and that could damage them. The cells were washed twice with 2 mL PBS, and 3 mL trypsin were added to the cells. Then, the flask was placed in the incubator for 3-4 minutes, in order for the trypsin to react and for the cells to be able to be detached from the bottom of the flask. After this period of time, the effective cells detachment was checked at the microscope. Once the cells were detached, 7 mL of fresh media were added to the mixture of cells and trypsin and homogenized, in order to neutralize the trypsin. The mixture of cells, trypsin and media was removed from

the flask and put in a test tube for centrifugation at 300 G for 5 minutes. After the centrifugation, the supernatant was discarded and 10 mL of new fresh media were added to the pellet and homogenized to re-disperse it. Trypan blue-stained cells (obtained by mixing 13 μ L cells solution and 13 μ L trypan blue dye) were counted with a haemocytometer to estimate cell concentration (cells/mL). According to the estimated cell concentration, a chosen volume of cell solution was put in a new 75 cm² flask and fresh media was added in order to reach 20 mL final volume. After that, the cells were stored in a humidified incubator, at 37°C, 5% CO₂, until the next sub-culture. The optimal amount of cells to place in the new flask depended on the doubling time of each cell line, so that the sub-culture of the cells would happen every 2-3 days. Therefore, the exact number of sub-cultured cells, which constituted the next generation, was stabilized and optimized during the work.

3.2.7 MTT assay (*in vitro* cytotoxicity)

The MTT assay for cell viability and proliferation is used to measure the cellular metabolic activity, as indicator of their viability. It is designed to test the relative cytotoxicity of various treatments against a particular cell line and this is done by assessing the metabolic status of the cells after a certain length of exposure to the drug. As shown in Figure 11, it is based on the reduction of a yellow tetrazolium salt (MTT, 3-[4,5-Dimethylthiazol-2-yl]-2,5-diphenyltetrazolium bromide) to purple formazan crystals by metabolically active cells, since the active and viable cells possess specific enzymes able to reduce the MTT to formazan. The insoluble formazan crystals are then dissolved and they produce a coloured solution, which provides information on the viability of the cells. The darker the colour (purple) obtained, the more viable the cells. In particular, the cytotoxicity of free CCI-001, encapsulated CCI-001, and only carrier (albumin nanoparticles), was tested using the MTT assay.

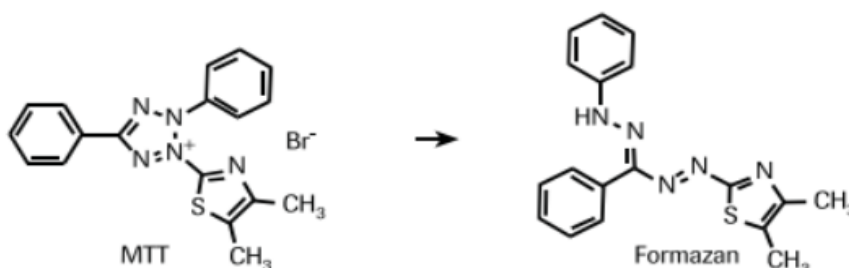


Figure 11: Reduction of MTT to Formazan crystals.

On day 1, the cells were seeded on 96-well plates (Figure 12) with media and they were incubated at 37°C for 24 hours. In particular, the 36 wells that constitute the external frame of the plate were filled with only media (200 µL/well), for preventing the evaporation of the wells, whereas the internal 60 wells were filled with cells and medium, for a total volume of 100 µL/well.

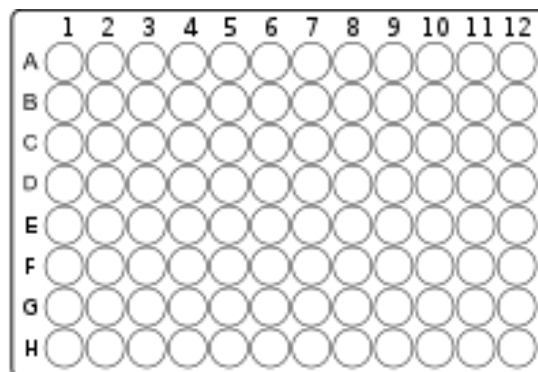


Figure 12: 96-wells plate.

The optimal cell density at which to seed the wells (in 100 µL total volume) had to be determined and optimized for each cell line: after some trials, it was chosen to use 2×10^3 cells/well for the HCT-116 cell line and 4×10^3 cells/well for the SW-620. As a general rule, the number of cells seeded in each well should be such as to provide a 40-60% confluency after 24 hours from the seeding, at the moment of treatment. The volume required for the insertion of the correct amount of cells had to be calculated by counting the cells with the haemocytometer (in the Burker chamber) during the sub-culture of the cells. It is important to remember to always consider some extra volume when filling the wells (excess). After plating, the cells were left to adhere to the plate overnight. After 24 hours from the seeding, it is important to check the condition of the cells and the percentage of confluency. After that, the treatment (free drug, blank nanoparticles or drug-loaded nanoparticles) was added to the wells at different concentrations (10 concentrations, chosen appropriately, from the lowest to the highest concentration) and incubated at 37°C. The important thing to carry in mind is that, before the addition of the treatment, the wells are already filled with 100 µL of cells + media from the day before. Therefore, when other 100 µL (treatment) are added to the wells, the cells are subjected to a 1:2 dilution. That is the reason why the 10 concentrations of the treatment should be doubled before the addition to the cells, in order for the cells to receive the right and chosen concentrations of the treatment. After having treated the cells, from the lowest concentration to the highest one, the 96-wells plates were incubated at 37°C for 48 or 72 hours. After the period of incubation (48 or 72 hours), in order to evaluate the viability of the cells, the MTT solution was prepared (5 mg/mL in distilled water, 20 µL/well). The MTT solution, previously filtered in order to remove any bacteria or fungi present in it, was added to the cells, homogenized (with the Titer Plate Shaker, Thermo Scientific) and incubated at 37°C for 3-4 hours. The reduction of MTT in presence of cellular

dehydrogenases yields formazan crystals on the bottom of the wells. After checking the effective presence of the crystals at the microscope, the wells were emptied and 100 μ L DMSO was added to each well and mixed thoroughly on the shaker, in order to dissolve the crystals. The plates were analysed and the cell viability was detected by measuring the optical absorbance at 570 nm. The mean absorbance of each treatment was determined and converted to the percentage of viable cells relative to the control. The IC₅₀ (the concentration of a drug or formulation required for a 50% inhibition *in vitro*) of the specific treatment was calculated from the plot of the % of viable cells versus log CCI-001 concentration. The analysis of the plates was performed at 48 and 72 hours since the IC₅₀ value should vary depending on different cell lines and times of incubation.

3.2.7.1 Free CCI-001

Before testing the obtained formulations, the cell lines were first treated with the free drug, to evaluate the activity of the main compound. In fact, it is important to make a comparison between the efficacy of the free drug and the encapsulated drug, to detect any possible improvement or worsening caused by the formulation. Ten stocks of drug in DMSO were prepared, at ten different concentrations: 0 nM, 25 nM, 50 nM, 200 nM, 400 nM, 800 nM, 6.4 μ M, 25.6 μ M and 51.2 μ M. Each stock was diluted 1:50 in media, so that the new stocks contained media and the 2% of the previously prepared stocks composed of drug and DMSO. The new resulting stocks, therefore, had concentrations of: 0 nM, 0.5 nM, 1 nM, 2 nM, 4 nM, 8 nM, 16 nM, 128 nM, 512 nM and 1024 nM. From these, 100 μ L were taken and put in each well, previously filled with other 100 μ L of media + cells. Therefore, the concentrations of treatment received by the cells were: 0 nM, 0.25 nM, 0.5 nM, 1 nM, 2 nM, 4 nM, 8 nM, 64 nM, 256 nM and 512 nM. It is important not to exceed the 1% DMSO in each well, otherwise the cells would be damaged. By following this procedure, each well contained exactly 1% DMSO.

3.2.7.2 CCI-001-loaded HSA nanoparticles

The cell lines were then treated with different concentrations of CCI-001-loaded HSA nanoparticles. The nanoparticles, obtained with the process described in the previous chapter, were re-dispersed in 1 mL PBS and filtered, to remove any possible bacteria or fungi. From the initial stock, ten serial dilutions in media were produced, in order to reach the ten desired concentrations. In particular, the resulting stocks had the following

concentrations: 1000 nM, 500 nM, 125 nM, 15.6 nM, 7.8 nM, 3.9 nM, 1.9 nM, 0.98 nM, 0.48 nM and 0 nM (control: no particles, just media + PBS). From each stock, 100 μ L was taken and added to the wells, previously filled with other 100 μ L of media + cells. Therefore, the concentrations of the treatment received by the cells resulted to be, respectively: 500 nM, 250 nM, 62 nM, 7.5 nM, 3.9 nM, 1.8 nM, 0.9 nM, 0.4 nM, 0.2 nM and 0 nM. The concentration of PBS should be under 20% in each well.

3.2.7.3 *Blank HSA nanoparticles*

Apart from the efficacy of the free drug and the encapsulated drug, it is also important to consider the effect of the vehicle on the cell viability, to take into consideration all the possible contributions to the cytotoxicity of the formulation. For this reason, the cells were also treated with blank crosslinked albumin nanoparticles (without drug, just the carrier), obtained by performing the same serial dilutions, at the same nanoparticles concentrations (from 0.25 mg/mL to 0) to see if glutaraldehyde, even in traces, could be toxic to the treated cell lines. In this way, it was possible to evaluate in a reliable way the efficacy of the drug-loaded nanoparticles, distinguishing the contributes of the encapsulated drug and the carrier. Furthermore, in this way, it was possible to see if there was a synergistic, additive or antagonistic effect between the drug and the carrier.

4 Results and discussion

4.1 Preparation of CCI-001-loaded albumin nanoparticles

4.1.1 Nab-technology[®]

4.1.1.1 Sonication

Unfortunately, due to the nature of the drug and the low affinity between the cargo and the carrier, nab-technology was not able to provide good results, in terms of size, zeta potential, stability of the formulation and encapsulation efficiency of the drug. Higher energies of the sonicator allowed to obtain smaller nanoparticles, perhaps due to the fact that more energy was transferred to the system and it was able to create more and finer nanoparticles, but the results were not good enough. Even by using a hand homogenizer to mix further the water and oil phases, no difference was noticed. After only two hours from the first measurement, the characteristics of the nanoparticles changed, demonstrating that the formulation was not stable. Replacing the ethanol and chloroform with acetonitrile, which is able to dissolve the drug, but at the same time is miscible with water, being less lipophilic than chloroform, did not make any significant difference. Often, the filtered samples provided worse results than the non-filtered ones: perhaps this was due to the fact that nanoparticles aggregated after filtration, or because they adhered to the filter, since the majority of the formulation was constituted of microparticles. More nanoparticles were obtained when two centrifugations were performed: the first one to eliminate the microparticles and the unencapsulated drug, removing them from the upper phase, and the second one to collect the nanoparticles. Still, the formulation was not stable and the size distribution resulted to be multimodal. Modifying the method and reducing the volumes allowed to improve the characteristics of the nanoparticles obtained, perhaps due to the fact that the energy produced by the sonicator was addressed to smaller volumes. The size, PDI and zeta potential of the obtained formulation were good this time and showed the presence of some nanoparticles, as opposed to the previous trials, where the formulation was mainly made of microparticles. However, the amount of drug entrapped in the nanoparticles was close to zero, confirming the evidence that with this technique, regardless of the modifications and optimizations, it was very difficult to make the drug, which is not attracted by albumin at all, enter the nanoparticles. Even though nab-technology and its variations were the most effective techniques used to produce

formulations such as Abraxane, they seemed not to work with CCI-001, because of the extremely high lipophilicity of the compound and its low binding affinity to albumin. Therefore, even though some nanoparticles were obtained, the yield of the process was very low, since the majority of the formulation was made of micro and macroparticles: this could be the reason why the filtration did not work appropriately and the centrifugation at higher speed provided better results, separating in a more efficient way the micro/macroparticles. Since no encapsulation was obtained, in this case the process was not efficient and not reproducible.

4.1.1.2 High-pressure homogenization

Even by using a high speed and a high-pressure homogenizer, which allowed the achievement of paclitaxel-loaded albumin nanoparticles, instead of a sonicator, the results were not satisfying with CCI-001. The particles obtained were quite good and stable, but almost no drug was encapsulated and, again, the majority of the particles were microparticles. As a proof of this fact, a mass balance was performed, in order to evaluate the distribution of the drug in the formulation and have a rough estimate of the efficiency of the encapsulation method. After evaporating the organic solvents, the formulation was centrifuged twice, at different speeds, in order to collect the nanoparticles, if present. The amount of drug in the nanoparticles was measured but, not surprisingly, most of the drug was not present neither in the upper phase nor in the nanoparticles, probably due to the fact that the majority of the drug precipitated, or it was encapsulated in the microparticles, which most likely constituted the majority of the formulation. To prove that, the original sample was centrifuged just once at 14000 rpm for 25 minutes, in order to precipitate the nanoparticles, the microparticles and the precipitated (unloaded) drug: ethanol was added to the pellet to make the unloaded drug dissolved in it. Furthermore, also the drug dissolved in the supernatant was analysed. Of the original 44 mg drug used at the beginning (the original amount was 60 mg in 55 mL, but only 40 mL of the solution was obtained after high-pressure homogenization), 28.48 mg resulted to be precipitated drug and 3.36 mg was drug in solution, unencapsulated. Of the remaining 12.16 mg of encapsulated drug, just 2% (around 1 mg) was present in the nanoparticles, whereas the majority was belonging to the microparticles. This provided further evidence that, even by using the high-pressure homogenizer, superior to the sonicator, the formulation

obtained was not effective, due to the nature of the drug. After these unsuccessful trials, a new method for the improvement of the formulation was tested.

4.1.2 Desolvation

The desolvation technique seemed to be more reliable and reproducible than nab-technology. It allowed to obtain nanoparticles of proper size, PDI and zeta potential. Furthermore, the nanoparticles resulted to be stable, since two days later the characteristics remained almost the same. However, although the particles obtained were appropriate, the low encapsulation efficiency made it necessary to optimize the process and modulate the parameters in order to obtain an overall effective formulation. Therefore, different trials have been performed and every time the volumes were changed, the ratios ethanol/water were altered and modifications of the centrifugation and washing processes were made, in order to try and obtain a better formulation characterized by higher encapsulation. Replacing the ethanol with acetone allowed to obtain slightly smaller nanoparticles, but did not make any significant difference in terms of encapsulation efficiency. The pH was changed, in order to see if basic or acidic solutions affected the achievement of the formulation (considering the pI of albumin=5.16). The pH of the BSA solution influenced greatly the characteristics of the formulation: increasing the pH, obtaining therefore a basic solution, by adding a higher volume of NaOH to the formulation, allowed to achieve smaller and smaller nanoparticles. On the other hand, the addition of HCl (acidic solution) caused an aggregation of albumin, that formed small precipitates, perhaps due to the fact that the pH obtained was near the isoelectric point of albumin, the pH at which the net charge becomes zero and the repulsive forces are not present. The addition of cholesterol, which was thought to increase the strength of the interaction between albumin and the drug²⁴⁶, did not provide any significant difference to the formulation.

4.1.3 Modified version of desolvation

The last technique adopted was the most effective one and provided the best formulations in terms of stability, size, zeta potential and encapsulation efficiency. The overnight incubation of the drug with the already crosslinked albumin nanoparticles, at 37°C and while shaking at 75-100 rpm, allowed a higher entrapment and entrance of the drug inside the drug delivery system, and it was the only solution to overcome some of the obstacles

encountered with the other methods, caused by the high lipophilicity and low affinity of the drug for the carrier. Since the carrier and the cargo did not show high interaction, the only solution was to find a way to let the drug enter as much as possible into the nanoparticles. In fact, despite the low entrapment and presence of the drug inside the nanoparticles, the extremely high potency of the compound (IC_{50} in the range of nM) allows to use and test the formulation on the cancer cell lines anyway. In this technique, the presence of the crosslinking agent affected greatly the achievement of the formulation: when the drug was incubated overnight with the albumin nanoparticles (not crosslinked), nanoparticles were not obtained. On the other hand, when crosslinked nanoparticles were used, the drug was able to be encapsulated in the formulation overnight. Even in this modified version of desolvation, as in the traditional desolvation, the pH of the albumin solution played a role in determining the size of the particles obtained: the higher was the pH, the smaller were the nanoparticles. The variations in size were seen in particular for human serum albumin. The optimal amount of NaOH to use for achievement of good nanoparticles was 50 μ L for HSA and 25 μ L for BSA. Another factor that affected the characteristics of the nanoparticles was sonication: sonicating the nanoparticles for a few minutes after the production allowed the size to decrease of 2-5 nm. Since this method involves an incubation of a drug solution with already formed crosslinked albumin nanoparticles, it was vital to find the best parameters and conditions (such as volumes, ratios EtOH/H₂O, methods of shaking, proper glass vials, time of incubation etc) for the drug, to trigger its encapsulation. It was proven that shaking horizontally and vertically allowed to obtain the same results. Smaller glass vials to use in the water bath were preferred, since less space was left for the ethanol to evaporate from the formulation. Furthermore, the most important variable to modulate was the precise ratio EtOH/H₂O to use in the drug solution: at first, a ratio of 1:9 was used (0.5 mL ethanol and 4.5 mL water), but overnight it caused the drug to precipitate, since the amount of water used, compared to the amount of ethanol, was too much. Then, a ratio of 1:4 was used (1 mL ethanol and 4 mL water), resulting in the optimal ratio, so that the drug was perfectly solubilized and did not precipitate. The optimal shaking speeds for the incubation were found to be in the range between 75 and 100 rpm. Another parameter that was varied during the experiments was the ratio drug/albumin used: ratios of 1/50, 1/25, 1/15 and 1/10 were tested. Interestingly, by keeping constant the amount of drug used and reducing the amount of albumin, the characteristics of the nanoparticles remained almost the same, especially the encapsulation efficiency. Therefore, a lower amount of albumin was

preferred, since the loading amount (μg of drug per mg of carrier) would be higher. The formulations used for the *in vitro* release studies and cell toxicity studies were prepared by using a 1/10 drug-albumin ratio, the optimal one. Since this last technique was the one that provided the best and most reproducible results, all the formulation prepared from this time on were made by using the modified version of desolvation.

4.2 Characterization of CCI-001-loaded albumin nanoparticles

As already stated above, three techniques have been used to try and obtain CCI-001-loaded albumin-based nanoparticles. Among these three methods, only the last one, the modified version of desolvation, was able to provide good and effective nanoparticles. Despite the relatively low encapsulation efficiency, this technique was the one which allowed to obtain the highest drug entrapments possible and since the IC_{50} of the drug is very low, due to the high potency and cytotoxicity of the drug, the amount of drug present in the nanoparticles was enough to perform *in vitro* release studies and cell toxicity studies. Before doing any kind of analysis, the λ_{max} (wavelength of maximum absorbance) of CCI-001 was calculated by UV-Vis Spectroscopy (UV-2600i, UV-Vis Spectrophotometer, Shimadzu, Mandel). It is important to determine it, since the extent to which a sample absorbs light depends upon the wavelength of light. The wavelength at which a substance shows maximum absorbance (and therefore photon absorption) is called absorption maximum (λ_{max}). In particular, λ_{max} is characteristic of each compound, it provides information on the electronic structure of the analyte and it is the wavelength at which the drug shows maximum sensitivity. λ_{max} is determined by plotting absorbance vs wavelength, as it can be observed in Figure 13A. The λ_{max} obtained was 386 nm. Standards of the drug in ethanol were produced and a calibration curve was obtained, in order to be able to measure the drug concentration of unknown samples, providing a relationship between absorbance and concentration, as shown in Figure 13B.

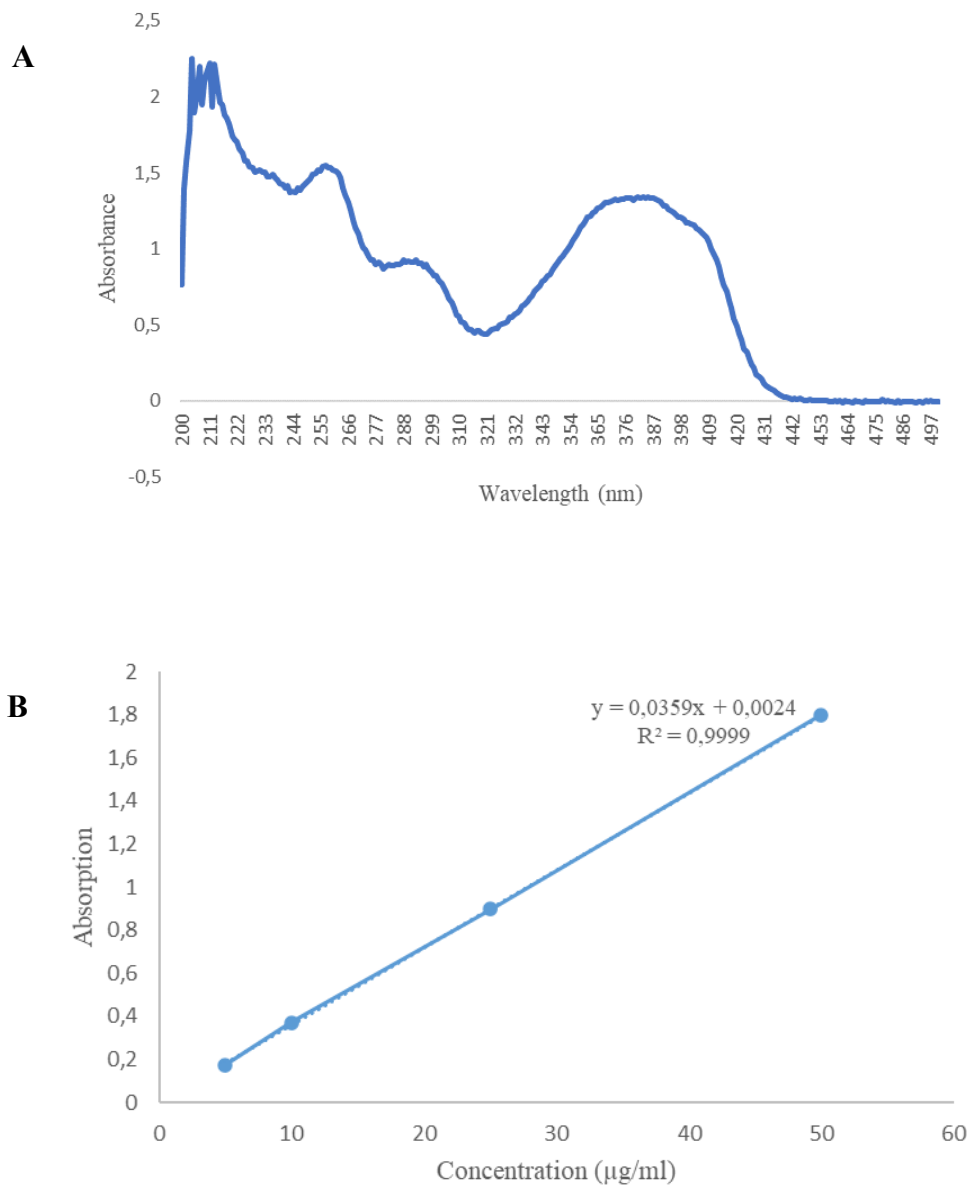


Figure 13: A) λ_{\max} CCI-001 B) Calibration curve of CCI-001.

Table 7 shows the characteristics of all the nanoparticles obtained, and allows to make a comparison between the different methods used. After having tested all the techniques, the third method was chosen and the other ones were abandoned. In particular, batch 6 (BSA) and 8 (HSA) were the best ones and the ones actually used for the various studies (release, cell toxicity).

Table 7: Characterization of the CCI-001-loaded BSA/HSA nanoparticles. Data represent average \pm SD (n=3).

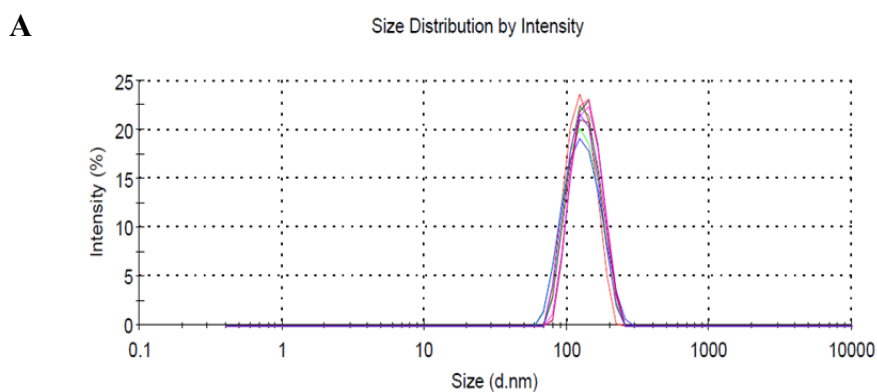
Nab-technology					
	<u>Size (nm)*</u>	<u>PDI*</u>	<u>Zeta potential (mV)*</u>	<u>Entrapment efficiency (%)*</u>	<u>$\mu\text{g drug/mg albumin}$</u>
	404.6 \pm 243.9	0.45 \pm 0.11	-11.3 \pm 15.7	2.5 \pm 0.8	-
Desolvation					
	<u>Size (nm)*</u>	<u>PDI*</u>	<u>Zeta potential (mV)*</u>	<u>Entrapment efficiency (%)*</u>	<u>$\mu\text{g drug/mg albumin}$</u>
	133.3 \pm 24.7	0.08 \pm 0.04	-29.8 \pm 6.9	3.9 \pm 0.86	-
Modified version of desolvation					
<u>Batch</u>	<u>Size (nm)*</u>	<u>PDI*</u>	<u>Zeta potential (mV)*</u>	<u>Entrapment efficiency (%)*</u>	<u>drug/albumin ($\mu\text{g/mg}$)</u>
1	114.87 \pm 8.9	0.05 \pm 0.01	-30.45 \pm 0.77	-	-
2	147.57 \pm 21	0.04 \pm 0.05	-29.8 \pm 1.35	8.1 \pm 0.44	1.62
3	96.59 \pm 2.14	0.043 \pm 0.009	-29.2 \pm 0.59	7.6 \pm 1.06	1.52
4	124.36 \pm 13.1	0.045 \pm 0.01	-28.5 \pm 1.1	6.9 \pm 0.89	2.76
5	127.55 \pm 9.6	0.037 \pm 0.02	-26 \pm 2.3	6.2 \pm 1.12	4.1
6	127.72 \pm 4.99	0.04 \pm 0.03	-25.67 \pm 2.4	5.8 \pm 0.72	5.8
7	209.2 \pm 4.5	0.034 \pm 0.02	-28.3 \pm 1.2	5.2 \pm 0.64	5.2
8	129.25 \pm 3.88	0.0395 \pm 0.01	-29.65 \pm 3.04	6.1 \pm 0.9	6.1

*Hydrodynamic diameter, polydispersity index and zeta potential estimated by DLS.

*Encapsulation efficiency measured by UV-Vis spectrophotometer.

As it is possible to observe from Table 7, the modified version of desolvation allowed to obtain the best and the most reproducible results, in terms of size and zeta potential and encapsulation efficiency. In fact, reproducibility is a very important requirement when designing and synthesizing a formulation. Taking into consideration the modified version of desolvation, which is the method of choice followed in this research project, the size ranges are between 100 and 200 nm, which is considered an optimal size for the targeting of tumours (especially for passive targeting, since small particles, characterized by sizes under 300 nm, are potentially more able to leak through the defective vascular endothelium of cancer blood vessels and passively accumulate in tumours) and the formulation are characterized by a narrow size distribution. The zeta potential ranges are between -20 and -30 mV, which highlight the stability of the formulations. In general, the drug-loaded HSA nanoparticles resulted to be bigger (around 10 nm) than the drug-loaded BSA nanoparticles and their zeta potential was lower (more negative). The encapsulation efficiency range is between 2 and 10%, which is certainly low for a drug delivery system, but most likely high enough for being effective as a treatment, since the IC₅₀ range of the free CCI-001 was proven to be between 2 and 10 nM in various cancer cell lines. Even though their encapsulation efficiency was not the highest, the batches 6 (BSA + drug) and 8 (HSA + drug) were the most effective ones and they were used in all the next experiments and analysis. This is due to the fact that the drug loading ($\mu\text{g drug/mg albumin}$) was higher, since the albumin used, 10 mg, was lower than in any other batches. This parameter is even more important than the encapsulation efficiency and that is the reason why the batches 6 and 8 were considered the best formulated ones.

4.2.1 Size and zeta potential



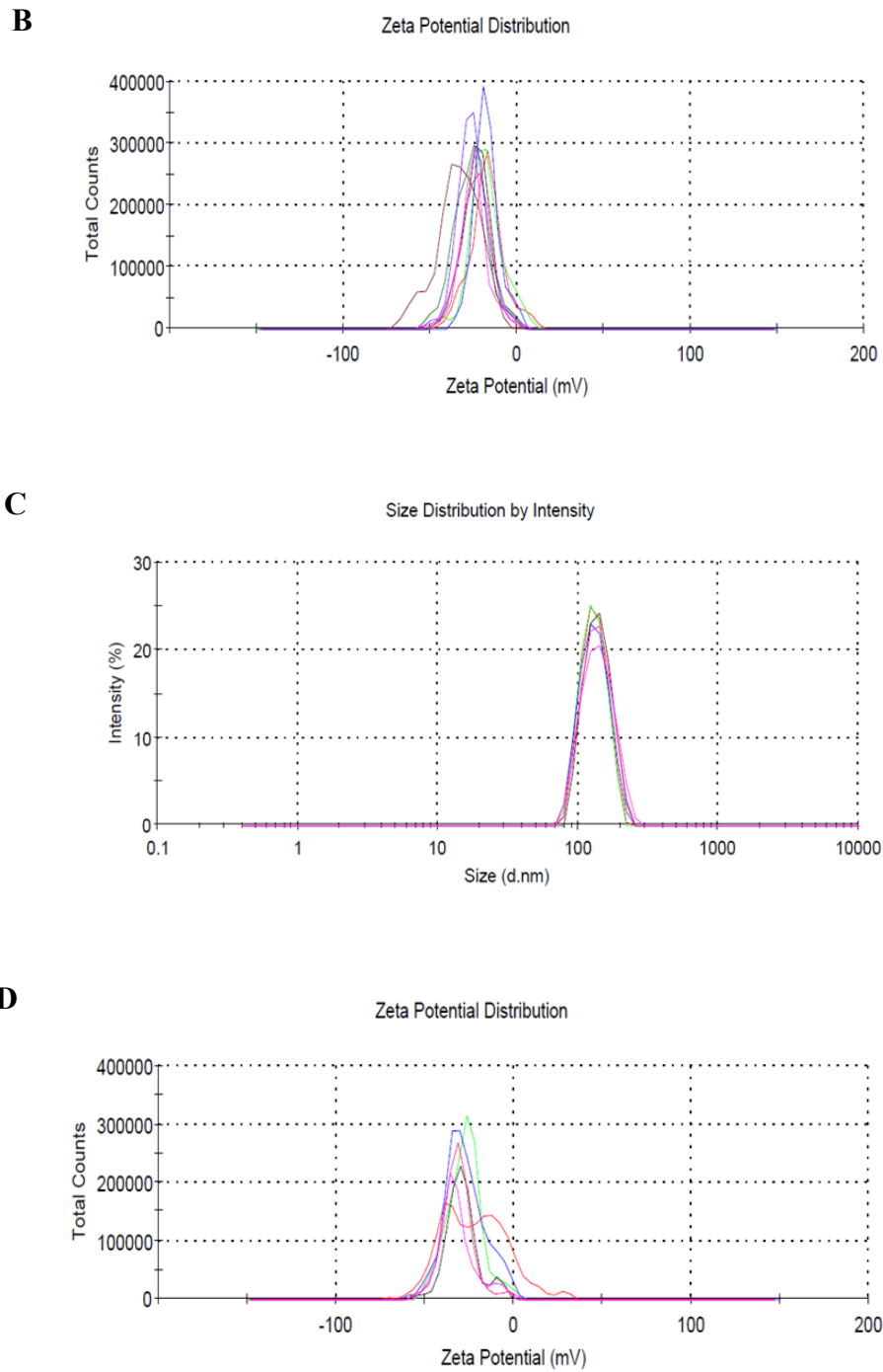


Figure 14: Size distribution of A) CCI-loaded BSA nanoparticles (batch 6) and C) CCI-00-loaded HSA nanoparticles (batch 8). Zeta potential of B) CCI-001-loaded BSA nanoparticles and D) CCI-001-loaded HSA nanoparticles.

Figure 14 shows the size and zeta potential distribution of drug-loaded BSA and HSA nanoparticles. In both the two formulations, BSA and HSA-based nanoparticles, the dimensions of the nanoparticles loaded with drug resulted to be slightly bigger than the ones of the blank nanoparticles (Figure 15A). In the same way, the zeta potential of the nanoparticles loaded with drug was more negative than the ones of the blank nanoparticles (Figure 15B). The data for this analysis are taken from the batches 6 (BSA) and 8 (HSA), which resulted to be the best ones.

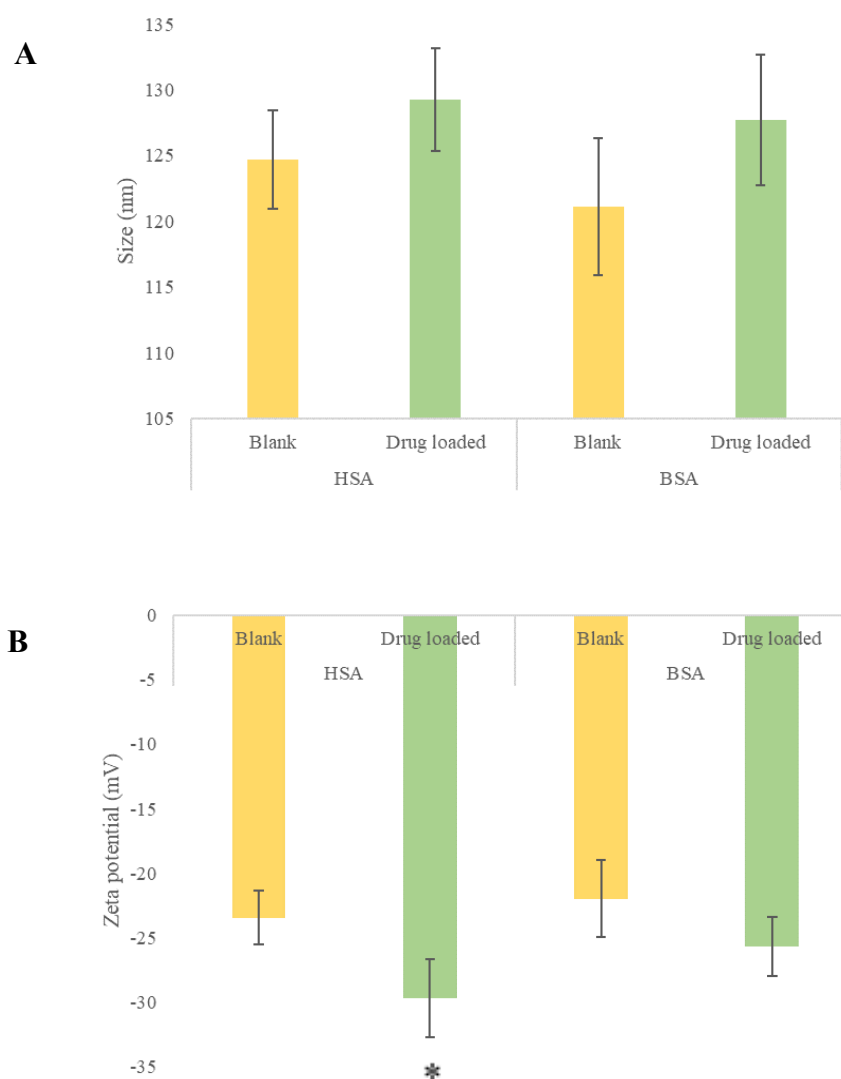


Figure 15: A) Size comparison of CCI-001-loaded BSA/HSA nanoparticles and blank BSA/HSA nanoparticles. B) Zeta potential comparison of CCI-001-loaded BSA/HSA nanoparticles and blank BSA/HSA nanoparticles. Data represent average \pm SD (n=3). * means statistically different from the blank NPs ($\alpha < 0.05$, Student *t*-test).

The nanoparticles obtained by the modified version of desolvation displayed not only similar sizes, but also resulted in physical stability, without aggregation and sedimentation at room temperature: the size and the zeta potential of the same formulation was measured for 5 days and they did not show particular differences, as it is possible to observe in Figure 16. The stability of the nanoparticles was most likely due to the presence of the crosslinking agent, which prevented the aggregation of the nanoparticles and allows the size, polydispersity index and zeta potential to remain constant. In fact, the glutaraldehyde treatment crosslinks albumin molecules both on the surface and in the interior of the nanoparticles, improving the stability of the formulations.

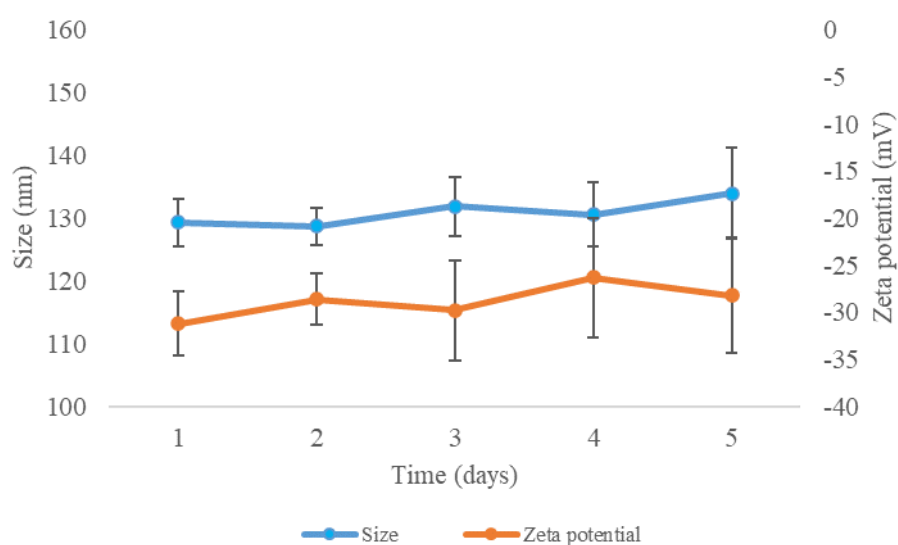


Figure 16: Stability of CCI-001-loaded albumin nanoparticles. Data represent average \pm SD (n=3).

4.2.2 Freeze-drying

The freeze-drying allowed to obtain the nanoparticles in the form of solid powder. As stated above, the nanoparticles were lyophilized both with trehalose and without, in order to evaluate the differences and see if the use of a cryoprotectant could be avoided or not. As it is possible to notice from Figure 17, the use of a cryoprotectant was vital for the achievement of good and stable nanoparticles, characterized by size and zeta potential similar to those of the fresh nanoparticles. On the other hand, the lack of trehalose influenced negatively the particles, determining their aggregation and instability. The freeze-dried powder reconstituted well in solution.

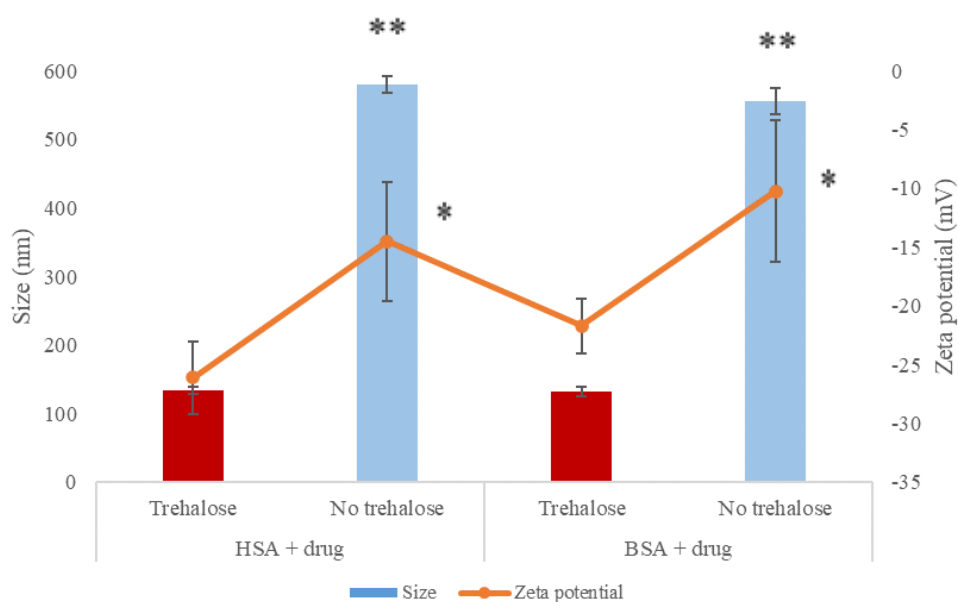


Figure 17: Influence of the use of trehalose on the size and zeta potential of freeze-dried nanoparticles. Data represent average \pm SD (n=3). ** means statistically different from the formulation with trehalose ($\alpha < 0.01$, Student *t*-test). * means statistically different from the formulation with trehalose ($\alpha < 0.05$, Student *t*-test).

4.2.3 Encapsulation efficiency and drug loading

The encapsulation efficiency (amount of drug encapsulated in the nanoparticles divided by the amount of drug originally used for the production of the formulation) falls between 5 and 9%, for both CCI-001 BSA nanoparticles and CCI-001 HSA nanoparticles: although not high, due to the nature of the affinity between the protein and the drug, it is still high enough to test the formulations on cancer cell lines and be effective, since the IC_{50} of the free drug is in the range of nM. Even more important is the parameter that expresses the μg of drug encapsulated per mg of carrier. The interesting fact to point out is that by reducing the quantity of albumin used, up to 10 mg, the encapsulation efficiency remained the same, as shown in Figure 18. That is the reason why batches 6 and 8, which used 10 mg of albumin instead of 15, 25 or 50 mg, were preferred and considered the most suitable ones, with $\sim 6 \mu\text{g}$ drug/mg albumin. With almost the same encapsulation efficiency, they allowed to reach higher drug loading, since less albumin was used.

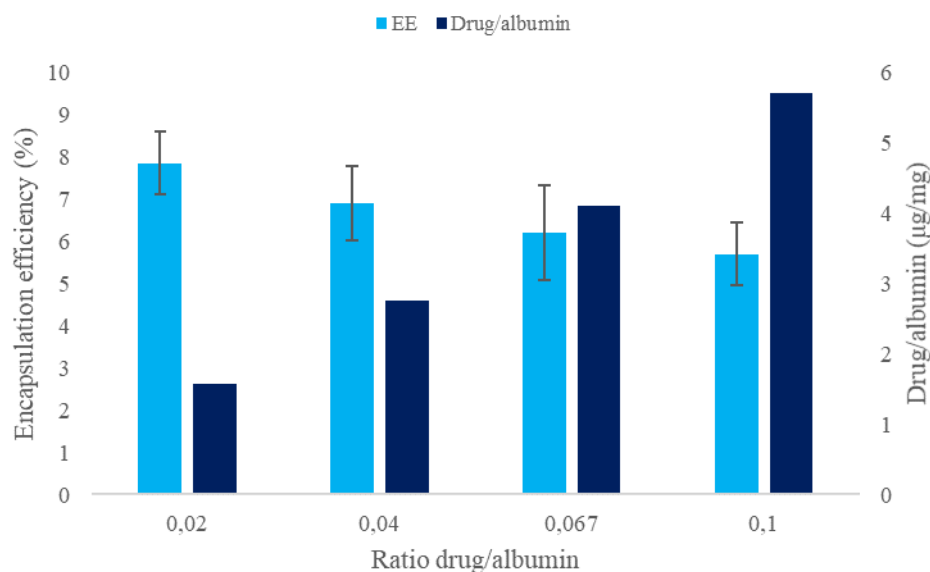


Figure 18: Encapsulation efficiency (%) and amount of drug/albumin ($\mu\text{g}/\text{mg}$). Data represent average \pm SD (n=3).

4.2.4 Yield

The yield of the nanoparticle was $\sim 65\%$. After the production, 5 batches were lyophilized together, generating 162 mg of solid powder (weight of the formulation). Each batch was composed of 10 mg albumin, 1 mg drug and 40 mg trehalose (weights of each component of the freeze-dried formulation). Dividing the weight of the final solid formulation by the summation of the weights of each component, it is possible to find a yield of around 65%.

4.2.5 Morphology

In order to visualise the existence of the nanoparticles in the size range between 100 and 200 nm, SEM imaging was used. SEM pictures (at 45000-fold and 16000-fold magnification) for CCI-001-loaded HSA nanoparticles and CCI-001-loaded BSA nanoparticles are illustrated in Figure 19. The nanoparticles resulted to be spherical and the CCI-001-loaded HSA nanoparticles seemed to be slightly more homogeneous and uniform than the CCI-001-loaded BSA ones.

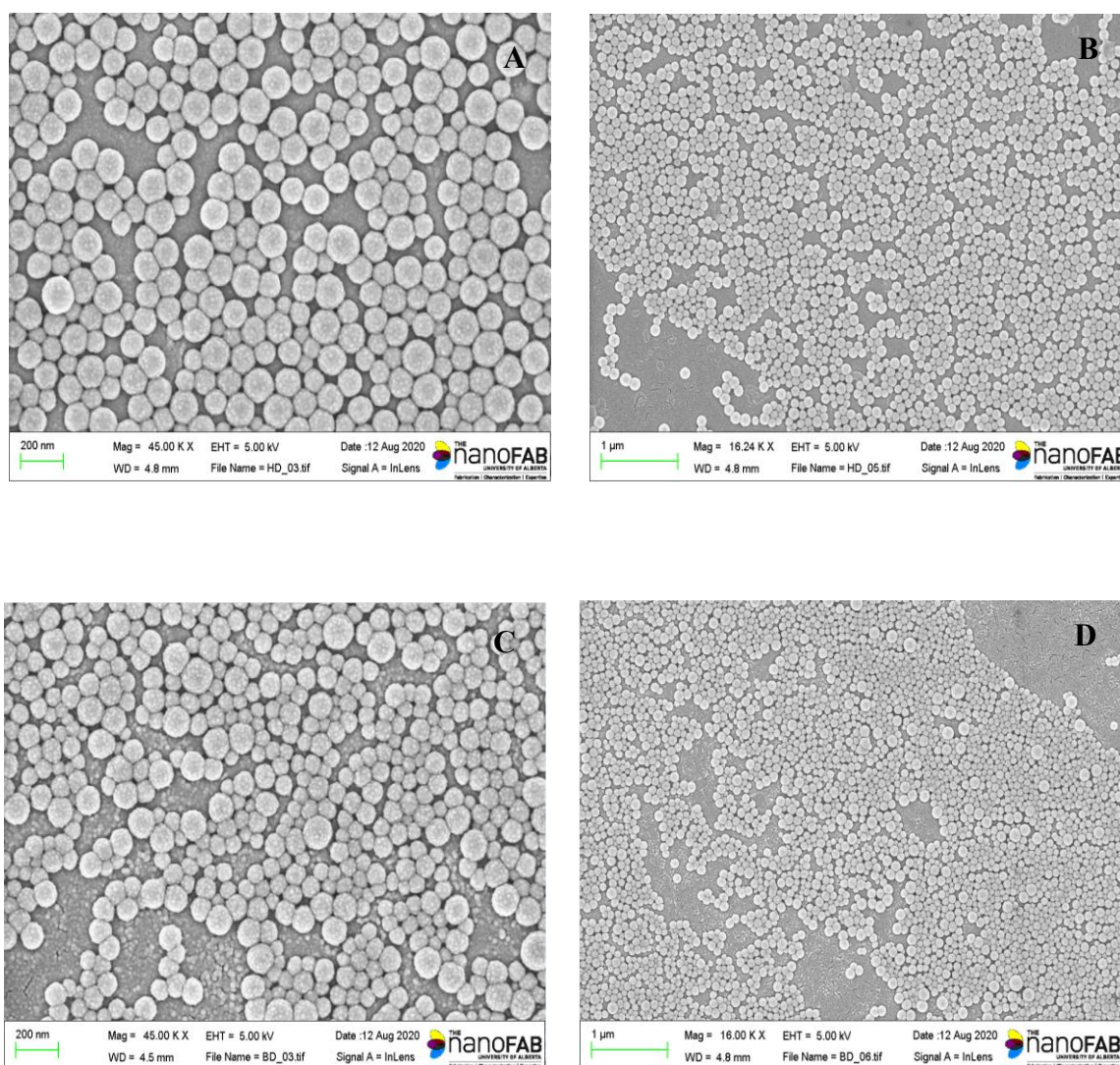


Figure 19: Sem images of A) CCI-001-loaded HSA NPs 45k-fold magnification, B) CCI-001-loaded HSA NPs 16k-fold magnification, C) CCI-001-loaded BSA NPs 45k-fold magnification, D) CCI-001-loaded BSA NPs 16k-fold magnification.

4.2.6 Effect of the stirring speed

As stated above, by modulating some of the process parameters, it was possible to tune the characteristics of the nanoparticles obtained. One of the most significant variables in the process was the stirring speed. The magnetic stirrer used, Corning PC-353, has a stirring speed range of 80-1000 rpm. During the process of generation of the nanoparticles by desolvation, the speed of the magnetic stirrer affected the size of the obtained nanoparticles. In particular, the size of albumin nanoparticles decreased if the stirring speed increased, as shown in Figure 20.

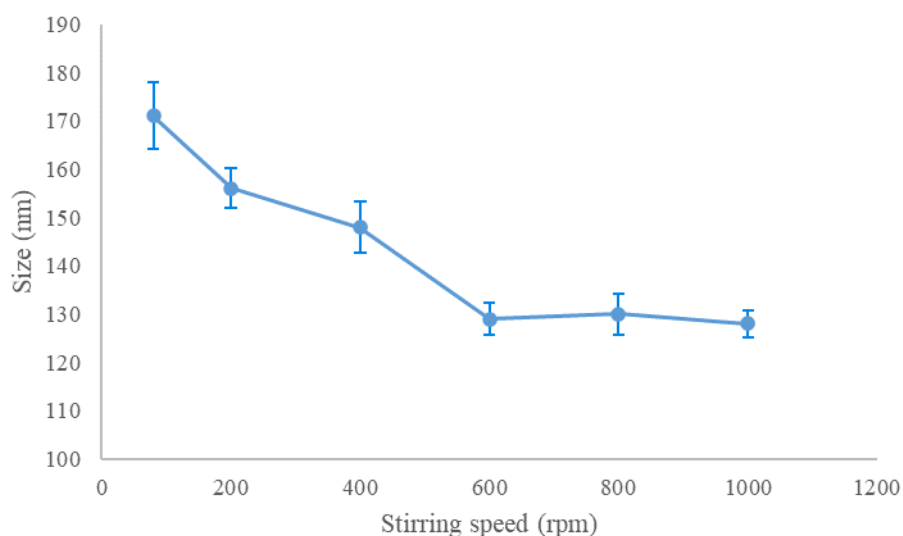


Figure 20: Influence of the stirring speed on the size of the nanoparticles. Data represent average \pm SD (n=3).

As it is possible to observe, from a certain speed on (600 rpm), the size of the albumin nanoparticles remained almost constant. Therefore, the speed adopted for the optimal formulations (batch 6 and 8), used for the characterization and cell toxicity studies, was 600 rpm, which allowed to obtain the minimum size of the nanoparticles.

4.2.7 Effect of pH

The pH of the albumin solution was another parameter that affected the characteristics of the nanoparticles obtained. The desolvation process (and therefore, the modified version of desolvation process) is usually carried out in a pH range of 7-9, in which the nanoparticles are stable and have optimal sizes (< 300 nm). To adjust the pH, a 0.1% NaOH solution was used: the more NaOH was added, the more the pH increased. As shown in Figure 21, the size of the nanoparticles was reduced at higher pH values. This may be due to the fact that at increasing pH values, the ionization of the albumin increased, leading to repulsion of the albumin molecules. On the other hand, deviating from the pH range chosen, and approaching the pI of albumin (around 4.7 for human serum albumin), which is the pH at which the overall charge of the protein is zero, due to the lack of the electrostatic forces, the nanoparticles resulted to be unstable and as a result, they aggregated. That is the reason why when managing protein-based nanoparticles, such as albumin nanoparticles, it is vital to avoid neutral particle surface charges.

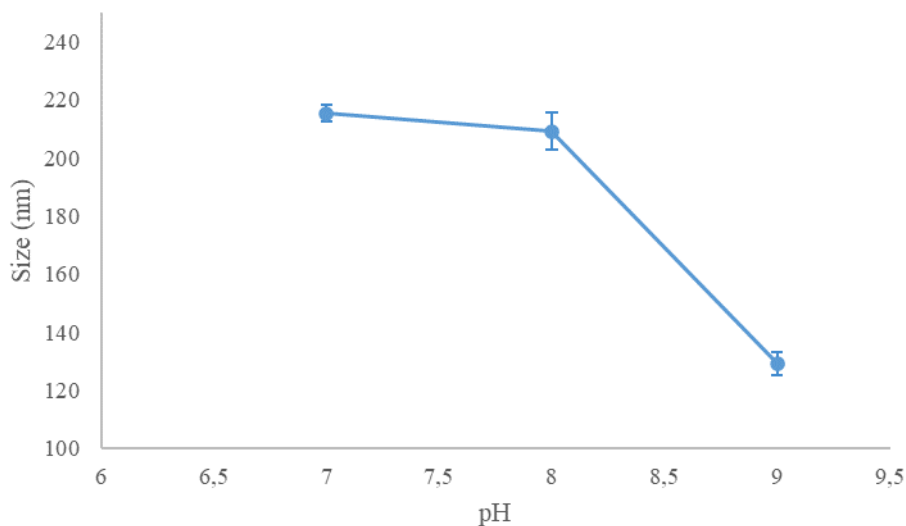


Figure 21: Influence of the pH on the size of the nanoparticles. Data represent average \pm SD (n=3).

Since smaller sizes are preferable, the optimal formulations that were tested on the cell lines were produced at pH 8.5-9.

4.2.8 Effect of the glutaraldehyde

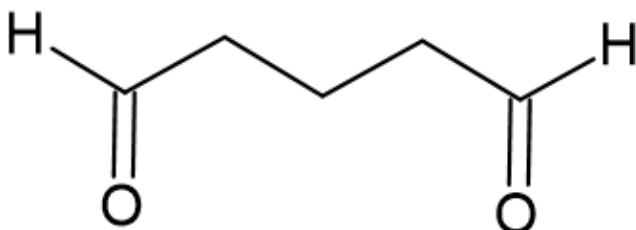


Figure 22: Glutaraldehyde.

The process of desolvation, frequently used to produce drug-loaded nanoparticles, such as albumin nanoparticles, often requires a crosslinking step, which is fundamental for the achievement of stable

nanoparticles, affecting the biodegradability and the release from the carrier system²⁴⁷. Glutaraldehyde (Figure 22) is one of the most commonly and frequently adopted crosslinking agents, mainly due to the fact that is cheap, easily accessible and has been investigated for a long time. It is often chosen for its high efficacy in the stabilization of biomaterials. However, glutaraldehyde has been demonstrated to be toxic to the cells. That is the most important reason why there has been an increasing need for alternative and non-toxic crosslinkers that are able, at the same level of glutaraldehyde, to produce stable and biocompatible products.

In the study, different concentrations of glutaraldehyde have been tested: 1.175, 0.588 and 0.235 μL of an 8% solution of glutaraldehyde per mg of albumin, which correspond respectively to 40, 100 and 200% of the necessary amount to react with the 59 amino-groups of lysine in the HSA molecules, as reported by Langer et al²⁴⁸. The differences in the characteristics of the nanoparticles were evaluated. The lowest concentration of glutaraldehyde was not enough to crosslink the nanoparticles and therefore, the influence on the size of the nanoparticles was investigated just for the 100 and 200%. From the experiments performed, the glutaraldehyde concentration resulted not to affect much the size of the nanoparticles and the encapsulation efficiency, as it is possible to observe in Table 8, in agreement with the previous results of Rahimnejad et al²⁴⁹.

Table 8: Influence of glutaraldehyde concentration on the particle size. Data represent average \pm SD (n=3).

** means statistically different from the other glutaraldehyde concentration ($\alpha < 0.01$, Student *t*-test).

Glutaraldehyde concentration (%)	Particle size (nm)	Polydispersity index
40%	-	-
100%	144 \pm 3.42	0.016 \pm 0.056
200%	129 \pm 2.98**	0.09 \pm 0.021

Langer et al²⁴⁸ demonstrated that glutaraldehyde crosslinking of the protein particles tends to result in a decrease in the pI of the nanoparticles: they found out that the pI value of the protein decreased with the increasing concentration of crosslinking, altering the electrostatic forces and the hydrophobic interactions with other compounds, therefore possibly modifying also the encapsulation efficiency. For this reason, the encapsulation efficiency was calculated for the nanoparticles crosslinked with both 100 and 200% glutaraldehyde (both in the process of desolvation and the modified version of desolvation), but the results did not show any difference, perhaps due to the nature of the drug, characterized by high lipophilicity and low affinity for albumin.

4.3 *In vitro* drug release

Albumin nanoparticle formulations, prepared under the experimental conditions described in the previous chapter, were tested for *in vitro* release at 37°C. The release studies performed showed quite a sustained release pattern, over 24-25 hours for both CCI-001-loaded BSA nanoparticles and CCI-001-loaded HSA nanoparticles, without any initial burst release. On the other hand, the release of the free drug through the dialysis membrane was really fast, reaching 100% in less than 4 hours: here all CCI-001 molecules are free in solution and they diffuse through the dialysis membrane much faster. Although not particularly prolonged, the release of the drug from the nanoparticles was slower and more gradual than the one of the free drug. This aspect provides evidence that the nanoparticle formulation potentially helps to protect the drug from degradation and to prolong its release. The slower release of CCI-001 from albumin nanoparticles could be the result of the gradual diffusion from the stable matrix of the nanoparticles (and most likely not of degradation, since the albumin nanoparticles are crosslinked). The CCI-001 molecules could be partly loaded on the surface of the nanoparticles and partly entrapped inside the nanoparticles, but most likely, since the release of the drug happens quite fast, the molecules of the drug are weakly attached to the surface of the nanoparticles, considering the low affinity between the drug and the protein and the relatively low encapsulation efficiency. This could be the reason why also the release from the nanoparticles is not particularly slow and prolonged. Figure 23 shows the plot of the data expressed as cumulative amounts of “encapsulated” CCI-001, released from the albumin nanoparticles, and the free CCI-001, released from the ethanolic solution, as function of time. The release profiles were compared (CCI-001 released from HSA and CCI-001 released from BSA nanoparticles, both compared with free CCI-001) using similarity factor f_2 and they resulted to be significantly different from each other ($f_2 = 17.88$ and $f_2 = 23.7$, respectively. In both cases, $f_2 < 50$).

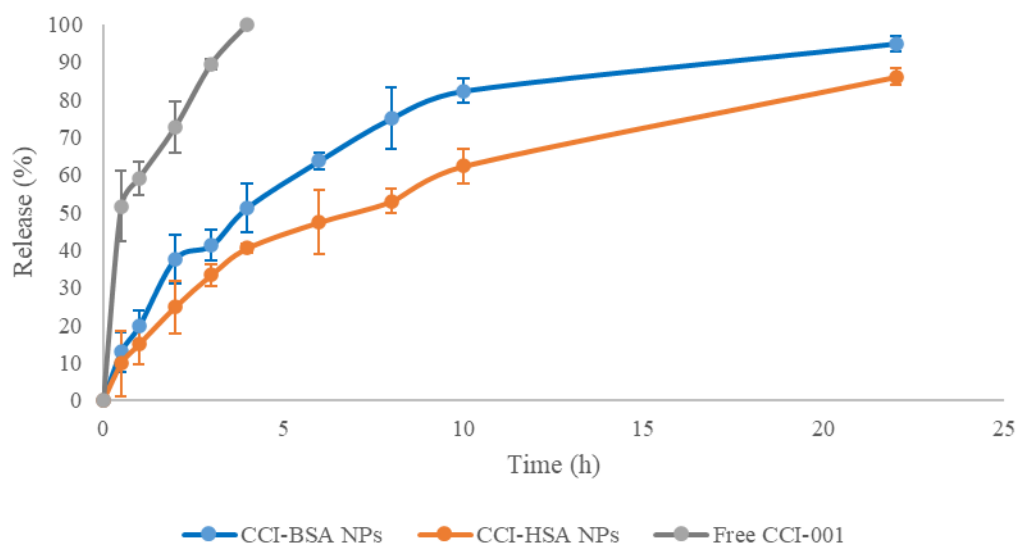


Figure 23: In vitro CCI-001 release profiles. Data represent average \pm SD (n=3).

4.4 Cell toxicity

The cytotoxicity studies of the free CCI-001, of the CCI-001-loaded HSA nanoparticles and of the blank HSA nanoparticles (at the same nanoparticles concentrations) were evaluated using the MTT assay. Generally, the results showed that the loaded nanoparticles exhibited even greater efficacy (lower IC_{50} s), compared to the positive control free CCI-001, by killing a higher amount of cells at lower concentrations. This may be due to the fact that the nanoparticles interact with cancer cells more than the free drug (since albumin possesses high affinity for the gp60 and SPARC receptors, overexpressed in cancer cells), or because of the higher solubility of the drug in the nanoparticles or because of the higher stability conferred to the drug inside the nanoparticles. However, the most likely reason why the nanoparticles resulted to be more effective than the free drug could be the presence of glutaraldehyde, that increases the cytotoxicity of the formulation. In fact, the results of the MTT assay of the blank HSA nanoparticles showed a reduction in cell viability, providing evidence that the presence of glutaraldehyde played a role in the cytotoxicity of the nanoparticles. In particular, the comparison between the activity of the free drug, the loaded nanoparticles and the carrier has been evaluated at 48 and 72 hours from the treatment (and the obtained IC_{50} s of the free drug at 48 and 72 hours were in agreement with the ones calculated by Dr Tuszynski's group). Table 9 shows the IC_{50} s of CCI-001-loaded HSA nanoparticles and

free CCI-001, calculated at 48 and 72 hours. In particular, the drug is very effective in both cancer cell lines, with lower IC₅₀s in SW-620 cell line.

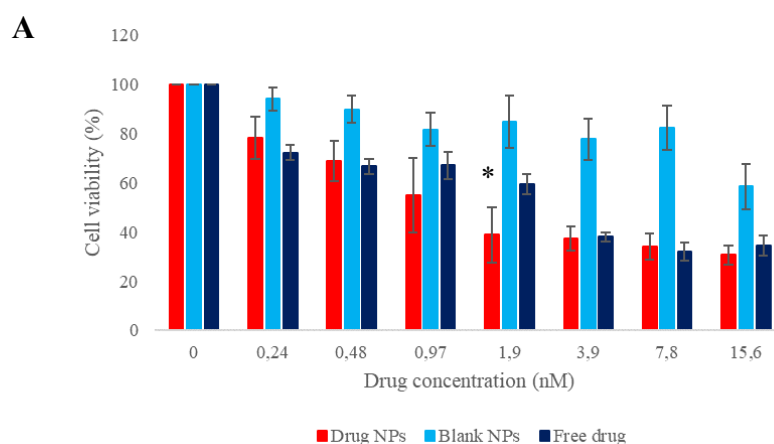
Table 9: IC₅₀s of CCI-001-loaded HSA nanoparticles and free CCI-001, in SW-620 and HCT-116 cancer cell lines, at 48 and 72 hours. Data represent average \pm SD (n=3).

* means statistically different from free drug ($\alpha < 0.05$, Student *t*-test).

** means statistically different from free drug ($\alpha < 0.01$, Student *t*-test).

IC ₅₀ (nM)				
	SW-620		HCT-116	
	<u>Free drug</u>	<u>Drug NPs</u>	<u>Free drug</u>	<u>Drug NPs</u>
48h	2.36 \pm 0.32	1.077 \pm 0.57*	4.392 \pm 0.27	1.269 \pm 0.21**
72h	2.058 \pm 0.29	0.62 \pm 0.31**	4.235 \pm 0.198	0.927 \pm 0.1**

Figure 24 shows the cytotoxicity of the drug-loaded nanoparticles, the carrier alone and the free drug in the cancer cell lines SW-620 at 48h (A) and at 72h (B), and HCT-116 at 48h (C) and at 72h (D).



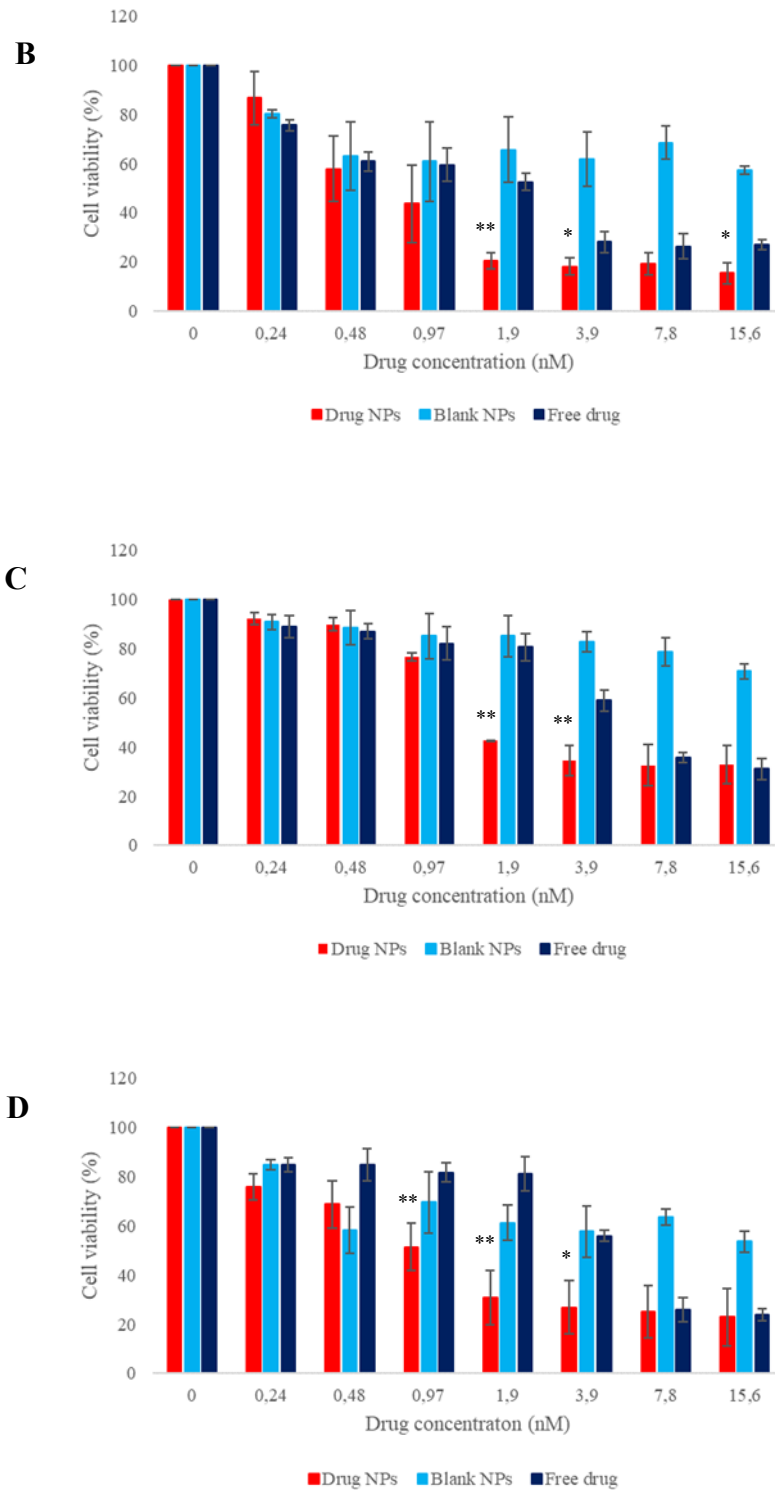


Figure 24: Comparison between the cytotoxicity of CCI-001-loaded HSA NPs, blank NPs and free CCI-001 in: A) SW-620 48h, B) SW-620 72h, C) HCT-116 48h, D) HCT-116 72h. Data represent average \pm SD (n=3).

* means statistically different from free drug ($\alpha < 0.05$, Student *t*-test).

** means statistically different from free drug ($\alpha < 0.01$, Student *t*-test).

At all the incubation times, the drug-loaded nanoparticles resulted to be more cytotoxic than the free drug. In particular, it is important to observe how at both 48h and 72h, the IC_{50} of the drug-loaded nanoparticles was lower than the one of the free drug, providing evidence that the nanoparticle formulation started to be cytotoxic earlier, at lower concentrations. The carrier alone showed a certain cytotoxicity, which was mainly time and concentration-dependent, since it showed higher cytotoxicity at 72h, compared to 48h, and at higher nanoparticles concentrations (which means also higher amount of glutaraldehyde). The positive aspect is that at the IC_{50} , which is the most important concentration to consider, the carrier did not show high toxicities. From the results obtained, it seems that from the IC_{50} on, at the higher concentrations, the cell lines did not show a dose-response, since the cell viability remained constant. Figure 25 shows the trend of the cell viability for the CCI-001-HSA nanoparticles in SW-620 and HCT-116 cancer cell lines. As it is possible to observe, the efficacy of the formulation was time-dependent: at 72h, the nanoparticles exhibited more cytotoxicity than at 48h, as it was expected.

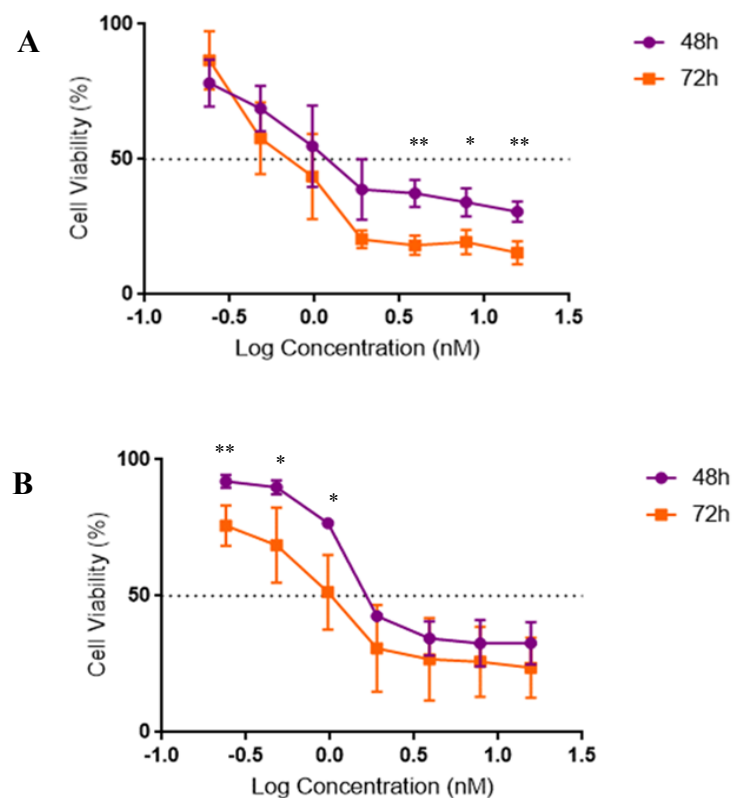


Figure 25: Comparison of the drug-loaded NPs effects at 48 and 72h in: A) SW-620, B) HCT-116. Data represent average \pm SD (n=3).

* means statistically different from 72h ($\alpha < 0.05$, Student *t*-test).

** means statistically different from 72h ($\alpha < 0.01$, Student *t*-test).

5 Conclusions

Cancer is one of the leading causes of death worldwide and new smart and effective treatments are needed in order to reduce the mortality. Therefore, many drug development studies and drug delivery studies are being performed. In fact, the outcome of a treatment not only depends on the active ingredient chosen and used, but also on the particular delivery system adopted to transport the compound inside the body. That is the reason why nowadays there is an urgent need to find new carriers for the delivery of anti-cancer agents. Over the past three decades, different complex formulations have been produced. However, only ten nanoparticles-based preparations have been FDA approved and of the formulations that reached phase III clinical trials, only 14% have been successful at demonstrating efficacy²⁵⁰. Nanoparticles have been beneficial and have been proven to be very effective at delivering chemotherapeutics. Furthermore, nanomedicine has improved patient tolerance by reducing systemic toxicity. In this research project, albumin has been chosen as a possible carrier for the very lipophilic compound, CCI-001, a colchicine derivative. Its capability to bind even the least water soluble compounds, its biocompatibility, biodegradability, non-toxicity and wide availability make the protein a very appealing carrier in drug delivery.

After various trials and different techniques adopted, the results of the present study demonstrated that a modified version of the already known desolvation method, based on an incubation process, allowed to produce stable CCI-001-loaded albumin nanoparticles, characterized by an average diameter of ~ 130 nm, with a narrow size distribution, and a negative charge, with a zeta potential of ~ -30 mV. The nanoparticles exhibited a spherical, uniform and homogeneous morphology. The features of the nanoparticles obtained could be modulated by modifying some of the process parameters. The smallest and most uniform nanoparticles were produced by using ethanol as desolvating agent, glutaraldehyde as crosslinking agent, stirring speed of around 600 rpm, and adjusting the pH by adding 50 μ L NaOH for human serum albumin and 25 μ L NaOH for bovine serum albumin. The incubation overnight at 37°C allowed to achieve, even though in low amount, the entrapment of the drug inside the protein nanoparticles (some of the drug might be encapsulated in the protein matrix, but the majority was most likely weakly attached to the surface of the protein). In particular, the ratio ethanol/water used for the drug solution played a vital role in the achievement of the formulation: the optimal ratio,

1:4, allowed to obtain a clear drug solution, essential requirement for the incubation overnight with the already crosslinked albumin nanoparticles, and prevented the formation of precipitates. Loaded human serum albumin and loaded bovine serum albumin nanoparticles showed almost the same characteristics, with the only differences that the former ones were slightly bigger than the latter ones and they showed a higher homogeneity in size. In both cases, the drug-loaded nanoparticles exhibited a bigger size and a more negative zeta potential than the relative blank nanoparticles (without drug), which probably was a sign of the successful attachment or encapsulation of the drug. For evaluating the interaction and affinity between the protein and the drug, two parameters were calculated: the entrapment efficiency and the drug loading. In the first case, the amount of encapsulated drug was compared to the amount of originally supplied drug, whereas the second parameter, even more significant, was obtained by comparing the amount of encapsulated drug to the amount of carrier (albumin) used in the formulation. The best formulations showed an encapsulation efficiency of ~ 6%, and the maximum drug loading, ~ 6 µg drug per mg albumin (which was still good due to the extremely high potency and cytotoxicity of CCI-001, characterized by a very low IC₅₀, in the range of nM), was obtained using a drug/albumin ratio of 1:10. The nanoparticles *in vitro* release studies of CCI-001 from albumin nanoparticles showed a sustained release pattern over 24-25 hours without any initial burst release. On the other hand, the free drug was released faster, reaching a 100% release in around 4 hours. Although it was not a very slow and prolonged release profile, the loaded albumin nanoparticles had the ability to control the release of CCI-001 in physiological conditions. Furthermore, in theory, the carrier chosen should reduce the off-target distribution and improve drastically the selectivity of the anti-cancer drug, due to the potential ability of albumin to specifically target the tumours through both passive targeting, and mainly active targeting (recognition by gp60 receptor and SPARC pathways), without the need of external ligands, which is one of the key strengths of albumin as a carrier. Although improved and prolonged, even the release from albumin nanoparticles was not very slow, compared to other formulations in the market. This is most likely due to the fact that the compound and the carrier do not interact strongly with each other, and the majority of CCI-001 is weakly attached to the surface of the nanoparticles, instead of being all encapsulated inside the albumin matrix and being gradually released through diffusion. Lyophilized loaded nanoparticles were obtained by freeze-drying in presence of the cryoprotectant trehalose and they showed the same characteristics (size and zeta potential) and release profiles of the fresh nanoparticles. In

particular, the presence of a cryoprotectant resulted to be fundamental for the achievement of stable solid powder: without trehalose, the nanoparticles aggregated and showed no stability. A cytotoxicity study on colorectal cancer cells (SW-620 and HCT-116) was performed to evaluate the efficiency and the activity of the encapsulated drug, compared to the free drug. Furthermore, it was important to evaluate the effects of blank nanoparticles on the cancer cells, to see if the carrier used in the formulations exerted toxic effects on biological systems (mainly to investigate the influence of glutaraldehyde). The CCI-001-loaded HSA nanoparticles exhibited cytotoxicity on all the cancer cell lines, with IC_{50} values which were even lower than the ones of the free drug: this fact provided evidence of the efficacy of the formulation, since the nanoparticles maintained the efficacy of the free compound. Since their IC_{50} was lower, they exhibited even greater activity than the free CCI-001, which could be partly due to improved selectivity of the formulation and higher uptake by the cells, but most likely to the additive effect of the crosslinking agent, glutaraldehyde, which has been previously shown to exert some toxicities on the cells²⁴⁷.

6 Limitations and future directions

In this study, the crosslinking agent chosen and adopted for the formulation of the crosslinked drug-loaded albumin nanoparticles was glutaraldehyde, one of the most effective and commonly used crosslinkers. As the cell toxicity studies showed, unfortunately the carrier of the nanoparticles resulted to be slightly cytotoxic, in a time and concentration-dependent manner. The contribution of glutaraldehyde could be the main reason why the nanoparticles showed a lower IC_{50} and an even greater efficacy, compared to the free drug, in an additive, and not synergistic, way. The results obtained in the cell toxicity studies of the carrier are in agreement with the observation of Niknejad et al²⁴⁷, who demonstrated that cells treated with nanoparticles crosslinked with glutaraldehyde exhibited a cell viability of $40.04\% \pm 6.6$. In the same way, they found out that crosslinking with UV and glucose, separately, produced even higher toxicity, determining a cell viability of $16.48\% \pm 3.87\%$ and $14.29\% \pm 3.60\%$, respectively. On the other hand, crosslinking with the combination of UV and glucose was much less harmful to the cells, causing a cell viability of $76.59\% \pm 7.67\%$. Various papers indicate the toxic effects of glutaraldehyde, including skin sensitivity resulting in dermatitis and irritation of the eyes and nose²⁵¹. In particular, a study conducted in North Carolina²⁵² in the human TK6 lymphoblast cell line and in primary cultures of rat hepatocytes demonstrated that the cause of glutaraldehyde's toxicity lies in the fact that the compound is able to induce DNA-protein crosslinking in a concentration-dependent manner, inducing mutations²⁵², and even extremely low concentrations of glutaraldehyde were capable of inducing significant DNA-protein crosslinking. This provides further evidence of glutaraldehyde's ability to react rapidly and irreversibly with proteins. Furthermore, glutaraldehyde was used in a two-component surgical adhesive with albumin (BioGlue) and, although it provided strong adherence to tissues and synthetic materials, its release could cause *in vitro* and *in vivo* side effects²⁵³, which included edema, inflammation and toxic necrosis. The remaining of toxic aldehyde residues in the nanoparticles are the problem of using glutaraldehyde as a crosslinker. For these reasons, a possible future direction would be to try and replace the glutaraldehyde with more biocompatible alternatives, such as the combination of UV + glucose, which exhibited lower cellular toxicity, even though each one alone was toxic for the cells, or natural alternatives, such as citric acid, ascorbic acid, tannic acid and sorbitol, which have demonstrated to possess the same crosslinking effects²⁵⁴, or genipin, which is a naturally obtained substance, that

offers excellent crosslinking ability in biological tissues and biopolymers through covalent coupling. It is safer and degrades slower than glutaraldehyde²⁵⁵. Genipin has been used as a crosslinking agent in a Chinese study, conducted in 2018, in which researchers developed human serum albumin fragments (HSAFs) nanoparticles to carry paclitaxel¹⁸⁰. Another possibility, already adopted by Chinese researchers in 2016, would be to use a Schiff base- containing vanillin as a crosslinking agent²⁵⁶. Schiff base has been demonstrated to have therapeutic potential, including antibacterial, anticancer and antiproliferative activities. Vanillin, a water-soluble aromatic compound, has been proven to be nontoxic and generally safe. The crosslinking, as in the case of glutaraldehyde, involves the chemical reaction between the amino groups of albumin and the aldehyde groups of vanillin, generating imine groups. Furthermore, hydrogen bonds can be formed between the hydroxyl groups of vanillin and albumin. Another alternative would be to use glyoxal, a recently discovered crosslinking agent belonging to the same family of glutaraldehyde, but which has shown to be much less toxic and to have less influence on cell viability²⁵⁷.

In this study, we were not able to obtain a very high encapsulation efficiency, regardless of the technique and method adopted. This was probably due to the extremely high lipophilicity of the compound, which did not show high attraction to and interaction with the protein carrier, as opposed to what happens with other lipophilic agents, such as colchicine. The interaction between colchicine and human serum albumin was investigated by fluorescence and UV-Vis spectroscopy. The results exhibited the formation of colchicine-HSA complexes, where Van der Waals interactions and hydrogen bonds played a vital role in the stability of the complex²⁵⁸. In particular, the binding site for colchicine on human serum albumin is located in sub-domain IIA (Trp²¹⁴). For this reason, being a derivative of colchicine, it was thought that albumin could be a smart and efficient delivery system for CCI-001. However, CCI-001 exhibits a solubility in water at pH 7.4 of 0.007 mg/mL, very low compared to the 7 mg/mL of colchicine and that could be one of the reasons why it interacts much less with the carrier. For these reasons, although the results of this study indicate the potential use of these NPs as drug carriers in biological systems, the formulation should be further investigated and modified, to improve its characteristics and provide higher loaded drug levels for a more efficient delivery to tumours and further animal or human studies. A possibility could be to replace the lipophilic drug with a more hydrophilic version, such as the ammine derivative of the

drug. An increased hydrophilicity would probably allow a higher encapsulation capacity and interaction with the cargo.

Another possible future direction in this study could be to perform a cellular uptake study, in order to investigate the capability of the protein carrier to be internalized by the cells. As stated above, albumin has been extensively proven to be recognized and internalized by its receptor gp60 and by the SPARC pathway. For this reason, the formulation should be able to improve the selectivity and the specificity of the drug, reducing the off-target side effects, letting the compound enter directly the target site. In this study, due to the lack of time, no uptake study was performed. The results of the cytotoxicity assays showed that the IC_{50} of the drug-loaded nanoparticles are even lower than the one of the free drug and that could be due to the contribution of glutaraldehyde, which exert cytotoxicity on the cells, but also due to the augmented uptake of the formulation by the cells, compared to the free drug. That is the reason why conducting some cellular uptake studies would be very useful to investigate better the reasons for the improved efficacy of the formulation and the advantages of the nanoparticle formulation over the free compound. Furthermore, it would provide a clear idea of the period of time required to the cells for the internalization of the drug-loaded albumin nanoparticles.

Another future direction to investigate would be the possibility of a chemical conjugation between the drug and the protein carrier, which would allow to overcome the obstacles of the low encapsulation efficiency and the hydrophobic interactions. Therefore, instead of analysing a physical interaction between albumin and the drug, it would be smart to analyse further a chemical attachment of the drug to the protein. Albumin, as already stated, possesses numerous functional groups that can be used to attach various compounds. The chemical conjugation can happen by covalent linking of the cargo directly or *via* linker. Albumin has cysteine residues that can attach to a maleimide group. If a linker is used, it is possible to connect a drug to a linker with a maleimide group and attach it to the Cys-34 residue of albumin, allowing the covalent attachment of protein and the payload. For this reason, the ammine derivative of CCI-001, conjugated with a linker that may interact and bind covalently to albumin, could be useful. An important aspect to keep in mind is that a chemical conjugation of the drug would involve a much more stable attachment with the carrier, which would certainly alter the release profile

and the pharmacokinetics parameters, compared with a physical interaction, based on hydrophobic forces between the compound and the carrier.

7 References

1. Fouad, Y. A. & Aanei, C. Revisiting the hallmarks of cancer. *Am. J. Cancer Res.* **7**, 1016–1036 (2017).
2. Schirmacher, V. From chemotherapy to biological therapy: A review of novel concepts to reduce the side effects of systemic cancer treatment (Review). *Int. J. Oncol.* **54**, 407–419 (2018).
3. Benjamin, D. J. The efficacy of surgical treatment of cancer – 20years later. *Med. Hypotheses* **82**, 412–420 (2014).
4. Baskar, R., Lee, K. A., Yeo, R. & Yeoh, K.-W. Cancer and Radiation Therapy: Current Advances and Future Directions. *Int. J. Med. Sci.* **9**, 193–199 (2012).
5. Chabner, B. A. & Roberts, T. G. Chemotherapy and the war on cancer. *Nat. Rev. Cancer* **5**, 65–72 (2005).
6. Esfahani, K. *et al.* A review of cancer immunotherapy: from the past, to the present, to the future. *Curr. Oncol.* **27**, S87–S97 (2020).
7. Seebacher, N. A., Stacy, A. E., Porter, G. M. & Merlot, A. M. Clinical development of targeted and immune based anti-cancer therapies. *J. Exp. Clin. Cancer Res.* **38**, 156 (2019).
8. Amer, M. H. Gene therapy for cancer: present status and future perspective. *Mol. Cell. Ther.* **2**, (2014).
9. Soares, S., Sousa, J., Pais, A. & Vitorino, C. Nanomedicine: Principles, Properties, and Regulatory Issues. *Front. Chem.* **6**, (2018).

10. Bozzuto, G. & Molinari, A. Liposomes as nanomedical devices. *Int. J. Nanomedicine* **975** (2015) doi:10.2147/IJN.S68861.
11. Islam, W. *et al.* Augmentation of the Enhanced Permeability and Retention Effect with Nitric Oxide-Generating Agents Improves the Therapeutic Effects of Nanomedicines. *Mol. Cancer Ther.* **17**, 2643–2653 (2018).
12. Tahara, Y. *et al.* Encapsulation of a nitric oxide donor into a liposome to boost the enhanced permeation and retention (EPR) effect. *MedChemComm* **8**, 415–421 (2017).
13. Praetorius, N. & Mandal, T. Engineered Nanoparticles in Cancer Therapy. *Recent Pat. Drug Deliv. Formul.* **1**, 37–51 (2007).
14. Lowe, S., O'Brien-Simpson, N. M. & Connal, L. A. Antibiofouling polymer interfaces: poly(ethylene glycol) and other promising candidates. *Polym. Chem.* **6**, 198–212 (2014).
15. Perry, J. L. *et al.* PEGylated PRINT Nanoparticles: The Impact of PEG Density on Protein Binding, Macrophage Association, Biodistribution, and Pharmacokinetics. *Nano Lett.* **12**, 5304–5310 (2012).
16. Toy, R. & Roy, K. Engineering nanoparticles to overcome barriers to immunotherapy. *Bioeng. Transl. Med.* **1**, 47–62 (2016).
17. Pollard, T. D. & Borisy, G. G. Cellular Motility Driven by Assembly and Disassembly of Actin Filaments. *Cell* **112**, 453–465 (2003).
18. Melak, M., Plessner, M. & Grosse, R. Actin visualization at a glance. *J. Cell Sci.* **130**, 525–530 (2017).

19. Buehler, M. J. Mechanical Players—The Role of Intermediate Filaments in Cell Mechanics and Organization. *Biophys. J.* **105**, 1733–1734 (2013).
20. Eriksson, J. E. *et al.* Introducing intermediate filaments: from discovery to disease. *J. Clin. Invest.* **119**, 1763–1771 (2009).
21. Sanghvi-Shah, R. & Weber, G. F. Intermediate Filaments at the Junction of Mechanotransduction, Migration, and Development. *Front. Cell Dev. Biol.* **5**, (2017).
22. Heald, R. & Nogales, E. Microtubule dynamics. *J. Cell Sci.* **115**, 3–4 (2002).
23. Muroyama, A. & Lechler, T. Microtubule organization, dynamics and functions in differentiated cells. *Development* **144**, 3012–3021 (2017).
24. Akhmanova, A. & Steinmetz, M. O. Tracking the ends: a dynamic protein network controls the fate of microtubule tips. *Nat. Rev. Mol. Cell Biol.* **9**, 309–322 (2008).
25. Brouhard, G. J. & Rice, L. M. Microtubule Dynamics: an interplay of biochemistry and mechanics. *Nat. Rev. Mol. Cell Biol.* **19**, 451–463 (2018).
26. Lasser, M., Tiber, J. & Lowery, L. A. The Role of the Microtubule Cytoskeleton in Neurodevelopmental Disorders. *Front. Cell. Neurosci.* **12**, (2018).
27. Horio, T. & Murata, T. The role of dynamic instability in microtubule organization. *Front. Plant Sci.* **5**, (2014).
28. Microtubule assembly during mitosis – from distinct origins to distinct functions? | Journal of Cell Science. <https://jcs.biologists.org/content/125/12/2805>.

29. Gadadhar, S., Bodakuntla, S., Natarajan, K. & Janke, C. The tubulin code at a glance. *J. Cell Sci.* **130**, 1347–1353 (2017).
30. Janke, C. & Magiera, M. M. The tubulin code and its role in controlling microtubule properties and functions. *Nat. Rev. Mol. Cell Biol.* 1–20 (2020) doi:10.1038/s41580-020-0214-3.
31. Huzil, J. T., Ludueña, R. F. & Tuszynski, J. Comparative modelling of human β tubulin isotypes and implications for drug binding. *Nanotechnology* **17**, S90 (2006).
32. Leandro-García, L. J. *et al.* Tumoral and tissue-specific expression of the major human β -tubulin isotypes. *Cytoskeleton* **67**, 214–223 (2010).
33. Janke, C. & Magiera, M. M. The tubulin code and its role in controlling microtubule properties and functions. *Nat. Rev. Mol. Cell Biol.* (2020) doi:10.1038/s41580-020-0214-3.
34. Wehenkel, A. & Janke, C. Towards elucidating the tubulin code. *Nat. Cell Biol.* **16**, 303–305 (2014).
35. Janke, C. The tubulin code: Molecular components, readout mechanisms, and functions. *J. Cell Biol.* **206**, 461–472 (2014).
36. Ferreira, L. T., Figueiredo, A. C., Orr, B., Lopes, D. & Maiato, H. Dissecting the role of the tubulin code in mitosis. in *Methods in Cell Biology* vol. 144 33–74 (Elsevier, 2018).
37. Binarová, P. & Tuszynski, J. Tubulin: Structure, Functions and Roles in Disease. *Cells* **8**, (2019).

38. Dumontet, C. & Jordan, M. A. Microtubule-binding agents: a dynamic field of cancer therapeutics. *Nat. Rev. Drug Discov.* **9**, 790–803 (2010).
39. Bates, D. & Eastman, A. Microtubule destabilising agents: far more than just antimetabolic anticancer drugs. *Br. J. Clin. Pharmacol.* **83**, 255–268 (2017).
40. Kaul, R., Risinger, A. L. & Mooberry, S. L. Microtubule-Targeting Drugs: More than Antimetabolites. *J. Nat. Prod.* **82**, 680–685 (2019).
41. Lee, J. J. & Swain, S. M. Peripheral neuropathy induced by microtubule-stabilizing agents. *J. Clin. Oncol. Off. J. Am. Soc. Clin. Oncol.* **24**, 1633–1642 (2006).
42. Schwartz, E. L. Antivascular Actions of Microtubule-Binding Drugs. *Clin. Cancer Res.* **15**, 2594–2601 (2009).
43. Siemann, D. W. The Unique Characteristics of Tumor Vasculature and Preclinical Evidence for its Selective Disruption by Tumor-Vascular Disrupting Agents. *Cancer Treat. Rev.* **37**, 63–74 (2011).
44. Hillen, F. & Griffioen, A. W. Tumour vascularization: sprouting angiogenesis and beyond. *Cancer Metastasis Rev.* **26**, 489–502 (2007).
45. Wu, C. Focal Adhesion. *Cell Adhes. Migr.* **1**, 13–18 (2007).
46. Lampugnani, M. G. Endothelial adherens junctions and the actin cytoskeleton: an ‘infinity net’? *J. Biol.* **9**, 16 (2010).
47. Ganguly, A. & Cabral, F. New insights into mechanisms of resistance to microtubule inhibitors. *Biochim. Biophys. Acta* **1816**, 164–171 (2011).

48. Mohammad, I. S., He, W. & Yin, L. Understanding of human ATP binding cassette superfamily and novel multidrug resistance modulators to overcome MDR. *Biomed. Pharmacother.* **100**, 335–348 (2018).
49. Choi, C.-H. ABC transporters as multidrug resistance mechanisms and the development of chemosensitizers for their reversal. *Cancer Cell Int.* **5**, 30 (2005).
50. Choi, Y. H. & Yu, A.-M. ABC Transporters in Multidrug Resistance and Pharmacokinetics, and Strategies for Drug Development. *Curr. Pharm. Des.* **20**, 793–807 (2014).
51. Li, W. *et al.* Overcoming ABC transporter-mediated multidrug resistance: Molecular mechanisms and novel therapeutic drug strategies. *Drug Resist. Updat.* **27**, 14–29 (2016).
52. Amin, Md. L. P-glycoprotein Inhibition for Optimal Drug Delivery. *Drug Target Insights* **7**, 27–34 (2013).
53. Naito, M. & Tsuruo, T. Reversal of Tumour Drug Resistance with Monoclonal Antibodies: Prospects and Problems. *Clin. Immunother.* **5**, 91–95 (1996).
54. Heike, Y. *et al.* Monoclonal Anti-P-glycoprotein Antibody-dependent Killing of Multidrug-resistant Tumor Cells by Human Mononuclear Cells. *Jpn. J. Cancer Res. Gann* **81**, 1155–1161 (1990).
55. Tew, K. D. Glutathione-Associated Enzymes In Anticancer Drug Resistance. *Cancer Res.* **76**, 7–9 (2016).
56. Bansal, A. & Simon, M. C. Glutathione metabolism in cancer progression and treatment resistance. *J. Cell Biol.* **217**, 2291–2298 (2018).

57. Prasad, A., Pospíšil, P. & Tada, M. Editorial: Reactive Oxygen Species (ROS) Detection Methods in Biological System. *Front. Physiol.* **10**, (2019).
58. Murphy, M. P. *et al.* Unravelling the Biological Roles of Reactive Oxygen Species. *Cell Metab.* **13**, 361–366 (2011).
59. Hayes, J. D. & McLellan, L. I. Glutathione and glutathione-dependent enzymes represent a co-ordinately regulated defence against oxidative stress. *Free Radic. Res.* **31**, 273–300 (1999).
60. Galadari, S., Rahman, A., Pallichankandy, S. & Thayyullathil, F. Reactive oxygen species and cancer paradox: To promote or to suppress? *Free Radic. Biol. Med.* **104**, 144–164 (2017).
61. Hayes, J. D. & McLellan, L. I. Glutathione and glutathione-dependent enzymes represent a co-ordinately regulated defence against oxidative stress. *Free Radic. Res.* **31**, 273–300 (1999).
62. Pljesa-Ercegovac, M. *et al.* Glutathione Transferases: Potential Targets to Overcome Chemoresistance in Solid Tumors. *Int. J. Mol. Sci.* **19**, (2018).
63. Vogelstein, B., Lane, D. & Levine, A. J. Surfing the p53 network. *Nature* **408**, 307–310 (2000).
64. Aubrey, B. J., Kelly, G. L., Janic, A., Herold, M. J. & Strasser, A. How does p53 induce apoptosis and how does this relate to p53-mediated tumour suppression? *Cell Death Differ.* **25**, 104–113 (2018).
65. Brady, C. A. & Attardi, L. D. p53 at a glance. *J. Cell Sci.* **123**, 2527–2532 (2010).

66. Zhou, X., Hao, Q. & Lu, H. Mutant p53 in cancer therapy—the barrier or the path. *J. Mol. Cell Biol.* **11**, 293–305 (2018).
67. Hientz, K., Mohr, A., Bhakta-Guha, D. & Efferth, T. The role of p53 in cancer drug resistance and targeted chemotherapy. *Oncotarget* **8**, 8921–8946 (2016).
68. Martinez-Rivera, M. & Siddik, Z. H. Resistance and gain-of-resistance phenotypes in cancers harboring wild-type p53. *Biochem. Pharmacol.* **83**, 1049–1062 (2012).
69. Haupt, S. Apoptosis - the p53 network. *J. Cell Sci.* **116**, 4077–4085 (2003).
70. Czabotar, P. E., Lessene, G., Strasser, A. & Adams, J. M. Control of apoptosis by the BCL-2 protein family: implications for physiology and therapy. *Nat. Rev. Mol. Cell Biol.* **15**, 49–63 (2014).
71. Youle, R. J. & Strasser, A. The BCL-2 protein family: opposing activities that mediate cell death. *Nat. Rev. Mol. Cell Biol.* **9**, 47–59 (2008).
72. Kale, J., Osterlund, E. J. & Andrews, D. W. BCL-2 family proteins: changing partners in the dance towards death. *Cell Death Differ.* **25**, 65–80 (2018).
73. Antonsson, B. & Martinou, J.-C. The Bcl-2 Protein Family. *Exp. Cell Res.* **256**, 50–57 (2000).
74. Hardwick, J. M. & Soane, L. Multiple Functions of BCL-2 Family Proteins. *Cold Spring Harb. Perspect. Biol.* **5**, a008722 (2013).
75. Adams, J. M. The Bcl-2 Protein Family: Arbiters of Cell Survival. *Science* **281**, 1322–1326 (1998).

76. Fujita, N. & Tsuruo, T. In vivo veritas: Bcl-2 and Bcl-XL mediate tumor cell resistance to chemotherapy. *Drug Resist. Updat.* **3**, 149–154 (2000).
77. García-Aranda, M., Pérez-Ruiz, E. & Redondo, M. Bcl-2 Inhibition to Overcome Resistance to Chemo- and Immunotherapy. *Int. J. Mol. Sci.* **19**, (2018).
78. Azmi, A. S., Wang, Z., Philip, P. A., Mohammad, R. M. & Sarkar, F. H. Emerging Bcl-2 inhibitors for the treatment of cancer. *Expert Opin. Emerg. Drugs* **16**, 59–70 (2011).
79. Czabotar, P. E., Lessene, G., Strasser, A. & Adams, J. M. Control of apoptosis by the BCL-2 protein family: implications for physiology and therapy. *Nat. Rev. Mol. Cell Biol.* **15**, 49–63 (2014).
80. Gores, G. J. & Kaufmann, S. H. Selectively targeting Mcl-1 for the treatment of acute myelogenous leukemia and solid tumors. *Genes Dev.* **26**, 305–311 (2012).
81. Wertz, I. E. *et al.* Sensitivity to antitubulin chemotherapeutics is regulated by MCL1 and FBW7. *Nature* **471**, 110–114 (2011).
82. Mukhtar, E., Adhami, V. M. & Mukhtar, H. Targeting Microtubules by Natural Agents for Cancer Therapy. *Mol. Cancer Ther.* **13**, 275–284 (2014).
83. Stengel, C. *et al.* Class III β -tubulin expression and in vitro resistance to microtubule targeting agents. *Br. J. Cancer* **102**, 316–324 (2010).
84. High Expression of Class III β -Tubulin Predicts Good Response to Neoadjuvant Taxane and Doxorubicin/Cyclophosphamide-Based Chemotherapy in Estrogen Receptor-Negative Breast Cancer | Request PDF. *ResearchGate*
https://www.researchgate.net/publication/233876873_High_Expression_of_Class_III

_b-

Tubulin_Predicts_Good_Response_to_Neoadjuvant_Taxane_and_DoxorubicinCyclophosphamide-Based_Chemotherapy_in_Estrogen_Receptor-Negative_Breast_Cancer
doi:10.1016/j.clbc.2012.11.003.

85. McCarroll, J. A., Gan, P. P., Liu, M. & Kavallaris, M. β III-Tubulin Is a Multifunctional Protein Involved in Drug Sensitivity and Tumorigenesis in Non-Small Cell Lung Cancer. *Cancer Res.* **70**, 4995–5003 (2010).
86. Kavallaris, M. Microtubules and resistance to tubulin-binding agents. *Nat. Rev. Cancer* **10**, 194–204 (2010).
87. Resistance to anti-tubulin agents: From vinca alkaloids to epothilones. <https://cdrjournal.com/article/view/2991> doi:doi : 10.20517/cdr.2019.06.
88. Monzó, M. *et al.* Paclitaxel Resistance in Non-Small-Cell Lung Cancer Associated With Beta-Tubulin Gene Mutations. *J. Clin. Oncol.* **17**, 1786–1786 (1999).
89. Moudi, M., Go, R., Yien, C. Y. S. & Nazre, Mohd. Vinca Alkaloids. *Int. J. Prev. Med.* **4**, 1231–1235 (2013).
90. Rowinsky, E. The Vinca Alkaloids. *Holl.-Frei Cancer Med. 6th Ed.* (2003).
91. Dumontet, C. & Sikic, B. I. Mechanisms of Action of and Resistance to Antitubulin Agents: Microtubule Dynamics, Drug Transport, and Cell Death. *J. Clin. Oncol.* **17**, 1061–1061 (1999).
92. Anticancer activity of Vinca Alkaloids | Request PDF. *ResearchGate* https://www.researchgate.net/publication/216127874_Anticancer_activity_of_Vinca_Alkaloids.

93. Steinmetz, M. O. & Prota, A. E. Microtubule-Targeting Agents: Strategies To Hijack the Cytoskeleton. *Trends Cell Biol.* **28**, 776–792 (2018).
94. Perez, E. A. Microtubule inhibitors: Differentiating tubulin-inhibiting agents based on mechanisms of action, clinical activity, and resistance. *Mol. Cancer Ther.* **8**, 2086–2095 (2009).
95. Johnson, I. S., Armstrong, J. G., Gorman, M. & Burnett, J. P. The Vinca Alkaloids: A New Class of Oncolytic Agents. *Cancer Res.* **23**, 1390–1427 (1963).
96. Lee, C.-T., Huang, Y.-W., Yang, C.-H. & Huang, K.-S. Drug Delivery Systems and Combination Therapy by Using Vinca Alkaloids. *Curr. Top. Med. Chem.* **15**, 1491–1500 (2015).
97. Yassine, F., Salibi, E. & Gali-Muhtasib, H. Overview of the Formulations and Analogs in the Taxanes' Story. *Curr. Med. Chem.* **23**, 4540–4558 (2016).
98. Snyder, J. P., Nettles, J. H., Cornett, B., Downing, K. H. & Nogales, E. The binding conformation of Taxol in β -tubulin: A model based on electron crystallographic density. *Proc. Natl. Acad. Sci.* **98**, 5312–5316 (2001).
99. Safavy, A. Recent developments in taxane drug delivery. *Curr. Drug Deliv.* **5**, 42–54 (2008).
100. Bueno, O. *et al.* High-affinity ligands of the colchicine domain in tubulin based on a structure-guided design. *Sci. Rep.* **8**, 4242 (2018).
101. (PDF) Pharmacological and Clinical Basis of Treatment of Familial Mediterranean Fever (FMF) with Colchicine or Analogues: An Update. *ResearchGate* https://www.researchgate.net/publication/8013645_Pharmacological_and_Clinical_B

asis_of_Treatment_of_Familial_Mediterranean_Fever_FMF_with_Colchicine_or_Analogues_An_Update doi:10.2174/1568010053622984.

102. Chen, J., Liu, T., Dong, X. & Hu, Y. Recent Development and SAR Analysis of Colchicine Binding Site Inhibitors. *Mini-Rev. Med. Chem.* **9**, 1174–1190 (2009).
103. Chen, J., Liu, T., Dong, X. & Hu, Y. Recent Development and SAR Analysis of Colchicine Binding Site Inhibitors. *Mini-Rev. Med. Chem.* **9**, 1174–1190 (2009).
104. Leung, Y. Y., Hui, L. L. Y. & Kraus, V. B. Colchicine --- update on mechanisms of action and therapeutic uses. *Semin. Arthritis Rheum.* **45**, 341–350 (2015).
105. Lu, Y., Chen, J., Xiao, M., Li, W. & Miller, D. D. An Overview of Tubulin Inhibitors That Interact with the Colchicine Binding Site. *Pharm. Res.* **29**, 2943–2971 (2012).
106. Spasevska, I. *et al.* Modeling the Colchicum autumnale Tubulin and a Comparison of Its Interaction with Colchicine to Human Tubulin. *Int. J. Mol. Sci.* **18**, (2017).
107. Patterson, D. M. & Rustin, G. J. S. Vascular Damaging Agents. *Clin. Oncol.* **19**, 443–456 (2007).
108. Arnst, K. E. *et al.* Colchicine Binding Site Agent DJ95 Overcomes Drug Resistance and Exhibits Antitumor Efficacy. *Mol. Pharmacol.* **96**, 73–89 (2019).
109. Lu, Y., Chen, J., Xiao, M., Li, W. & Miller, D. D. An Overview of Tubulin Inhibitors That Interact with the Colchicine Binding Site. *Pharm. Res.* **29**, 2943–2971 (2012).

110. Singh, B. *et al.* Colchicine derivatives with potent anticancer activity and reduced P-glycoprotein induction liability. *Org. Biomol. Chem.* **13**, 5674–5689 (2015).
111. Muvaffak, A., Gurhan, I. & Hasirci, N. Prolonged cytotoxic effect of colchicine released from biodegradable microspheres. *J. Biomed. Mater. Res.* **71B**, 295–304 (2004).
112. Hao, Y., Zhao, F., Li, N., Yang, Y. & Li, K. Studies on a high encapsulation of colchicine by a niosome system. *Int. J. Pharm.* **244**, 73–80 (2002).
113. Doorty, K. B. *et al.* Poly(N-isopropylacrylamide) co-polymer films as potential vehicles for delivery of an antimitotic agent to vascular smooth muscle cells. *Cardiovasc. Pathol.* **12**, 105–110 (2003).
114. Ibim, S. M. *et al.* In Vitro Release of Colchicine Using Poly(phosphazenes): The Development of Delivery Systems for Musculoskeletal Use. *Pharm. Dev. Technol.* **3**, 55–62 (1998).
115. Gladwin S. Das, Gundu H. R. Rao, Ro. Colchicine Encapsulation within Poly(Ethylene Glycol)-Coated Poly(Lactic Acid)/Poly(?-Caprolactone) Microspheres- Controlled Release Studies. *Drug Deliv.* **7**, 129–138 (2000).
116. Shen, Q., Wang, Y. & Zhang, Y. Improvement of colchicine oral bioavailability by incorporating eugenol in the nanoemulsion as an oil excipient and enhancer. *Int. J. Nanomedicine* **6**, 1237–1243 (2011).
117. Bazylińska, U., Zieliński, W., Kulbacka, J., Samoć, M. & Wilk, K. A. New diamidequat-type surfactants in fabrication of long-sustained theranostic

- nanocapsules: Colloidal stability, drug delivery and bioimaging. *Colloids Surf. B Biointerfaces* **137**, 121–132 (2016).
118. Singh, H. P., Utreja, P., Tiwary, A. K. & Jain, S. Elastic Liposomal Formulation for Sustained Delivery of Colchicine: In Vitro Characterization and In Vivo Evaluation of Anti-gout Activity. *AAPS J.* **11**, 54–64 (2009).
119. Abdulbaqi, I. M., Darwis, Y., Assi, R. A. & Khan, N. A. K. Transethosomal gels as carriers for the transdermal delivery of colchicine: statistical optimization, characterization, and ex vivo evaluation. *Drug Des. Devel. Ther.* **12**, 795–813 (2018).
120. Cauda, V. *et al.* Colchicine-Loaded Lipid Bilayer-Coated 50 nm Mesoporous Nanoparticles Efficiently Induce Microtubule Depolymerization upon Cell Uptake. *Nano Lett.* **10**, 2484–2492 (2010).
121. AbouAitah, K. *et al.* Targeted Nano-Drug Delivery of Colchicine against Colon Cancer Cells by Means of Mesoporous Silica Nanoparticles. *Cancers* **12**, 144 (2020).
122. Nasr, M., Younes, H. & Abdel-Rashid, R. S. Formulation and evaluation of cubosomes containing colchicine for transdermal delivery. *Drug Deliv. Transl. Res.* (2020) doi:10.1007/s13346-020-00785-6.
123. Zhang, L. *et al.* A novel colchicine/gadolinium-loading tubulin self-assembly nanocarrier for MR imaging and chemotherapy of glioma. *Nanotechnology* **31**, 255601 (2020).
124. Hu, Y.-J., Liu, Y., Zhao, R.-M. & Qu, S.-S. Interaction of colchicine with human serum albumin investigated by spectroscopic methods. *Int. J. Biol. Macromol.* **37**, 122–126 (2005).

125. Slobodnick, A., Shah, B., Pillinger, M. H. & Krasnokutsky, S. COLCHICINE: OLD AND NEW. *Am. J. Med.* **128**, 461–470 (2015).
126. Bladder cancer paper_JT_PB_June_26 (1)(1) copy.pdf.
127. CR42-24.pdf.
128. Yeh, L.-C. C. *et al.* Effect of CH-35, a novel anti-tumor colchicine analogue, on breast cancer cells overexpressing the β III isotype of tubulin. *Invest. New Drugs* **34**, 129–137 (2016).
129. OncolinesProfiler report CR42-24.pdf.
130. micellar formulation of CR 42024 March 2014_updated 17 March.pdf.
131. Larsen, M. T., Kuhlmann, M., Hvam, M. L. & Howard, K. A. Albumin-based drug delivery: harnessing nature to cure disease. *Mol. Cell. Ther.* **4**, 3 (2016).
132. Kouchakzadeh, H., Safavi, M. S. & Shojaosadati, S. A. Efficient Delivery of Therapeutic Agents by Using Targeted Albumin Nanoparticles. in *Advances in Protein Chemistry and Structural Biology* vol. 98 121–143 (Elsevier, 2015).
133. Fanali, G. *et al.* Human serum albumin: From bench to bedside. *Mol. Aspects Med.* **33**, 209–290 (2012).
134. Fu, Q. *et al.* Nanoparticle Albumin - Bound (NAB) Technology is a Promising Method for Anti-Cancer Drug Delivery. *Recent Patents Anticancer Drug Discov.* **4**, 262–272 (2009).
135. Caraceni, P., Tufoni, M. & Bonavita, M. E. Clinical use of albumin. *Blood Transfus.* **11**, s18–s25 (2013).

136. Carvalho, J. R. & Machado, M. V. New Insights About Albumin and Liver Disease. *Ann. Hepatol.* **17**, 547–560 (2018).
137. Levitt, D. G. & Levitt, M. D. Human serum albumin homeostasis: a new look at the roles of synthesis, catabolism, renal and gastrointestinal excretion, and the clinical value of serum albumin measurements. *Int. J. Gen. Med.* **9**, 229–255 (2016).
138. Bertucci, C. & Domenici, E. Reversible and Covalent Binding of Drugs to Human Serum Albumin: Methodological Approaches and Physiological Relevance. *Curr. Med. Chem.* **9**, 1463–1481 (2002).
139. Arroyo, V., García-Martínez, R. & Salvatella, X. Human serum albumin, systemic inflammation, and cirrhosis. *J. Hepatol.* **61**, 396–407 (2014).
140. Ge, P. *et al.* Albumin Binding Function: The Potential Earliest Indicator for Liver Function Damage. *Gastroenterol. Res. Pract.* **2016**, 1–7 (2016).
141. Phan, H. T. M., Bartelt-Hunt, S., Rodenhausen, K. B., Schubert, M. & Bartz, J. C. Investigation of Bovine Serum Albumin (BSA) Attachment onto Self-Assembled Monolayers (SAMs) Using Combinatorial Quartz Crystal Microbalance with Dissipation (QCM-D) and Spectroscopic Ellipsometry (SE). *PLOS ONE* **10**, e0141282 (2015).
142. Elzoghby, A. O., Samy, W. M. & Elgindy, N. A. Albumin-based nanoparticles as potential controlled release drug delivery systems. *J. Controlled Release* **157**, 168–182 (2012).

143. Hilton, J., Dearman, R. J., Sattar, N., Basketter, D. A. & Kimber, I. Characteristics of antibody responses induced in mice by protein allergens. *Food Chem. Toxicol.* **35**, 1209–1218 (1997).
144. Mogues, T., Li, J., Coburn, J. & Kuter, D. J. IgG antibodies against bovine serum albumin in humans—their prevalence and response to exposure to bovine serum albumin. *J. Immunol. Methods* **300**, 1–11 (2005).
145. Perrudet-Badoux, A. & Frei, P. C. Immunogenicity of Bovine Serum Albumin in Adult Rabbits of Various Strains. *Int. Arch. Allergy Immunol.* **40**, 928–933 (1971).
146. Lv, L., Chi, Y., Chen, C. & Xu, W. Structural and Functional Properties of Ovalbumin Glycated by Dry-Heating in the Presence of Maltodextrin. *Int. J. Food Prop.* **18**, 1326–1333 (2015).
147. Huntington, J. A. & Stein, P. E. Structure and properties of ovalbumin. *J. Chromatogr. B. Biomed. Sci. App.* **756**, 189–198 (2001).
148. Zheng, N., Zhu, S., Liu, L. & Yu, X. Rat serum albumin is not equal to human serum albumin. *Fertil. Steril.* **95**, e81 (2011).
149. Hoogenboezem, E. N. & Duvall, C. L. Harnessing albumin as a carrier for cancer therapies. *Adv. Drug Deliv. Rev.* **130**, 73–89 (2018).
150. Li, C. *et al.* Current multifunctional albumin-based nanoplatfoms for cancer multi-mode therapy. *Asian J. Pharm. Sci.* **15**, 1–12 (2020).
151. Loureiro, A., G. Azoia, N., C. Gomes, A. & Cavaco-Paulo, A. Albumin-Based Nanodevices as Drug Carriers. *Curr. Pharm. Des.* **22**, 1371–1390 (2016).

152. Sindhvani, S. *et al.* The entry of nanoparticles into solid tumours. *Nat. Mater.* **19**, 566–575 (2020).
153. Nakamura, Y., Mochida, A., Choyke, P. L. & Kobayashi, H. Nanodrug Delivery: Is the Enhanced Permeability and Retention Effect Sufficient for Curing Cancer? *Bioconjug. Chem.* **27**, 2225–2238 (2016).
154. Kinoshita, R. *et al.* Improved anticancer effects of albumin-bound paclitaxel nanoparticle via augmentation of EPR effect and albumin-protein interactions using S-nitrosated human serum albumin dimer. *Biomaterials* **140**, 162–169 (2017).
155. Desai, N. Nanoparticle Albumin-Bound Paclitaxel (Abraxane®). in *Albumin in Medicine* (eds. Otagiri, M. & Chuang, V. T. G.) 101–119 (Springer Singapore, 2016). doi:10.1007/978-981-10-2116-9_6.
156. Bern, M., Sand, K. M. K., Nilsen, J., Sandlie, I. & Andersen, J. T. The role of albumin receptors in regulation of albumin homeostasis: Implications for drug delivery. *J. Controlled Release* **211**, 144–162 (2015).
157. Sand, K. M. K. *et al.* Unraveling the Interaction between FcRn and Albumin: Opportunities for Design of Albumin-Based Therapeutics. *Front. Immunol.* **5**, (2015).
158. Roopenian, D. C. & Akilesh, S. FcRn: the neonatal Fc receptor comes of age. *Nat. Rev. Immunol.* **7**, 715–725 (2007).
159. Chaudhury, C., Brooks, C. L., Carter, D. C., Robinson, J. M. & Anderson, C. L. Albumin binding to FcRn: distinct from the FcRn-IgG interaction. *Biochemistry* **45**, 4983–4990 (2006).

160. Yoo, J., Park, C., Yi, G., Lee, D. & Koo, H. Active Targeting Strategies Using Biological Ligands for Nanoparticle Drug Delivery Systems. *Cancers* **11**, 640 (2019).
161. Zu. Preparation, characterization, and in vitro targeted delivery of folate-decorated paclitaxel-loaded bovine serum albumin nanoparticles. *Int. J. Nanomedicine* **669** (2010) doi:10.2147/IJN.S12918.
162. Fanciullino, R., Ciccolini, J. & Milano, G. Challenges, expectations and limits for nanoparticles-based therapeutics in cancer: A focus on nano-albumin-bound drugs. *Crit. Rev. Oncol. Hematol.* **88**, 504–513 (2013).
163. Qu, N. *et al.* Docetaxel-loaded human serum albumin (HSA) nanoparticles: synthesis, characterization, and evaluation. *Biomed. Eng. OnLine* **18**, (2019).
164. Jokerst, J. V., Lobovkina, T., Zare, R. N. & Gambhir, S. S. Nanoparticle PEGylation for imaging and therapy. *Nanomed.* **6**, 715–728 (2011).
165. Gradishar, W. J. Albumin-bound paclitaxel: a next-generation taxane. *Expert Opin. Pharmacother.* **7**, 1041–1053 (2006).
166. Gupta, N., Hatoum, H. & Dy, G. First line treatment of advanced non-small-cell lung cancer - Specific focus on albumin bound paclitaxel. *Int. J. Nanomedicine* **9**, 209–221 (2014).
167. Rajeshkumar, N. V. *et al.* Superior therapeutic efficacy of nab -paclitaxel over cremophor-based paclitaxel in locally advanced and metastatic models of human pancreatic cancer. *Br. J. Cancer* **115**, 442–453 (2016).
168. Stinchcombe, T. E. Nanoparticle albumin-bound paclitaxel: a novel Cremphor-EL[®] -free formulation of paclitaxel. *Nanomed.* **2**, 415–423 (2007).

169. Hawkins, M. J., Soon-Shiong, P. & Desai, N. Protein nanoparticles as drug carriers in clinical medicine. *Adv. Drug Deliv. Rev.* **60**, 876–885 (2008).
170. Villaruz, L. C. & Socinski, M. A. Is there a role of nab-paclitaxel in the treatment of advanced non-small cell lung cancer? The data suggest yes. *Eur. J. Cancer* **56**, 162–171 (2016).
171. Vishnu, P. & Roy, V. Safety and Efficacy of nab-Paclitaxel in the Treatment of Patients with Breast Cancer. *Breast Cancer Basic Clin. Res.* **5**, 53–65 (2011).
172. Chen, N. *et al.* Albumin-bound nanoparticle (nab) paclitaxel exhibits enhanced paclitaxel tissue distribution and tumor penetration. *Cancer Chemother. Pharmacol.* **76**, 699–712 (2015).
173. Moriyama, T., Sasaki, K., Karasawa, K., Uchida, K. & Nitta, K. Intracellular transcytosis of albumin in glomerular endothelial cells after endocytosis through caveolae. *J. Cell. Physiol.* **232**, 3565–3573 (2017).
174. Cucinotto, I. *et al.* Nanoparticle Albumin Bound Paclitaxel in the Treatment of Human Cancer: Nanodelivery Reaches Prime-Time? *Journal of Drug Delivery* vol. 2013 e905091 <https://www.hindawi.com/journals/jdd/2013/905091/> (2013).
175. Lee, J. E. *et al.* Self-assembled PEGylated albumin nanoparticles (SPAN) as a platform for cancer chemotherapy and imaging. *Drug Deliv.* **25**, 1570–1578 (2018).
176. Ruttala, H. B. & Ko, Y. T. Liposomal co-delivery of curcumin and albumin/paclitaxel nanoparticle for enhanced synergistic antitumor efficacy. *Colloids Surf. B Biointerfaces* **128**, 419–426 (2015).

177. Yi, X. *et al.* Co-delivery of Pirarubicin and Paclitaxel by Human Serum Albumin Nanoparticles to Enhance Antitumor Effect and Reduce Systemic Toxicity in Breast Cancers. *Mol. Pharm.* **12**, 4085–4098 (2015).
178. Karmali, P. P. *et al.* Targeting of albumin-embedded paclitaxel nanoparticles to tumors. *Nanomedicine Nanotechnol. Biol. Med.* **5**, 73–82 (2009).
179. Xiong, J., Han, S., Ding, S., He, J. & Zhang, H. Antibody-nanoparticle conjugate constructed with trastuzumab and nanoparticle albumin-bound paclitaxel for targeted therapy of human epidermal growth factor receptor γ 2-positive gastric cancer. *Oncol. Rep.* (2018) doi:10.3892/or.2018.6201.
180. Ge, L. *et al.* Human Albumin Fragments Nanoparticles as PTX Carrier for Improved Anti-cancer Efficacy. *Front. Pharmacol.* **9**, 582 (2018).
181. Kelly, C. & Alken. Benefit risk assessment and update on the use of docetaxel in the management of breast cancer. *Cancer Manag. Res.* 357 (2013) doi:10.2147/CMAR.S49321.
182. Sulkes, A. *et al.* Docetaxel (Taxotere) in advanced gastric cancer: results of a phase II clinical trial. EORTC Early Clinical Trials Group. *Br. J. Cancer* **70**, 380–383 (1994).
183. Cheng, K., Sun, S. & Gong, X. Preparation, characterization, and antiproliferative activities of biotin-decorated docetaxel-loaded bovine serum albumin nanoparticles. *Braz. J. Pharm. Sci.* **54**, (2018).

184. Tang, X. *et al.* Enhanced tolerance and antitumor efficacy by docetaxel-loaded albumin nanoparticles. *Drug Deliv.* 1–11 (2015) doi:10.3109/10717544.2015.1049720.
185. Desale, J. P., Swami, R., Kushwah, V., Katiyar, S. S. & Jain, S. Chemosensitizer and docetaxel-loaded albumin nanoparticle: overcoming drug resistance and improving therapeutic efficacy. *Nanomed.* **13**, 2759–2776 (2018).
186. Patel, A. G. & Kaufmann, S. H. How does doxorubicin work? *eLife* **1**, (2012).
187. Thorn, C. F. *et al.* Doxorubicin pathways: pharmacodynamics and adverse effects. *Pharmacogenet. Genomics* **21**, 440–446 (2011).
188. Hanna, A. D., Lam, A., Tham, S., Dulhunty, A. F. & Beard, N. A. Adverse Effects of Doxorubicin and Its Metabolic Product on Cardiac RyR2 and SERCA2A. *Mol. Pharmacol.* **86**, 438–449 (2014).
189. Zhao, N., Woodle, M. C. & Mixson, A. J. Advances in delivery systems for doxorubicin. *J. Nanomedicine Nanotechnol.* **9**, (2018).
190. Honary, S., Jahanshahi, M., Golbayani, P., Ebrahimi, P. & Ghajar, K. Doxorubicin-Loaded Albumin Nanoparticles: Formulation and Characterization. *J. Nanosci. Nanotechnol.* **10**, 7752–7757 (2010).
191. Abbasi, S., Paul, A., Shao, W. & Prakash, S. Cationic Albumin Nanoparticles for Enhanced Drug Delivery to Treat Breast Cancer: Preparation and *In Vitro* Assessment. *J. Drug Deliv.* **2012**, 1–8 (2012).

192. Onafuye, H. *et al.* Doxorubicin-loaded human serum albumin nanoparticles overcome transporter-mediated drug resistance in drug-adapted cancer cells. *Beilstein J. Nanotechnol.* **10**, 1707–1715 (2019).
193. Motevalli, S. M. *et al.* Co-encapsulation of curcumin and doxorubicin in albumin nanoparticles blocks the adaptive treatment tolerance of cancer cells. *Biophys. Rep.* **5**, 19–30 (2019).
194. Lu, Y. *et al.* Co-delivery of Cyclophosphamide and Doxorubicin Mediated by Bovine Serum Albumin Nanoparticles Reverses Doxorubicin Resistance in Breast Cancer by Down-regulating P-glycoprotein Expression. *J. Cancer* **10**, 2357–2368 (2019).
195. Teng, L. *et al.* Cabazitaxel-loaded human serum albumin nanoparticles as a therapeutic agent against prostate cancer. *Int. J. Nanomedicine* **Volume 11**, 3451–3459 (2016).
196. Meng, F. *et al.* Folate Receptor-Targeted Albumin Nanoparticles Based on Microfluidic Technology to Deliver Cabazitaxel. *Cancers* **11**, 1571 (2019).
197. Tziortzioti, R. Human Serum Albumin Nanoparticles as a Novel Delivery System for Cabazitaxel. *ANTICANCER Res.* **8** (2016).
198. Maiti, T. K., Ghosh, K. S., Debnath, J. & Dasgupta, S. Binding of all-trans retinoic acid to human serum albumin: Fluorescence, FT-IR and circular dichroism studies. *Int. J. Biol. Macromol.* **38**, 197–202 (2006).
199. Li, Y. *et al.* Specific cancer stem cell-therapy by albumin nanoparticles functionalized with CD44-mediated targeting. *J. Nanobiotechnology* **16**, 99 (2018).

200. Huang, H. *et al.* Co-delivery of all-trans-retinoic acid enhances the anti-metastasis effect of albumin-bound paclitaxel nanoparticles. *Chem. Commun.* **53**, 212–215 (2016).
201. Bedoui, Y. *et al.* Methotrexate an Old Drug with New Tricks. *Int. J. Mol. Sci.* **20**, (2019).
202. Taheri, A. *et al.* Nanoparticles of Conjugated Methotrexate-Human Serum Albumin: Preparation and Cytotoxicity Evaluations. *Journal of Nanomaterials* vol. 2011 e768201 <https://www.hindawi.com/journals/jnm/2011/768201/> (2011).
203. Gaies, E. & Jebabli, N. Methotrexate Side Effects: Review Article. *J. Drug Metab. Toxicol.* **3**, (2012).
204. Fiehn, C. *et al.* Albumin-coupled methotrexate (MTX-HSA) is a new anti-arthritis drug which acts synergistically to MTX. *Rheumatology* **43**, 1097–1105 (2004).
205. Burger, A. M., Hartung, G., Stehle, G., Sinn, H. & Fiebig, H. H. Pre-clinical evaluation of a methotrexate–albumin conjugate (MTX-HSA) in human tumor xenografts in vivo. *Int. J. Cancer* **92**, 718–724 (2001).
206. Wosikowski, K. *et al.* In Vitro and in Vivo Antitumor Activity of Methotrexate Conjugated to Human Serum Albumin in Human Cancer Cells. *Clin. Cancer Res.* **9**, 1917–1926 (2003).
207. Taheri, A. *et al.* Enhanced Anti-Tumoral Activity of Methotrexate-Human Serum Albumin Conjugated Nanoparticles by Targeting with Luteinizing Hormone-Releasing Hormone (LHRH) Peptide. *Int. J. Mol. Sci.* **12**, 4591–4608 (2011).

208. Taheri, A. *et al.* Use of biotin targeted methotrexate–human serum albumin conjugated nanoparticles to enhance methotrexate antitumor efficacy. *Int. J. Nanomedicine* **6**, 1863–1874 (2011).
209. Taheri, A., Dinarvand, R., Atyabi, F., Ghahremani, M. H. & Ostad, S. N. Trastuzumab decorated methotrexate–human serum albumin conjugated nanoparticles for targeted delivery to HER2 positive tumor cells. *Eur. J. Pharm. Sci.* **47**, 331–340 (2012).
210. S, Sripriyalakshmi., C. H, Anjali., C, G. P. Doss., B, R. & Ravindran, A. BSA Nanoparticle Loaded Atorvastatin Calcium - A New Facet for an Old Drug. *PLoS ONE* **9**, e86317 (2014).
211. Zhou, C. *et al.* Alternative and Injectable Preformed Albumin-Bound Anticancer Drug Delivery System for Anticancer and Antimetastasis Treatment. *ACS Appl. Mater. Interfaces* **11**, 42534–42548 (2019).
212. Cacemiro, M. da C. *et al.* Philadelphia-negative myeloproliferative neoplasms as disorders marked by cytokine modulation. *Hematol. Transfus. Cell Ther.* **40**, 120–131 (2018).
213. De Marinis, E. *et al.* Ruxolitinib binding to human serum albumin: bioinformatics, biochemical and functional characterization in JAK2V617F + cell models. *Sci. Rep.* **9**, 1–12 (2019).
214. A. A. Aljabali, A. *et al.* Albumin Nano-Encapsulation of Piceatannol Enhances Its Anticancer Potential in Colon Cancer Via Downregulation of Nuclear p65 and HIF-1 α . *Cancers* **12**, 113 (2020).

215. Nowak, R., Olech, M. & Nowacka, N. Plant Polyphenols as Chemopreventive Agents. in *Polyphenols in Human Health and Disease* 1289–1307 (Elsevier, 2014). doi:10.1016/B978-0-12-398456-2.00086-4.
216. Bush, M. A. *et al.* Safety, tolerability, pharmacodynamics and pharmacokinetics of albiglutide, a long-acting glucagon-like peptide-1 mimetic, in healthy subjects. *Diabetes Obes. Metab.* **11**, 498–505 (2009).
217. Baggio, L. L., Huang, Q., Cao, X. & Drucker, D. J. An albumin-exendin-4 conjugate engages central and peripheral circuits regulating murine energy and glucose homeostasis. *Gastroenterology* **134**, 1137–1147 (2008).
218. Ding, X. *et al.* Exendin-4, a glucagon-like protein-1 (GLP-1) receptor agonist, reverses hepatic steatosis in ob/ob mice. *Hepatology* **43**, 173–181 (2006).
219. Gajahi Soudahome, A. *et al.* Glycation of human serum albumin impairs binding to the glucagon-like peptide-1 analogue liraglutide. *J. Biol. Chem.* **293**, 4778–4791 (2018).
220. Plum, A., Jensen, L. B. & Kristensen, J. B. In Vitro Protein Binding of Liraglutide in Human Plasma Determined by Reiterated Stepwise Equilibrium Dialysis. *J. Pharm. Sci.* **102**, 2882–2888 (2013).
221. Rondeau, P. & Bourdon, E. The glycation of albumin: structural and functional impacts. *Biochimie* **93**, 645–658 (2011).
222. Léger, R. *et al.* Identification of CJC-1131-albumin bioconjugate as a stable and bioactive GLP-1(7–36) analog. *Bioorg. Med. Chem. Lett.* **14**, 4395–4398 (2004).

223. Mark S. Wallace, M. D. *et al.* A Phase II, multicenter, randomized, double-blind, placebo-controlled crossover study of CJC-1008—a long-acting, parenteral opioid analgesic—in the treatment of postherpetic neuralgia. *J. Opioid Manag.* **2**, 167–173 (2006).
224. Moore, D. C. Drug-Induced Neutropenia. *Pharm. Ther.* **41**, 765–768 (2016).
225. Ghidini, M. *et al.* New developments in the treatment of chemotherapy-induced neutropenia: focus on balugrastim. *Ther. Clin. Risk Manag.* **12**, 1009–1015 (2016).
226. Konkle, B. A., Huston, H. & Nakaya Fletcher, S. Hemophilia B. in *GeneReviews*® (eds. Adam, M. P. *et al.*) (University of Washington, Seattle, 1993).
227. Santagostino, E. *et al.* Long-acting recombinant coagulation factor IX albumin fusion protein (rIX-FP) in hemophilia B: results of a phase 3 trial. *Blood* **127**, 1761–1769 (2016).
228. Zollner, S. *et al.* Pharmacological characteristics of a novel, recombinant fusion protein linking coagulation factor VIIa with albumin (rVIIa-FP). *J. Thromb. Haemost. JTH* **12**, 220–228 (2014).
229. Gibbert, K., Schlaak, J., Yang, D. & Dittmer, U. IFN- α subtypes: distinct biological activities in anti-viral therapy. *Br. J. Pharmacol.* **168**, 1048–1058 (2013).
230. Cai, Y. *et al.* Reengineering of Albumin-Fused Cocaine Hydrolase Coch1 (TV-1380) to Prolong Its Biological Half-Life. *AAPS J.* **22**, 5 (2019).
231. Liang, H., Yang, F., Lee, N. & Wu, X. HSA-based anti-inflammatory therapy: a new and improved approach. *Future Med. Chem.* **6**, 119–121 (2014).

232. Yang, F. *et al.* Human serum albumin-based design of a diflunisal prodrug. *Eur. J. Pharm. Biopharm.* **84**, 549–554 (2013).
233. Stoddart, C. A. *et al.* Albumin-conjugated C34 Peptide HIV-1 Fusion Inhibitor. *J. Biol. Chem.* **283**, 34045–34052 (2008).
234. Kitchen, C. M., Nuño, M., Kitchen, S. G. & Krogstad, P. Enfuvirtide antiretroviral therapy in HIV-1 infection. *Ther. Clin. Risk Manag.* **4**, 433–439 (2008).
235. Grishin, A. V. *et al.* Fusion of Lysostaphin to an Albumin Binding Domain Prolongs Its Half-Life and Bactericidal Activity in the Systemic Circulation. *Molecules* **24**, (2019).
236. Elsadek, B. & Kratz, F. Impact of albumin on drug delivery — New applications on the horizon. *J. Controlled Release* **157**, 4–28 (2012).
237. Van Roy, M. *et al.* The preclinical pharmacology of the high affinity anti-IL-6R Nanobody® ALX-0061 supports its clinical development in rheumatoid arthritis. *Arthritis Res. Ther.* **17**, 135 (2015).
238. Kratz, F. Albumin as a drug carrier: Design of prodrugs, drug conjugates and nanoparticles. *J. Controlled Release* **132**, 171–183 (2008).
239. Gounden, V. & Jialal, I. Hypoalbuminemia. in *StatPearls* (StatPearls Publishing, 2020).
240. Wiedenmann, N. *et al.* 130-nm albumin-bound paclitaxel enhances tumor radiocurability and therapeutic gain. *Clin. Cancer Res. Off. J. Am. Assoc. Cancer Res.* **13**, 1868–1874 (2007).

241. Nanjwade, B. K., Derkar, G. K., Bechra, H. & Manvi, F. V. Nanosized Technological Approaches for the Delivery of Poorly Water Soluble Drugs. *Iran. J. Pharm. Sci.* **6**, 149–162 (2010).
242. Hosseinifar, N., Sharif, A. A. M., Goodarzi, N., Amini, M. & Dinarvand, R. Preparation of human serum albumin nanoparticles using a chemometric technique. *J. Nanostructure Chem.* **7**, 327–335 (2017).
243. Lee, M. K., Kim, M. Y., Kim, S. & Lee, J. Cryoprotectants for freeze drying of drug nano-suspensions: Effect of freezing rate. *J. Pharm. Sci.* **98**, 4808–4817 (2009).
244. Corradini, D., Strekalova, E. G., Stanley, H. E. & Gallo, P. Microscopic mechanism of protein cryopreservation in an aqueous solution with trehalose. *Sci. Rep.* **3**, (2013).
245. Young, L., Sung, J., Stacey, G. & Masters, J. R. Detection of Mycoplasma in cell cultures. *Nat. Protoc.* **5**, 929–934 (2010).
246. Thao, L. Q. *et al.* Pharmaceutical potential of tacrolimus-loaded albumin nanoparticles having targetability to rheumatoid arthritis tissues. *Int. J. Pharm.* **497**, 268–276 (2016).
247. Niknejad, H. & Mahmoudzadeh, R. Comparison of Different Crosslinking Methods for Preparation of Docetaxel-loaded Albumin Nanoparticles. *Iran. J. Pharm. Res. IJPR* **14**, 385–394 (2015).
248. Langer, K. *et al.* Optimization of the preparation process for human serum albumin (HSA) nanoparticles. *Int. J. Pharm.* **257**, 169–180 (2003).

249. Rahimnejad, M., Jahanshahi, M., Najafpour, G. D. & Mehdinia, M. Fabrication of Bovine Serum Albumin Nanoparticles Self-assembled Coacervation Method for Drug Delivery Systems. *Iran. J. Energy Environ.* **1**, (2010).
250. Challenging paradigms in tumour drug delivery. *Nat. Mater.* **19**, 477–477 (2020).
251. Wiggins, P., McCurdy, S. A. & Zeidenberg, W. Epistaxis due to glutaraldehyde exposure. *J. Occup. Med. Off. Publ. Ind. Med. Assoc.* **31**, 854–856 (1989).
252. St Clair, M. B., Bermudez, E., Gross, E. A., Butterworth, B. E. & Recio, L. Evaluation of the genotoxic potential of glutaraldehyde. *Environ. Mol. Mutagen.* **18**, 113–119 (1991).
253. W, F. & A, B. Release of glutaraldehyde from an albumin-glutaraldehyde tissue adhesive causes significant in vitro and in vivo toxicity. *The Annals of thoracic surgery* vol. 79 <https://pubmed.ncbi.nlm.nih.gov/15854927/> (2005).
254. Amighi, F., Emam-Djomeh, Z. & Labbafi-Mazraeh-Shahi, M. Effect of different cross-linking agents on the preparation of bovine serum albumin nanoparticles. *J. Iran. Chem. Soc.* **17**, 1223–1235 (2020).
255. Manickam, B., Sreedharan, R. & Elumalai, M. ‘Genipin’ – The Natural Water Soluble Cross-linking Agent and Its Importance in the Modified Drug Delivery Systems: An Overview. *Curr. Drug Deliv.* **11**, 139–145 (2014).
256. Li, F. *et al.* Enhanced tumor delivery and antitumor response of doxorubicin-loaded albumin nanoparticles formulated based on a Schiff base. *Int. J. Nanomedicine* **11**, 3875–3890 (2016).

257. Wang, L. & Stegemann, J. P. Glyoxal Crosslinking of Cell-Seeded Chitosan/Collagen Hydrogels for Bone Regeneration. *Acta Biomater.* **7**, 2410–2417 (2011).
258. Hu, Y.-J., Liu, Y., Zhao, R.-M. & Qu, S.-S. Interaction of colchicine with human serum albumin investigated by spectroscopic methods. *Int. J. Biol. Macromol.* **37**, 122–126 (2005).